Int. J. Anal. Appl. (2026), 24:144

International Journal of Analysis and Applications

Tri-valued Neutrosophic Soft Structures with Graphics and Machine-Learning-Assisted Visualizations

Jamil J. Hamja[1], Diana Amin Mohammad Mahmoud[2], Raed Hatamleh[3], Haitham Qawaqneh[4], Shoaib Arbab[5], Alaa M. Abd El-latif[6], Mohammed Mamoun Ahmed Abubakr[7], Arif Mehmood[8,*], Cris L. Armada[9,10]

[1]*Department of Mathematics, College of Mathematical Sciences, Mindanao State University Tawi-Tawi College of Technology and Oceanography, Philippines*

[2]*Amman Arab University, College of Arts and Sciences, Department of Mathematics, P.O. Box 2234, Amman 11953, Jordan*

[3]*Department of Mathematics, Faculty of Science, Jadara University, P.O. Box 733, Irbid 21110, Jordan*

[4]*Al-Zaytoonah University of Jordan, Amman 11733, Jordan*

[5]*Department of Mathematics, Islamia College Peshawar, Peshawar 25120, Khyber Pakhtunkhwa, Pakistan*

[6]*Department of Mathematics, College of Science, Northern Border University, Arar 91431, Saudi Arabia*

[7]*College of Business Administration, Northern Border University, Arar 91431, Saudi Arabia*

[8*]*Department of Mathematics, Institute of Numerical Sciences, Gomal University, Dera Ismail Khan 29050, KPK, Pakistan*

[9]*Vietnam National University Ho Chi Minh City, Linh Trung Ward, Thu Duc City, Ho Chi Minh City, Vietnam*

[10]*Department of Applied Mathematics, Faculty of Applied Science, Ho Chi Minh City University of Technology (HCMUT), 268 Ly Thuong Kiet, Ward 14, District 10, Ho Chi Minh City, Vietnam*

**Corresponding author:* mehdaniyal@gmail.com

ABSTRACT: The notion of the tri-valued neutrosophic soft set (TVNSS), its basic operations, and examples of each operation are first explained in this paper as worked problems that are subsequently displayed as understandable graphics. Based on this, we further offer the tri-valued neutrosophic topological space (TVNSTS), outline its

Received Sep. 22, 2025

2020 Mathematics Subject Classification. 03E72.

Key words and phrases. neutrosophic set; neutrosophic soft set; TVNSS; TVNSTS; cosine similarity; machine-learning techniques.

https://doi.org/10.28924/2291-8639-24-2026-144

ISSN: 2291-8639

fundamental functions, and provide instances once more, illustrating the outcomes with excellent graphical representations. We also employ the chosen machine-learning and statistical techniques to provide comparative visualizations in order to improve and triangulate these constructs. Next, we use these tools to depict patient-disease similarity at complementary angles on a 5x5 grid. A 3D bar chart (grouped into a 3D) and a cool-to-warm Heatmaps both agree on the single best match, P2 -D1 = 0.9107, which we identify and emphasize. Additionally, the corner highs at P1D5 and P3D5 are steady, the majority of the patients have high scores at the region, and there is a noticeable high ridge at D4. Likewise, P2D3, P4D4, and P5D5 are among the strong pairs in the 0.87–0.91 range, whereas P4D1 and P2D5 are near the lower end of the scale. With no change in narrative, min-max normalization to [0,1] then saturates the contrast: row-wise maxima are apparent at P1 -D5, P3 -D4, P4 -D4, and P5 -D5, while P2 -D1 is the global maximum at 1.000. The signal is strong on metrics and scales when a Pearson correlation representation in a red-yellow-green palette regularly follows the cosine pattern and, after normalization, isolates the same dominant cells. Finally, PCA with k-means is used to describe the form of these visuals: in the raw matrix, two small clusters, {P2, P3, P5} and {P1, P4}, form. These clusters are primarily concentrated on PC1 at about 81% variance; during normalization, P2 is an outlier that is enjoyable on its own, and the remaining four are tightly clustered by PC1 and PC2, which account for about 94% of the variation. When taken together, these associated opinions show a repeated high ridge along D4, a solid unification of classification, and a single definitive assignment of the patient and condition.

1. Introduction

The issue of uncertainty, imprecision, and incompleteness modeling has gained interest in various areas of science and engineering over the last few decades. Classical binary logic and probability theory tend to be inadequate in case of indeterminate or inconsistent information. These limitations were overcome by the introduction of neutrosophy by Smarandache [1] which is an extension of classical and fuzzy logic, but which adds an additional element of indeterminacy. This was repeated in Smarandache [2], where neutrosophic logic, probability and statistics were unified in order to create a coherent system. The next important practical development was the introduction of single-valued neutrosophic sets (SVNSs) by Wang et al. [3], to simplify the representation of neutrosophic information to be used in real-world applications. Later on, there were numerous hybrid models. As an example, Alkhazaleh et al. [4] proposed possibility Fermatean neutrosophic soft sets and Mohanty and Tripathy [5] proposed a new method to neutrosophic soft sets that are used in decision-making. Parimala et al. [6] have reviewed the theoretical foundations of such structures and have analyzed the fuzzy soft, intuitionistic fuzzy soft, and neutrosophic soft topological spaces. The study by Liu and Shi [7] in the field of multi-criteria decision-making (MCDM) suggested the generalized hybrid weighted average operators with reference to interval neutrosophic hesitant sets. Neutrosophic sets were thoroughly compiled in a collection of MCDM techniques, edited by Kahraman and Otay [8]. Meanwhile, in image processing, Guo and Cheng [9] came up with a new neutrosophic algorithm of image segmentation. Abdel-Basset et al. [10] further extended the TOPSIS approach with the aid of type-2 neutrosophic numbers in selecting the suppliers. Smarandache [11] further refined the theory, introducing refined literal indeterminacy and laws of multiplication. Bashir et al. [12] came up with refined neutrosophic soft sets whereas Solang and Ye [13] advanced refined simplified neutrosophic similarity measures using trigonometric functions to make decisions relating to a group of suppliers. In addition to decision making, neutrosophic ideas have been applied in communication and information sciences, as discussed by Teodorescu and Ionescu [15]. Saeed et al. [16] presented axioms of separation in neutrosophic quadri-partition topological space in neutrosophic soft topological spaces. It was also shown by Smarandache [17] that neutrosophic sets are an extension of intuitionistic fuzzy sets. The pioneering seminal work on soft sets by Molodtsov [18], provided foundations to numerous hybrid models, which were then defined by Maji [19] who introduced neutrosophic soft sets. The further works of neutrosophic soft topological spaces were proposed by Bera and Mahapatra [20] and Ozturk et al. [21]. Recent developments are hyper-fuzzy VIKOR and DEMATEL techniques by Fujita [22], interval-valued Fermatean neutrosophic super hyper soft sets in healthcare by Abdalla et al. [23], bipolar fuzzy rough set based VIKOR by Gul [24], and CODAS techniques with bipolar complex fuzzy soft Frank aggregation operators by Jaleel et al [25].

1.1. Literature review

Goswami and Pamučar [26] used fuzzy MCDM in the selection of materials of the interiors of an electric vehicle, and Tarafdar et al. [27] combined T-spherical fuzzy models when assessing an EV. Palanikumar et al. [28] suggested trigonometric Pythagorean fuzzy normal aggregation operators to choose industrial robots. Wavelet-based methods (Lilik et al. [29]) and fuzzy single-stroke character recognition have also been developed to improve fuzzy and neutrosophic methods (Tormasi and Koczy [30]). Gondocs and Dorer [31] investigated AI prediction and human judgment in medical diagnosis, whereas Ballagi and Koczy [32] used fuzzy signature sets to work with multi-robot cooperation. Abubaker et al. [33] studied the numerical solutions of neutrosophic boundary value problems and Ahmad et al. [34] studied the applications of graph theory. Other extensions are complex tangent trigonometric treatments of rung fuzzy sets by Hatamleh et al. [35], symbolic n-plithogenic intervals by Hatamleh and Hazaymeh [36], and fixed point results in any metric space by Qawaqneh [41], Qawaqneh et al. [42], Qawaqneh et al. [43], Qawaqneh Elbes et al. [43], and Kanan et al. [44] described their applications of deep learning to detect the COVID-19 disease and IoT-based learning environments, respectively. Batiha et al. [45] designed fractional-order PID controllers. sssAbd El-latif and Alqahtani [46] have defined new types of supra soft continuous maps in the context of soft topological structures, and Abd El-latif et al. [47] have defined a strictly broader category of soft sets. Al-Omari and Alqahtani [48] introduced operators in soft primal spaces, and Abd El-latif et al. [49] introduced new forms of maps and connected spaces. Abd El-latif et al. [50] used soft somewhere dense sets and Alqahtani [51] proposed neutrosophic primal structures. Alqahtani [52] defined operators and separation axioms in diving topological spaces and Ibedou et al. [53] defined diving and floating structures. Alqahtani and Tkachenko [54] studied normality in topological groups. Further extensions of supra soft were given by El-Sheikh and Abd El-latif [55] and new Lindelofness and compactness conditions by Abd El-latif [56]. Soft operators and separation axioms were further studied by Abd El-latif and Alqahtani [57] and Alqahtani and Abd El-latif [58]. Ameen and Alqahtani [59] studied the idea of baire category soft sets, Alqahtani et al. [60] studied the nodecness of soft generalized topological spaces, and Ameen and Alqahtani studied soft functions modulo soft sets of the first category [61]. Congruence representations via soft ideals were presented by Ameen and Alqahtani [62], and a novel class of separation axioms via C-open sets by Alqahtani and Saleh [63]. Lastly, Fermatean double-valued neutrosophic soft topological spaces were introduced by Hatamleh et al. [64], and Abd El-Latif [65] considered soft supra compactness.

1.2. Novelty and motivations for research

This paper provides a tri-valued neutrosophic soft set with full specifications and a complete operator toolkit. Each operator is related to a proposed example with full visualization of the data, making the algebra always directly proportional to what a reader is looking at on data. The stability and proximity of neutrosophic evidence are made tangible and testable on real matrices by characterizing a three-valued neutrosophic topological space that is consistent with the soft-set layer. It employs a visualization-first methodology in which grouped bar charts, Heatmaps, and 3D surfaces serve as guarantees of model behavior rather than as decorations. The cross-metric validation within the same cohesive pipeline is the second source of uniqueness. Cosine similarity, Pearson correlation, and min-max normalization all identify the same dominating cells, demonstrating that the findings are independent of the scale. Row-wise maxima are maintained and the global maximum P2D1 size selection is fixed at 1.000 after normalization, demonstrating normalization invariance on the 5x5 patient disease matrix. In order to recover latent structure that is related to the visuals, PCA is also utilized. Two small groups of patients appear along PC1 at about 81% explained variance in the original matrix, and P2 splits as a glaring outlier. The remaining four patients cluster closely around PC1 and PC2, representing about 94% of the total variance. invariance on the 5x5 matrix of patient diseases.

Finally, by showing a high ridge in all D4 views, the analysis provides a good visual observation, a suspected feature, and a reproducible discovery. Together, these provide a cooking process that can be used to neutrosophic research: specify the operators, illustrate the procedures, cross-check measurements and scales, and use basic machine learning to comprehend the structure to produce results that are readable, reliable, and repeatable.

2. Preliminaries

The prerequisites that are crucial for the other sections are covered in the first section

Definition 2.1 [17]. On the universe of discourse X, a neutrosophic set A is defined as follows:

$A = \{(\varkappa, \text{T}_A(\varkappa), \text{I}'_A(\varkappa), \text{F}_A(\varkappa)) : \varkappa \in X\}$,

where $\text{T}, \text{I}', \text{F}: X \to]0^-, 1^+[$ and $0^- \leq \text{T}_A(\varkappa) + \text{I}'_A(\varkappa) + \text{F}_A(\varkappa) \leq 3^+$

According to philosophy, the values of the neutrosophic set are derived from the actual non-standard or standard subsets of $]0^-, 1^+[$. However, it is difficult to use a neutrosophic set with values from a real standard or non-standard subset of]0−,1+[when applying this idea to real scientific and engineering problems.

Definition 2.2 [18] . Let $P(X)$ be the power set of X, let Ĕ be a set of parameters, and let X be a starting universe. When F is a mapping with the formula $\text{F} : \breve{\text{E}} \to P(X)$, the pair $(\text{F}, \breve{\text{E}})$ is referred to as a soft set over X. Stated otherwise, the set is the set of e-approximate elements of the soft sets, or $(\text{F}, \breve{\text{E}}) = \{(\grave{e}, \text{F}(\grave{e})) : \grave{e} \in \breve{\text{E}}, \text{F}: \breve{\text{E}} \to P(X)\}$ or a parameterized family of subsets of set X for e-elements of the soft set $(\text{F}, \breve{\text{E}})$.

Definition 2.3 [19]. Let Ĕ be the set of parameters and X be the set of beginning universes. Let $P(X)$ be the set of all possible sets of X that are neutrosophic. Then, a set defined by a set valued function F that represents a mapping $\text{F} : \breve{\text{E}} \to P(X)$ is referred to as a neutrosophic soft set $(\text{F}, \breve{\text{E}})$ over X. F is also known as the approximate function of the neutrosophic soft set $(\text{F}, \breve{\text{E}})$. Stated differently, the neutrosophic soft set can be expressed as a set of ordered pairs,

$(\text{F}, \breve{\text{E}}) = \left\{\left(\grave{e}, \left(\varkappa, \text{T}_{\text{F}(\grave{e})}(\varkappa), \text{I}'_{\text{F}(\grave{e})}(\varkappa), \text{F}_{\text{F}(\grave{e})}(\varkappa) : \varkappa \in X\right)\right) : \grave{e} \in \breve{\text{E}}\right\}$,

We refer to the truth-membership, indeterminacy-membership, and falsity-membership functions of $\text{F}(\grave{e})$ as $\text{T}_{\text{F}(\grave{e})}(\varkappa), \text{I}'_{\text{F}(\grave{e})}(\varkappa)$ and $\text{F}_{\text{F}(\grave{e})}(\varkappa) \in [0,1]$, respectively. Since each T, I' and F has a supremum of 1, it follows that the inequality

$0 \leq \text{T}_{\text{F}(\grave{e})}(\varkappa) + \text{I}'_{\text{F}(\grave{e})}(\varkappa) + \text{F}_{\text{F}(\grave{e})}(\varkappa) \leq 3$ is obvious.

Definition 2.4 [20]. If $(\text{F}, \breve{\text{E}})$ is a NSS over universe set X, then $(\text{F}, \breve{\text{E}})^c$ is the complement of $(\text{F}, \breve{\text{E}})$ and is defined as follows:

$(\text{F}, \breve{\text{E}})^c = \left\{\left(\grave{e}, \left(\varkappa, \text{F}_{\text{F}(\grave{e})}(\varkappa), 1 - \text{I}'_{\text{F}(\grave{e})}(\varkappa), \text{T}_{\text{F}(\grave{e})}(\varkappa) : \varkappa \in X\right)\right) : \grave{e} \in \breve{\text{E}}\right\}$.

It should be clear that $((\text{F}, \breve{\text{E}})^c)^c = (\text{F}, \breve{\text{E}})$.

Definition 2.5[19]. If $(\text{F}, \breve{\text{E}})$ and $(\text{G}, \breve{\text{E}})$ are two NSSs over set X. We state that $(\text{F}, \breve{\text{E}}) \subseteq (\text{G}, \breve{\text{E}})$ if and only if $\grave{e} \in \breve{\text{E}}$ and $\forall\, \varkappa \in X$ and , the following conditions holds

$$\text{T}_{\text{F}(\grave{e})}(\varkappa) \leq \text{T}_{\text{G}(\grave{e})}(\varkappa), \text{I}'_{\text{F}(\grave{e})}(\varkappa) \leq \text{I}'_{\text{G}(\grave{e})}(\varkappa), \text{F}_{\text{F}(\grave{e})}(\varkappa) \geq \text{F}_{\text{G}(\grave{e})}(\varkappa).$$

Definition 2.6 [21]. Given two NSSs $(\text{F}_1, \breve{\text{E}})$ and $(\text{F}_2, \breve{\text{E}})$ over the universe set X, their union is represented by $(\text{F}_1, \breve{\text{E}}) \cup (\text{F}_2, \breve{\text{E}}) = (\text{F}_3, \breve{\text{E}})$, which is defined as follows:

$(\text{F}_3, \breve{\text{E}}) = \left\{\left(\grave{e}, \left(\varkappa, \text{T}_{\text{F}_3(\grave{e})}(\varkappa), \text{I}'_{\text{F}_3(\grave{e})}(\varkappa), \text{F}_{\text{F}_3(\grave{e})}(\varkappa)\right) : \varkappa \in X\right) : \grave{e} \in \breve{\text{E}}\right\}$,

Where, $\text{T}_{\text{F}_3(\grave{e})}(\varkappa) = \max\{\text{T}_{\text{F}_1(\grave{e})}(\varkappa), \text{T}_{\text{F}_2(\grave{e})}(\varkappa)\}$, $\text{T}_{\text{F}_3(\grave{e})}(\varkappa) = \max\{\text{I}'_{\text{F}_1(\grave{e})}(\varkappa), \text{I}'_{\text{F}_2(\grave{e})}(\varkappa)\}$,

$\text{T}_{\text{F}_3(\grave{e})}(\varkappa) = \min\{\text{F}_{\text{F}_1(\grave{e})}(\varkappa), \text{F}_{\text{F}_2(\grave{e})}(\varkappa)\}$.

Definition 2.7 [21]. Given two NSSs $(Ƒ_1, \breve{E})$ and $(Ƒ_2, \breve{E})$ over the universe set$X$, their intersection is represented by $(Ƒ_1, \breve{E}) \cap (Ƒ_2, \breve{E}) = (Ƒ_3, \breve{E})$, which is defined as follows:

$$(Ƒ_3, \breve{E}) = \left\{\left(è, \left(\varkappa, \mathrm{T}_{Ƒ_3(è)}(\varkappa), I'_{Ƒ_3(è)}(\varkappa), Ƒ_{Ƒ_3(è)}(\varkappa)\right) : \varkappa \in X\right) : è \in \breve{E}\right\},$$

Where, $\mathrm{T}_{Ƒ_3(è)}(\varkappa) = \min\{\mathrm{T}_{Ƒ_1(è)}(\varkappa), \mathrm{T}_{Ƒ_2(è)}(\varkappa)\}$, $\mathrm{T}_{Ƒ_3(è)}(\varkappa) = \min\{I'_{Ƒ_1(è)}(\varkappa), I'_{Ƒ_2(è)}(\varkappa)\}$,
$\mathrm{T}_{Ƒ_3(è)}(\varkappa) = \max\{Ƒ_{Ƒ_1(è)}(\varkappa), Ƒ_{Ƒ_2(è)}(\varkappa)\}$.

Definition 2.8 [21]. Given two NSSs $(Ƒ_1, \breve{E})$ and $(Ƒ_2, \breve{E})$, their difference is represented by $(Ƒ_1, \breve{E}) \setminus (Ƒ_2, \breve{E}) = (Ƒ_3, \breve{E})$, which is defined as follows: $(Ƒ_3, \breve{E}) = (Ƒ_1, \breve{E}) \cap (Ƒ_2, \breve{E})^c$, such that $(Ƒ_3, \breve{E}) = \left\{\left(è, \left(\varkappa, \mathrm{T}_{Ƒ_3(è)}(\varkappa), I'_{Ƒ_3(è)}(\varkappa), Ƒ_{Ƒ_3(è)}(\varkappa)\right) : \varkappa \in X\right)\right\}$, for all $è \in \breve{E}$. Where,
$\mathrm{T}_{Ƒ_3(è)}(\varkappa) = \min\{\mathrm{T}_{Ƒ_1(è)}(\varkappa), Ƒ_{Ƒ_2(è)}(\varkappa)\}$, $\mathrm{T}_{Ƒ_3(è)}(\varkappa) = \min\{I'_{Ƒ_1(è)}(\varkappa), 1 - I'_{Ƒ_2(è)}(\varkappa)\}$,
$\mathrm{T}_{Ƒ_3(è)}(\varkappa) = \max\{Ƒ_{Ƒ_1(è)}(\varkappa), \mathrm{T}_{Ƒ_2(è)}(\varkappa)\}$.

Definition 2.9 [21]. Given a family of NSSs over set X, $\{(Ƒ_i, \breve{E}) | i \in I'\}$, then

$$\bigcup_{i \in I'} (Ƒ_i, \breve{E}) = \left\{\left(è, \left(\varkappa, \sup[\mathrm{T}_{Ƒ_i(è)}(\varkappa)]_{i \in I'}, \sup[I'_{Ƒ_i(è)}(\varkappa)]_{i \in I'}, \inf[Ƒ_{Ƒ_i(è)}(\varkappa)]_{i \in I'}\right) : \varkappa \in X\right) : è \in \breve{E}\right\},$$

$$\cap_{i \in I'} (Ƒ_i, \breve{E}) = \left\{\left(è, \left(\varkappa, \inf[\mathrm{T}_{Ƒ_i(è)}(\varkappa)]_{i \in I'}, \inf[I'_{Ƒ_i(è)}(\varkappa)]_{i \in I'}, \sup[Ƒ_{Ƒ_i(è)}(\varkappa)]_{i \in I'}\right) : \varkappa \in X\right) : è \in \breve{E}\right\}.$$

Definition 2.10 [21]. Consider two NSSs over X, $(Ƒ_1, \breve{E})$ and $(Ƒ_2, \breve{E})$,. Then AND operation on them is represented by $(Ƒ_1, \breve{E}) \wedge (Ƒ_2, \breve{E}) = (Ƒ_3, \breve{E} \times \breve{E})$, and is defined as:

$$(Ƒ_3, \breve{E} \times \breve{E}) = \left\{\left((è_1, è_2), \left(\varkappa, \mathrm{T}_{Ƒ_3(è_1,è_2)}(\varkappa), I'_{Ƒ_3(è_1,è_2)}(\varkappa), Ƒ_{Ƒ_3(è_1,è_2)}(\varkappa)\right) : \varkappa \in X\right) : (è_1, è_2) \in \breve{E} \times \breve{E}\right\},$$

where$\mathrm{T}_{Ƒ_3(è_1,è_2)}(\varkappa) = \min\{\mathrm{T}_{Ƒ_1(è_1)}(\varkappa), \mathrm{T}_{Ƒ_2(è_2)}(\varkappa)\}$,

$$\mathrm{T}_{Ƒ_3(è_1,è_2)}(\varkappa) = \min\{I'_{Ƒ_1(è_1)}(\varkappa), I'_{Ƒ_2(è_2)}(\varkappa)\},$$
$$\mathrm{T}_{Ƒ_3(è_1,è_2)}(\varkappa) = \max\{Ƒ_{Ƒ_1(è_1)}(\varkappa), Ƒ_{Ƒ_2(è_2)}(\varkappa)\}.$$

Definition 2.11 [21].Consider two NSSs over X, $(Ƒ_1, \breve{E})$ and $(Ƒ_2, \breve{E})$. The OR operation on them, represented by $(Ƒ_1, \breve{E}) \vee (Ƒ_2, \breve{E}) = (Ƒ_3, \breve{E} \times \breve{E})$,
is defined as: $(Ƒ_3, \breve{E} \times \breve{E}) = \left\{\left((è_1, è_2), \left(\varkappa, \mathrm{T}_{Ƒ_3(è_1,è_2)}(\varkappa), I'_{Ƒ_3(è_1,è_2)}(\varkappa), Ƒ_{Ƒ_3(è_1,è_2)}(\varkappa)\right) : \varkappa \in X\right) : (è_1, è_2) \in \breve{E} \times \breve{E}\right\}$, where, $\mathrm{T}_{Ƒ_3(è_1,è_2)}(\varkappa) = \max\{\mathrm{T}_{Ƒ_1(è_1)}(\varkappa), \mathrm{T}_{Ƒ_2(è_2)}(\varkappa)\}$,

$$\mathrm{T}_{Ƒ_3(è_1,è_2)}(\varkappa) = \max\{I'_{Ƒ_1(è_1)}(\varkappa), I'_{Ƒ_2(è_2)}(\varkappa)\},$$
$$\mathrm{T}_{Ƒ_3(è_1,è_2)}(\varkappa) = \min\{Ƒ_{Ƒ_1(è)}(\varkappa), Ƒ_{Ƒ_2(è_2)}(\varkappa)\}.$$

Definition 2.12 [21].The following criteria must be met for a NSS $(Ƒ, \breve{E})$ over set X to be considered null neutrosophic soft set: è must be within $\breve{E}$ and $\varkappa$ must be within X.
$\mathrm{T}_{Ƒ(è)}(\varkappa) = 0$, $I'_{Ƒ(è)}(\varkappa) = 0$, $Ƒ_{Ƒ(è)}(\varkappa) = 1$. It is denoted by $0_{(X,\breve{E})}$.

Definition 2.13 [21]. The following criteria must be met for a NSS $(Ƒ, \breve{E})$ over set X to be considered absolute NSS: è must be within $\breve{E}$ and $\varkappa$ must be with in X.
$\mathrm{T}_{Ƒ(è)}(\varkappa) = 1$, $I'_{Ƒ(è)}(\varkappa) = 1$, $Ƒ_{Ƒ(è)}(\varkappa) = 0$. It is denoted by $1_{(X,\breve{E})}$.

3. Operations on Double-Valued and Triple-Valued Neutrosophic Soft Sets

DNSS equality of sets, DNSS complement of sets, DNSS subset, DNSS union, DNSS intersection, DNSS difference, family of DNSS sets, DNSS AND set, DNSS OR set, DNSS soft null set, and DNSS absolute sets are all covered in this section. Triple-valued neutrosophic sets (TVNSs), their complements, TVNSSs, equality of TVNSSs, the union of two TVNSSs, the intersection of two TVNSSs, and the difference of two TVNSSs are among the ideas.

Definition 3.1. Suppose X be the set of initial universe set and Ĕ be the set of parameters. Let $P(X)$ denotes the set of all DNSSs of X. A DNSS (Ƒ, Ĕ) is defined as set valued function

Ƒ : Ĕ $\rightarrow P(X)$, where Ƒ is called approximate function of the DNSS (Ƒ, Ĕ). In other words, a DNSS is a parameterized family of some elements of the set $P(X)$ and can be written as a set of ordered pairs:

$$(Ƒ, Ĕ) = \left\{\left(è, \left(\varkappa, T_{Ƒ(è)}(\varkappa), I'_{C_{Ƒ(è)}}(\varkappa), I'_{H_{Ƒ(è)}}(\varkappa), Ƒ_{Ƒ(è)}(\varkappa)\right) : è \in Ĕ\right) : \varkappa \in X\right\},$$

Where, $T_{Ƒ(è)}(\varkappa), I'_{C}(\varkappa), I'_{H_{Ƒ(è)}}(\varkappa), Ƒ_{Ƒ(è)}(\varkappa) \in [0,1]$, are respectively called the truth-membership, indeterminacy leans toward contradiction -membership, indeterminacy leans toward hesitation-membership and falsity-membership function of Ƒ(è). Since, supremum of each $T, I'_{C}, I'_{H}, Ƒ$ is 1, the following inequality $0 \le T_{Ƒ(è)}(\varkappa) + I'_{C_{Ƒ(è)}}(\varkappa) + I'_{H_{Ƒ(è)}}(\varkappa) + Ƒ_{Ƒ(è)}(\varkappa) \le 4$ is obvious.

Definition 3.2. Let (Ƒ, Ĕ) be DNSS over set X. The complement of (Ƒ, Ĕ) is symbolized by $(Ƒ, Ĕ)^c$ is defined as: $(Ƒ, Ĕ)^c = \left\{\left(è, \left(\varkappa, Ƒ_{Ƒ(è)}(\varkappa), 1 - I'_{C_{Ƒ(è)}}(\varkappa), 1 - I'_{H_{Ƒ(è)}}(\varkappa), T_{Ƒ(è)}(\varkappa)\right) : è \in Ĕ\right) : \varkappa \in X\right\}$,

clearly, $((Ƒ, Ĕ)^c)^c = (Ƒ, Ĕ)$.

Definition 3.3. Let (Ƒ, Ĕ) and (Ɠ, Ĕ) be two DNSSs over X. Then (Ƒ, Ĕ) is said to be DNSS subset of (Ɠ, Ĕ), dented by $(Ƒ, Ĕ) \subseteq (Ɠ, Ĕ)$,) if and only if $\forall\, \varkappa \in X$, è ∈ Ĕ, the following conditions are satisfied:

$T_{Ƒ(è)}(\varkappa) \le T_{Ɠ(è)}(\varkappa)$, $I'_{Ƒ(è)}(\varkappa) \le I'_{Ɠ(è)}(\varkappa)$,

Definition 3.4. Let (Ƒ, Ĕ) and (Ɠ, Ĕ) be two DNSSs over X. Then (Ƒ, Ĕ) is said to be equal to (Ɠ, Ĕ), denoted by $(Ƒ, Ĕ) \subseteq (Ɠ, Ĕ)$ If and only if both $(Ƒ, Ĕ) \subseteq (Ɠ, Ĕ)$ and $(Ɠ, Ĕ) \subseteq (Ƒ, Ĕ)$ hold. That is, for all $\varkappa \in X$ and è ∈ Ĕ, the following conditions must be satisfied:

From $(Ƒ, Ĕ) \subseteq (Ɠ, Ĕ)$: $T_{Ƒ(è)}(\varkappa) \le T_{Ɠ(è)}(\varkappa)$, $I'_{C_{Ƒ(è)}}(\varkappa) \le I'_{C_{Ɠ(è)}}(\varkappa)$, $(\varkappa) \le I'_{H_{Ɠ(è)}}(\varkappa)$,

$Ƒ_{Ƒ(è)}(\varkappa) \ge Ƒ_{Ɠ(è)}(\varkappa)$ and from $(Ɠ, Ĕ) \subseteq (Ƒ, Ĕ)$: $T_{Ɠ(è)}(\varkappa) \le T_{Ƒ(è)}(\varkappa)$, $I'_{C_{Ɠ(è)}}(\varkappa) \le I'_{C_{Ƒ(è)}}(\varkappa)$, $I'_{H_{Ɠ(è)}}(\varkappa) \le I'_{H_{Ƒ(è)}}(\varkappa)$, $Ƒ_{Ɠ(è)}(\varkappa) \ge Ƒ_{Ƒ(è)}(\varkappa)$.

Definition 3.5. Let $(Ƒ_1, Ĕ)$ and $(Ƒ_2, Ĕ)$ be DNSSs over set X, their union, denoted by

$(Ƒ_1, Ĕ) \cup (Ƒ_2, Ĕ) = (Ƒ_3, Ĕ)$ is defined as:

$$(Ƒ_3, Ĕ) = \left\{\left(è, \left(\varkappa, T_{Ƒ_3(è)}(\varkappa), I'_{C_{Ƒ_3(è)}}(\varkappa), I'_{H_{Ƒ_3(è)}}(\varkappa), Ƒ_{Ƒ_3(è)}(\varkappa)\right) : \varkappa \in X\right) : è \in Ĕ\right\},$$

where the membership functions are given by

$\mathrm{T}_{\digamma_3(\grave{e})}(\varkappa) = \max\{\mathrm{T}_{\digamma_1(\grave{e})}(\varkappa), \mathrm{T}_{\digamma_2(\grave{e})}(\varkappa)\}$, $\mathrm{I'}_{C_{\digamma_3(\grave{e})}}(\varkappa) = \max\left\{\mathrm{I'}_{C_{\digamma_1(\grave{e})}}(\varkappa), \mathrm{I'}_{C_{\digamma_2(\grave{e})}}(\varkappa)\right\}$,

$'\mathrm{H}_{\digamma_3(\grave{e})}(\varkappa) = \max\left\{\mathrm{I'}_{\mathrm{H}_{\digamma_1(\grave{e})}}(\varkappa), \mathrm{I'}_{\mathrm{H}_{\digamma_2(\grave{e})}}(\varkappa)\right\}$, $\digamma_{\digamma_3(\grave{e})}(\varkappa) = \min\{\digamma_{\digamma_1(\grave{e})}(\varkappa), \digamma_{\digamma_2(\grave{e})}(\varkappa)\}$.

Definition 3.6. Let $(\digamma_1, \breve{E})$ and $(\digamma_2, \breve{E})$ be DNSSs over set X, Their intersection, denoted by $(\digamma_1, \breve{E}) \cap (\digamma_2, \breve{E}) = (\digamma_3, \breve{E})$ is defined as:$(\digamma_3, \breve{E}) =$
$\left\{\left(\grave{e}, \left(\varkappa, \mathrm{T}_{\digamma_3(\grave{e})}(\varkappa), \mathrm{I'}_{C_{\digamma_3(\grave{e})}}(\varkappa), \mathrm{I'}_{\mathrm{H}_{\digamma_3(\grave{e})}}(\varkappa), \digamma_{\digamma_3(\grave{e})}(\varkappa)\right) : \varkappa \in X\right) : \grave{e} \in \breve{E}\right\}$. Where, the membership functions are given by:

$\mathrm{T}_{\digamma_3(\grave{e})}(\varkappa) = \min\{\mathrm{T}_{\digamma_1(\grave{e})}(\varkappa), \mathrm{T}_{\digamma_2(\grave{e})}(\varkappa)\}$, $\mathrm{I'}_{C_{\digamma_3(\grave{e})}}(\varkappa) = \min\left\{\mathrm{I'}_{C_{\digamma_1(\grave{e})}}(\varkappa), \mathrm{I'}_{C_{\digamma_2(\grave{e})}}(\varkappa)\right\}$,

$'\mathrm{H}_{\digamma_3(\grave{e})}(\varkappa) = \min\left\{\mathrm{I'}_{\mathrm{H}_{\digamma_1(\grave{e})}}(\varkappa), \mathrm{I'}_{\mathrm{H}_{\digamma_2(\grave{e})}}(\varkappa)\right\}$, $\digamma_{\digamma_3(\grave{e})}(\varkappa) = \max\{\digamma_{\digamma_1(\grave{e})}(\varkappa), \digamma_{\digamma_2(\grave{e})}(\varkappa)\}$.

Definition 3.7. Let $(\digamma_1, \breve{E})$ and $(\digamma_2, \breve{E})$ be DNSSs over X. The difference between them, denoted by $(\digamma_3, \breve{E}) = (\digamma_1, \breve{E}) \setminus (\digamma_2, \breve{E})$, is defined as the intersection of $(\digamma_1, \breve{E})$ with the complement of $(\digamma_2, \breve{E})$,i.e.,$(\digamma_3, \breve{E}) = (\digamma_1, \breve{E}) \cap (\digamma_2, \breve{E})^c$, Given:

$(\digamma_1, \breve{E}) = \left\{\left(\grave{e}, \left(\varkappa, \mathrm{T}_{\digamma_1(\grave{e})}(\varkappa), \mathrm{I'}_{C_{\digamma_1(\grave{e})}}(\varkappa), \mathrm{I'}_{\mathrm{H}_{\digamma_1(\grave{e})}}(\varkappa), \digamma_{\digamma_1(\grave{e})}(\varkappa)\right) : \grave{e} \in \breve{E}\right) : \varkappa \in X\right\}$,

$(\digamma_2, \breve{E}) = \left\{\left(\grave{e}, \left(\varkappa, \mathrm{T}_{\digamma_2(\grave{e})}(\varkappa), \mathrm{I'}_{C_{\digamma_2(\grave{e})}}(\varkappa), \mathrm{I'}_{\mathrm{H}_{\digamma_2(\grave{e})}}(\varkappa), \digamma_{\digamma_2(\grave{e})}(\varkappa)\right) : \grave{e} \in \breve{E}\right) : \varkappa \in X\right\}$,

$(\digamma_2, \breve{E})^c = \left\{\left(\grave{e}, \left(\varkappa, \digamma_{\digamma_2(\grave{e})}(\varkappa), 1 - \mathrm{I'}_{C_{\digamma_2(\grave{e})}}(\varkappa), 1 - \mathrm{I'}_{\mathrm{H}_{\digamma_2(\grave{e})}}(\varkappa), \mathrm{T}_{\digamma_2(\grave{e})}(\varkappa)\right) : \grave{e} \in \breve{E}\right) : \varkappa \in X\right\}$.

Therefore, the resulting DNSS $(\digamma_3, \breve{E})$ is: $(\digamma_3, \breve{E}) =$
$\left\{\left(\grave{e}, \left(\varkappa, \mathrm{T}_{\digamma_3(\grave{e})}(\varkappa), \mathrm{I'}_{C_{\digamma_3(\grave{e})}}(\varkappa), \mathrm{I'}_{\mathrm{H}_{\digamma_3(\grave{e})}}(\varkappa), \digamma_{\digamma_3(\grave{e})}(\varkappa)\right) : \grave{e} \in \breve{E}\right) : \varkappa \in X\right\}$, where:

$\mathrm{T}_{\digamma_3(\grave{e})}(\varkappa) = \min\{\mathrm{T}_{\digamma_1(\grave{e})}(\varkappa), \digamma_{\digamma_2(\grave{e})}(\varkappa)\}$, $\mathrm{I'}_{C_{\digamma_3(\grave{e})}}(\varkappa) = \min\left\{\mathrm{I'}_{C_{\digamma_1(\grave{e})}}(\varkappa), 1 - \mathrm{I'}_{C_{\digamma_2(\grave{e})}}(\varkappa)\right\}$,

$'\mathrm{H}_{\digamma_3(\grave{e})}(\varkappa) = \min\left\{\mathrm{I'}_{\mathrm{H}_{\digamma_1(\grave{e})}}(\varkappa), 1 - \mathrm{I'}_{\mathrm{H}_{\digamma_2(\grave{e})}}(\varkappa)\right\}$, $\digamma_{\digamma_3(\grave{e})}(\varkappa) = \max\{\digamma_{\digamma_1(\grave{e})}(\varkappa), \mathrm{T}_{\digamma_2(\grave{e})}(\varkappa)\}$.

Definition 3.8. Let $\{(\digamma_i, \breve{E}) | i \in \mathrm{I'}\}$ be a family of TVNSSs over X, then

$$\cup_{i\in \mathrm{I'}}(\digamma_i, \breve{E}) = \left\{\left(\grave{e}, \begin{pmatrix} \varkappa, \sup[\mathrm{T}_{\digamma_i(\grave{e})}(\varkappa)]_{i\in\mathrm{I'}}, \sup\left[\mathrm{I'}_{C_{\digamma_i(\grave{e})}}(\varkappa)\right]_{i\in\mathrm{I'}}, \sup\left[\mathrm{I'}_{\mathrm{H}_{\digamma_i(\grave{e})}}(\varkappa)\right]_{i\in\mathrm{I'}}, \\ \inf[\digamma_{\digamma_i(\grave{e})}(\varkappa)]_{i\in\mathrm{I'}} \end{pmatrix} : \grave{e} \in \breve{E}\right) : \varkappa \in X\right\},$$

$$\cap_{i\in \mathrm{I'}}(\digamma_i, \breve{E}) = \left\{\left(\grave{e}, \begin{pmatrix} \varkappa, \inf[\mathrm{T}_{\digamma_i(\grave{e})}(\varkappa)]_{i\in\mathrm{I'}}, \inf\left[\mathrm{I'}_{C_{\digamma_i(\grave{e})}}(\varkappa)\right]_{i\in\mathrm{I'}}, \inf\left[\mathrm{I'}_{\mathrm{H}_{\digamma_i(\grave{e})}}(\varkappa)\right]_{i\in\mathrm{I'}}, \\ \sup[\digamma_{\digamma_i(\grave{e})}(\varkappa)]_{i\in\mathrm{I'}} \end{pmatrix} : \grave{e} \in \breve{E}\right) : \varkappa \in X\right\}.$$

Definition 3.9. Let $(\digamma_1, \breve{E})$ and $(\digamma_2, \breve{E})$ be DNSS*s* over X, then AND operation on them is symbolized by $(\digamma_3, \breve{E} \times \breve{E}) = (\digamma_1, \breve{E}) \wedge (\digamma_2, \breve{E})$, defined by:

$$(\digamma_3, \breve{E} \times \breve{E}) = \left\{(\grave{e}_1, \grave{e}_2), \left(\begin{pmatrix} \varkappa, \mathrm{T}_{\digamma_3(\grave{e}_1,\grave{e}_2)}(\varkappa), \mathrm{I'}_{C_{\digamma_3(\grave{e}_1,\grave{e}_2)}}(\varkappa), \mathrm{I'}_{\mathrm{H}_{\digamma_3(\grave{e}_1,\grave{e}_2)}}(\varkappa), \\ \digamma_{\digamma_3(\grave{e}_1,\grave{e}_2)}(\varkappa) \end{pmatrix} : (\grave{e}_1, \grave{e}_2) \in \breve{E} \times \breve{E}\right) : \varkappa \in X\right\}$$

Where for each $\varkappa \in X$ and $(\grave{e}_1, \grave{e}_2) \in \check{E} \times \check{E}$: $T_{F_3(\grave{e}_1,\grave{e}_2)}(\varkappa) = \min\{T_{F_1(\grave{e}_1)}(\varkappa), T_{F_2(\grave{e}_2)}(\varkappa)\}$,$I'_{F_3(\grave{e}_1,\grave{e}_2)}(\varkappa) = \min\left\{I'_{C_{F_1(\grave{e}_1)}}(\varkappa), I'_{C_{F_2(\grave{e}_2)}}(\varkappa)\right\}$, $I'_{H_{F_3(\grave{e}_1,\grave{e}_2)}}(\varkappa) = \min\left\{I'_{H_{F_1(\grave{e}_1)}}(\varkappa), I'_{H_{F_2(\grave{e}_2)}}(\varkappa)\right\}$, $F_{F_3(\grave{e}_1,\grave{e}_2)}(\varkappa) = \max\{F_{F_1(\grave{e}_1)}(\varkappa), F_{F_2(\grave{e}_2)}(\varkappa)\}$.

Definition 3.10. Let $(F_1, \check{E})$ and $(F_2, \check{E})$ be DNSS*s* over X, then OR operation on them is symbolized by $(F_3, \check{E} \times \check{E}) = (F_1, \check{E}) \vee (F_2, \check{E})$ is defined by:

$$(F_3, \check{E} \times \check{E}) = \left\{(\grave{e}_1, \grave{e}_2), \left(\begin{pmatrix} \varkappa, T_{F_3(\grave{e}_1,\grave{e}_2)}(\varkappa), I'_{C_{F_3(\grave{e}_1,\grave{e}_2)}}(\varkappa), I'_{H_{F_3(\grave{e}_1,\grave{e}_2)}}(\varkappa), \\ F_{F_3(\grave{e}_1,\grave{e}_2)}(\varkappa) \end{pmatrix} : (\grave{e}_1, \grave{e}_2) \in \check{E} \times \check{E}\right) : \varkappa \in X\right\}$$

Where for each $\varkappa \in X$ and $(\grave{e}_1, \grave{e}_2) \in \check{E} \times \check{E}$: $T_{F_3(\grave{e}_1,\grave{e}_2)}(\varkappa) = \max\{T_{F_1(\grave{e}_1)}(\varkappa), T_{F_2(\grave{e}_2)}(\varkappa)\}$
$I'_{C_{F_3(\grave{e}_1,\grave{e}_2)}}(\varkappa) = \max\left\{I'_{C_{F_1(\grave{e}_1)}}(\varkappa), I'_{C_{F_2(\grave{e}_2)}}(\varkappa)\right\}$, $I'_{H_{F_3(\grave{e}_1,\grave{e}_2)}}(\varkappa) = \max\left\{I'_{H_{F_1(\grave{e}_1)}}(\varkappa), I'_{H_{F_2(\grave{e}_2)}}(\varkappa)\right\}$,
$F_{F_3(\grave{e}_1,\grave{e}_2)}(\varkappa) = \min\{F_{F_1(\grave{e}_1)}(\varkappa), F_{F_2(\grave{e}_2)}(\varkappa)\}$.

Definition 3.11. 1. Let $(F, \check{E})$ be TVNSS over X. Then:

2. $(F, \check{E})$ is said to be a null TVNSS if $T_{F(\grave{e})}(\varkappa) = 0, I'_{C_{F(\grave{e})}}(\varkappa) = 0, I'_{H_{F(\grave{e})}}(\varkappa) = 0, F_{F(\grave{e})}(\varkappa) = 1, \forall\, \grave{e} \in \check{E}, \varkappa \in X$. It is symbolized by $0_{(X,\check{E})}$. 2. $(F, \check{E})$ is said to be absolute TVNSS if

$T_{F(\grave{e})}(\varkappa) = 1, I'_{C_{F(\grave{e})}}(\varkappa) = 1, I'_{H_{F(\grave{e})}}(\varkappa) = 1, F_{F(\grave{e})}(\varkappa) = 0, \forall\, \grave{e} \in \check{E}, \varkappa \in X$. It is symbolized by $1_{(X,\check{E})}$. Clearly, $0^c_{(X,\check{E})} = 1_{(X,\check{E})}$ and $1^c_{(X,\check{E})} = 0_{(X,\check{E})}$.

Definition 3.12. A TVNS represented by A is defined as follows:
$A = \{(\S, AbT_A(\S), R\check{e}lT_A(\S), H_A(\S), R\check{e}F_A(\S), AF_A(\S)) : \S \in \acute{U}\}$, where $AbT, R\check{e}lT, H, R\check{e}lF, AbF : \acute{U} \to\ ]0^-, 1^+[$ and $0^- \leq AbT_A(\S) + R\check{e}lT_A(\S) + H_A(\S) + R\check{e}lF_A(\S) + AbF_A(\S) \leq 5^+$.

Definition 3.13. Let E be a set of parameters and Ú be an initial universe set. A TVNSS (F, E) over X is a set defined by a set valued function F, which represents a mapping: $F : E \to P(X)$, where F is an approximate function of the TVNSS (F, E). Let $P(X)$ represent the set of all pentapartitioned neutrosophic sets of X. $(F, \check{E}) =$
$\left\{\left(\check{e}, \left(\S, AbT_{F(\check{e})}(\S), R\check{e}lT_{F(\check{e})}(\S), H_{F(\check{e})}(\S), R\check{e}lF_{F(\check{e})}(\S), AbF_{F(\check{e})}(\S)\right) : \S \in \acute{U}\right) : \check{e} \in \check{E}\right\}$,
where $AbT_{F(\check{e})}(\S), R\check{e}lT_{F(\check{e})}(\S), R\check{e}lT_{F(\check{e})}(\S), H_{F(\check{e})}(\S), AbF_{F(\check{e})}(\S)$ are elements of [0,1], and respectively called the absolute truth-membership, relative truth-membership, hesitation-membership, relative false-membership and absolute false-membership function of $F(\check{e})$. The inequality $0 \leq AbT_{F(\check{e})}(\S) + R\check{e}lT_{F(\check{e})}(\S) + H_{F(\check{e})}(\S) + R\check{e}lF_{F(\check{e})}(\S) + AbF_{F(\check{e})}(\S) \leq 5$ holds obviously.

Definition 3.14. Let $(F, \check{E})$ be TVNSS over set Ú. The complement of $(F, \check{E})$, denoted by $(F, \check{E})^c$, is defined as $(F, \check{E})^c = \left\{\left(\check{e}, \left(\S, AbF_{F(\check{e})}(\S), R\check{e}lF_{F(\check{e})}(\S), 1 - H_{F(\check{e})}(\S), R\check{e}lT_{F(\check{e})}(\S), AbT_{F(\check{e})}(\S)\right) : \S \in \acute{U}\right) : \check{e} \in \check{E}\right\}$.

Definition 3.15. Let $(Ƒ, Ě)$ and $(G, Ě)$ be TVNSSs over set Ú, then $(Ƒ, Ě)$ is said to be TVNSSSS of $(G, Ě)$ if $AbT_{Ƒ(ě)}(§) \geq AbT_{G(ě)}(§)$, $RělT_{Ƒ(ě)}(§) \geq RělT_{G(ě)}(§)$, $H_{Ƒ(ě)}(§) \geq H_{G(ě)}(§)$, $RělF_{Ƒ(ě)}(§) \leq RělF_{G(ě)}(§)$, $AbF_{Ƒ(ě)}(§) \leq AbƑ_{G(ě)}(§), \forall\ § \in Ú, ě \in Ě$. It is symbolized by $(Ƒ, Ě) \subseteq (G, Ě)$.

Definition 3.16. Let $(Ƒ, Ě)$ and $(G, Ě)$ be TVNSS over set Ú, then $(Ƒ, Ě)$ is said to be TVNSS equals $(G, Ě)$, if $(Ƒ, Ě) \subseteq (G, Ě)$ i.e. $AbT_{Ƒ(ě)}(§) \geq AbT_{G(ě)}(§)$, $RělT_{Ƒ(ě)}(§) \geq RělT_{G(ě)}(§)$, $H_{Ƒ(ě)}(§) \geq H_{G(ě)}(§)$, $RělƑ_{Ƒ(ě)}(§) \leq RělƑ_{G(ě)}(§)$, $AF_{Ƒ(ě)}(§) \leq AbF_{G(ě)}(§), \forall\ ě \in Ě, § \in Ú$. If $(G, Ě) \subseteq (Ƒ, Ě)$ i.e.
$AbT_{G(ě)}(§) \geq AbT_{Ƒ(ě)}(§)$, $RělT_{G(ě)}(§) \geq RělT_{Ƒ(ě)}(§)$, $H_{G(ě)}(§) \geq H_{Ƒ(ě)}(§)$,
$RělF_{G(ě)}(§) \leq RělƑ_{Ƒ(ě)}(§)$, $AbF_{G(ě)}(§) \leq AbF_{Ƒ(ě)}(§)$. It is symbolized by $(Ƒ, Ě) = (G, Ě)$.

Definition 3.17. Let $(Ƒ_1, Ě)$ and $(Ƒ_2, Ě)$ be TVNSSs over set Ú. Then, their union is denoted by $(Ƒ_3, Ě) = (Ƒ_1, Ě) \cup (Ƒ_2, Ě)$ and is defined as:
$(Ƒ_3, Ě) = \left\{\left(ě, \left(§, AbT_{Ƒ_3(ě)}(§), RělT_{Ƒ_3(ě)}(§), H_{Ƒ_3(ě)}(§), RělF_{Ƒ_3(ě)}(§), AbF_{Ƒ_3(ě)}(§)\right) : § \in Ú\right) : ě \in Ě\right\}$, where
$AbT_{Ƒ_3(ě)}(§) = \max\left\{AbT_{Ƒ_1(ě)}(§), AbT_{Ƒ_2(ě)}(§)\right\}$, $RělT_{Ƒ_3(ě)}(§) = \max\left\{RělT_{Ƒ_1(ě)}(§), RělT_{Ƒ_2(ě)}(§)\right\}$,
$H_{Ƒ_3(ě)}(§) = \max\left\{H_{Ƒ_1(ě)}(§), H_{Ƒ_2(ě)}(§)\right\}$, $RělF_{Ƒ_3(ě)}(§) = \min\left\{RělƑ_{Ƒ_1(ě)}(§), RělF_{Ƒ_2(ě)}(§)\right\}$,
$AbƑ_{Ƒ_3(ě)}(§) = \min\left\{AbF_{Ƒ_1(ě)}(§), AbF_{Ƒ_2(ě)}(§)\right\}$.

Definition 3.18. Let $(Ƒ_1, Ě)$ and $(Ƒ_2, Ě)$ be TVNSSs over set Ú. Then, their intersection is denoted by $(Ƒ_3, Ě) = (Ƒ_1, Ě) \cap (Ƒ_2, Ě)$ and is defined as:
$(Ƒ_3, Ě) = \left\{\left(ě, \left(§, AbT_{Ƒ_3(ě)}(§), RělT_{Ƒ_3(ě)}(§), H_{Ƒ_3(ě)}(§), RělF_{Ƒ_3(ě)}(§), AbF_{Ƒ_3(ě)}(§)\right) : § \in Ú\right) : ě \in Ě\right\}$. Where, $AbT_{Ƒ_3(ě)}(§) = \min\left\{AbT_{Ƒ_1(ě)}(§), AbT_{Ƒ_2(ě)}(§)\right\}$, $RělT_{Ƒ_3(ě)}(§) = \min\left\{RělT_{Ƒ_1(ě)}(§), RělT_{Ƒ_2(ě)}(§)\right\}$,
$H_{Ƒ_3(ě)}(§) = \min\left\{H_{Ƒ_1(ě)}(§), H_{Ƒ_2(ě)}(§)\right\}$, $RělƑ_{Ƒ_3(ě)}(§) = \max\left\{RělF_{Ƒ_1(ě)}(§), RělF_{Ƒ_2(ě)}(§)\right\}$,
$AbƑ_{Ƒ_3(ě)}(§) = \max\left\{AbF_{Ƒ_1(ě)}(§), AbF_{Ƒ_2(ě)}(§)\right\}$.

Definition 3.19. Let $(Ƒ_1, Ě)$ and $(Ƒ_2, Ě)$ be TVNSSs. Then the difference of $(Ƒ_1, Ě)$ and $(Ƒ_2, Ě)$ operation on them is symbolized by $(Ƒ_3, Ě) = (Ƒ_1, Ě) \setminus (Ƒ_2, Ě)$ and is defined as:
$(Ƒ_3, Ě) = (Ƒ_1, Ě) \cap (Ƒ_2, Ě)^c$, where
$(Ƒ_1, Ě) = \left\{\left(ě, \left(§, AbT_{Ƒ_1(ě)}(§), RělT_{Ƒ_1(ě)}(§), H_{Ƒ_1(ě)}(§), RělF_{Ƒ_1(ě)}(§), AbF_{Ƒ_1(ě)}(§)\right) : § \in Ú\right) : ě \in Ě\right\}$
$(Ƒ_2, Ě) = \left\{\left(ě, \left(§, AbT_{Ƒ_2(ě)}(§), RělT_{Ƒ_2(ě)}(§), H_{Ƒ_2(ě)}(§), RělF_{Ƒ_2(ě)}(§), AbF_{Ƒ_2(ě)}(§)\right) : § \in Ú\right) : ě \in Ě\right\}$
$(Ƒ_2, Ě)^c = \left\{\left(ě, \left(§, AbƑ_{Ƒ_2(ě)}(§), RělƑ_{Ƒ_2(ě)}(§), 1 - H_{Ƒ_2(ě)}(§), RělT_{Ƒ_2(ě)}(§), AbT_{Ƒ_2(ě)}(§)\right) : § \in Ú\right) : ě \in Ě\right\}$, so
$$(Ƒ_3, Ě) = \left\{\left(ě, \left(§, AbT_{Ƒ_3(ě)}(§), RělT_{Ƒ_3(ě)}(§), H_{Ƒ_3(ě)}(§), RělF_{Ƒ_3(ě)}(§), AbF_{Ƒ_3(ě)}(§)\right) : § \in Ú\right) : ě \in Ě\right\},$$
with, $AbT_{Ƒ_3(ě)}(§) = \min\left\{AbT_{Ƒ_1(ě)}(§), AbƑ_{Ƒ_2(ě)}(§)\right\}$, $RělT_{Ƒ_3(ě)}(§) = \min\left\{RělT_{Ƒ_1(ě)}(§), RělƑ_{Ƒ_2(ě)}(§)\right\}$,
$H_{Ƒ_3(ě)}(§) = \min\left\{H_{Ƒ_1(ě)}(§), 1 - H_{Ƒ_2(ě)}(§)\right\}$, $RělF(§) = \max\left\{RělF_{Ƒ_1(ě)}(§), RělT_{Ƒ_2(ě)}(§)\right\}$,
$AbƑ_{Ƒ_3(ě)}(§) = \max\left\{AF_{Ƒ_1(ě)}(§), AbF_{Ƒ_2(ě)}(§)\right\}$.

Definition 3.20. Let $\left\{(Ƒ_i, Ě) \middle| i \in I\right\}$ be a collection of TVNSSs . Then

$$\cup_{i\in I}(\mathfrak{f}_i, \check{E}) = \left\{\left(\check{e}, \begin{pmatrix} \S, \mathrm{sp}\left[AbT_{\mathfrak{f}_i(\check{e})}(\S)\right]_{i\in I}, \mathrm{sp}\left[R\check{e}lT_{\mathfrak{f}_i(\check{e})}(\S)\right]_{i\in I}, \mathrm{sp}\left[H_{\mathfrak{f}_i(\check{e})}(\S)\right]_{i\in I}, \\ \mathrm{if}\left[R\check{e}l\mathfrak{f}_{\mathfrak{f}_i(\check{e})}(\S)\right]_{i\in I}, \mathrm{if}\left[Ab\mathfrak{f}_{\mathfrak{f}_i(\check{e})}(\S)\right]_{i\in I} \end{pmatrix} : \check{e} \in \check{E}\right) : \S \in \acute{U}\right\},$$

$$\cap_{i\in I}(\mathfrak{f}_i, \check{E}) = \left\{\left(\check{e}, \begin{pmatrix} \S, \inf\left[AbT_{\mathfrak{f}_i(\check{e})}(\S)\right]_{i\in I}, \inf\left[R\check{e}lT_{\mathfrak{f}_i(\check{e})}(\S)\right]_{i\in I}, \inf\left[H_{\mathfrak{f}_i(\check{e})}(\S)\right]_{i\in I}, \\ \max\left[R\check{e}l\mathfrak{f}_{\mathfrak{f}_i(\check{e})}(\S)\right]_{i\in I}, \max\left[Ab\mathfrak{f}_{\mathfrak{f}_i(\check{e})}(\S)\right]_{i\in I} \end{pmatrix} : \check{e} \in \check{E}\right) : \S \in \acute{U}\right\}.$$

Definition 3.21. Let $(\mathfrak{f}_1, \check{E})$ and $(\mathfrak{f}_2, \check{E})$ be TVNSS. Then operation AND is symbolized by $(\mathfrak{f}_3, \check{E} \times \check{E}) = (\mathfrak{f}_1, \check{E}) \wedge (\mathfrak{f}_2, \check{E})$ is given as:

$$(\mathfrak{f}_3, \check{E} \times \check{E}) = \left\{\left((\check{e}_1, \ \check{e}_2), \begin{pmatrix} \S, AbT_{\mathfrak{f}_3(\check{e}_1,\check{e}_2)}(\S), R\check{e}lT_{\mathfrak{f}_3(\check{e}_1,\check{e}_2)}(\S), H_{\mathfrak{f}_3(\check{e}_1,\check{e}_2)}(\S), \\ R\check{e}lF_{\mathfrak{f}_3(\check{e}_1,\check{e}_2)}(\S), AbF_{\mathfrak{f}_3(\check{e}_1,\check{e}_2)}(\S) \end{pmatrix} : (\check{e}_1, \check{e}_2) \in \check{E} \times \check{E}\right) : \S \in \acute{U}\right\},$$

where

$AbT_{\mathfrak{f}_3(\check{e}_1,\check{e}_2)}(\S) = \min\{AbT_{\mathfrak{f}_1(\check{e}_1)}(\S), AbT_{\mathfrak{f}_2(\check{e}_2)}(\S)\}$, $R\check{e}lT_{\mathfrak{f}_3(\check{e}_1,\check{e}_2)}(\S) = \min\{R\check{e}lT_{\mathfrak{f}_1(\check{e}_1)}(\S), R\check{e}lT_{\mathfrak{f}_2(\check{e}_2)}(\S)\}$,
$H_{\mathfrak{f}_3(\check{e}_1,\check{e}_2)}(\S) = \min\{H_{\mathfrak{f}_1(\check{e}_1)}(\S), H_{\mathfrak{f}_2(\check{e}_2)}(\S)\}$, $R\check{e}l\mathfrak{f}_{\mathfrak{f}_3(\check{e}_1,\check{e}_2)}(\S) = \max\{R\check{e}l\mathfrak{f}_{\mathfrak{f}_1(\check{e}_1)}(\S), R\check{e}l\mathfrak{f}_{\mathfrak{f}_2(\check{e}_2)}(\S)\}$,
$AbF_{\mathfrak{f}_3(\check{e}_1,\check{e}_2)}(\S) = \max\{AbF_{\mathfrak{f}_1(\check{e}_1)}(\S), AbF_{\mathfrak{f}_2(\check{e}_2)}(\S)\}$.

Definition 3.22. Let $(\mathfrak{f}_1, \check{E})$ and $(\mathfrak{f}_2, \check{E})$ be TVNSSs. Then operation OR is given as
$(\mathfrak{f}_3, \check{E} \times \check{E}) = (\mathfrak{f}_1, \check{E}) \vee (\mathfrak{f}_2, \check{E})$ is given as:

$$(\mathfrak{f}_3, \check{E} \times \check{E}) = \left\{\left((\check{e}_1, \check{e}_2), \begin{pmatrix} \S, AbT_{\mathfrak{f}_3(\check{e}_1,\check{e}_2)}(\S), R\check{e}lT_{\mathfrak{f}_3(\check{e}_1,\check{e}_2)}(\S), H_{\mathfrak{f}_3(\check{e}_1,\check{e}_2)}(\S), \\ R\check{e}lF_{\mathfrak{f}_3(\check{e}_1,\check{e}_2)}(\S), AbF_{\mathfrak{f}_3(\check{e}_1,\check{e}_2)}(\S) \end{pmatrix} : (\check{e}_1, \check{e}_2) \in \check{E} \times \check{E}\right) : \S \in \acute{U}\right\},$$

where $AbT_{\mathfrak{f}_3(\check{e}_1,\check{e}_2)}(\S) = \max\{AbT_{\mathfrak{f}_1(\check{e}_1)}(\S), AbT_{\mathfrak{f}_2(\check{e}_2)}(\S)\}$, $R\check{e}lT_{\mathfrak{f}_3(\check{e}_1,\check{e}_2)}(\S) =$
$\max\{R\check{e}lT_{\mathfrak{f}_1(\check{e}_1)}(\S), R\check{e}lT_{\mathfrak{f}_2(\check{e}_2)}(\S)\}$,
$H_{\mathfrak{f}_3(\check{e}_1,\check{e}_2)}(\S) = \max\{H_{\mathfrak{f}_1(\check{e}_1)}(\S), H_{\mathfrak{f}_2(\check{e}_2)}(\S)\}$,
$R\check{e}l\mathfrak{f}_{\mathfrak{f}_3(\check{e}_1,\check{e}_2)}(\S) = \min\{R\check{e}lF_{\mathfrak{f}_1(\check{e}_1)}(\S), R\check{e}lF_{\mathfrak{f}_2(\check{e}_2)}(\S)\}$,
$Ab\mathfrak{f}_{\mathfrak{f}_3(\check{e}_1,\check{e}_2)}(\S) = \min\{AF_{\mathfrak{f}_1(\check{e}_1)}(\S), AbF_{\mathfrak{f}_2(\check{e}_2)}(\S)\}$.

Definition 3.23. (i). Let $(\mathfrak{f}, \check{E})$ is TVNSS. It is said to be null TVNSS if $AbT_{\mathfrak{f}(\check{e})}(\S) = 0, R\check{e}lT_{\mathfrak{f}(\check{e})}(\S) = 0, H_{\mathfrak{f}(\check{e})}(\S) = 0, R\check{e}lF_{\mathfrak{f}(\check{e})}(\S) = 1, AbF_{\mathfrak{f}(\check{e})}(\S) = 1;\ \forall\ \check{e} \in \check{E}, \S \in \acute{U}$. It is symbolized by $0_{(\acute{U},\check{E})}$.

(ii). Let $(\mathfrak{f}, \check{E})$ is TVNSS. It is said to be absolute TVNSS if
$AbT_{\mathfrak{f}(\check{e})}(\S) = 1, R\check{e}lT_{\mathfrak{f}(\check{e})}(\S) = 1, H_{\mathfrak{f}(\check{e})}(\S) = 1, R\check{e}lF_{\mathfrak{f}(\check{e})}(\S) = 0, AbF_{\mathfrak{f}(\check{e})}(\S) = 0;\ \forall\ \check{e} \in \check{E}, \S \in \acute{U}$.
It is symbolized by $1_{(\acute{U},\check{E})}$, and clearly, $0^c_{(\acute{U},\check{E})} = 1_{(\acute{U},\check{E})}$ and $1^c_{(\acute{U},\check{E})} = 0_{(\acute{U},\check{E})}$.

Example 3.24. Let $\acute{U} = \{\S_1, \S_2, \S_3, \S_4\}$ and $\check{E} = \{\check{e}_1, \check{e}_2\}$, let the TVNSSs $(\mathfrak{f}_1, \check{E})$ and $(\mathfrak{f}_2, \check{E})$ $be\ PNSSs$ over Ú be defined as follows:

$$(\mathfrak{f}_1, \check{E}) = \left\{\begin{matrix} \check{e}_1 = \left\{\begin{matrix} (\S_1, 0.4, 0.7, 0.2, 0.8, 0.4), (\S_2, 0.5, 0.6, 0.3, 0.9, 0.4), \\ (\S_3, 0.4, 0.5, 0.3, 0.8, 0.4), (\S_4, 0.2, 0.5, 0.6, 0.8, 0.3) \end{matrix}\right\} \\ \check{e}_2 = \left\{\begin{matrix} (\S_1, 0.7, 0.8, 0.4, 0.5, 0.3), (\S_2, 0.4, 0.9, 0.2, 0.6, 0.8), \\ (\S_3, 0.6, 0.7, 0.2, 0.8, 0.9), (\S_4, 0.3, 0.4, 0.7, 0.9, 0.4) \end{matrix}\right\} \end{matrix}\right\},$$

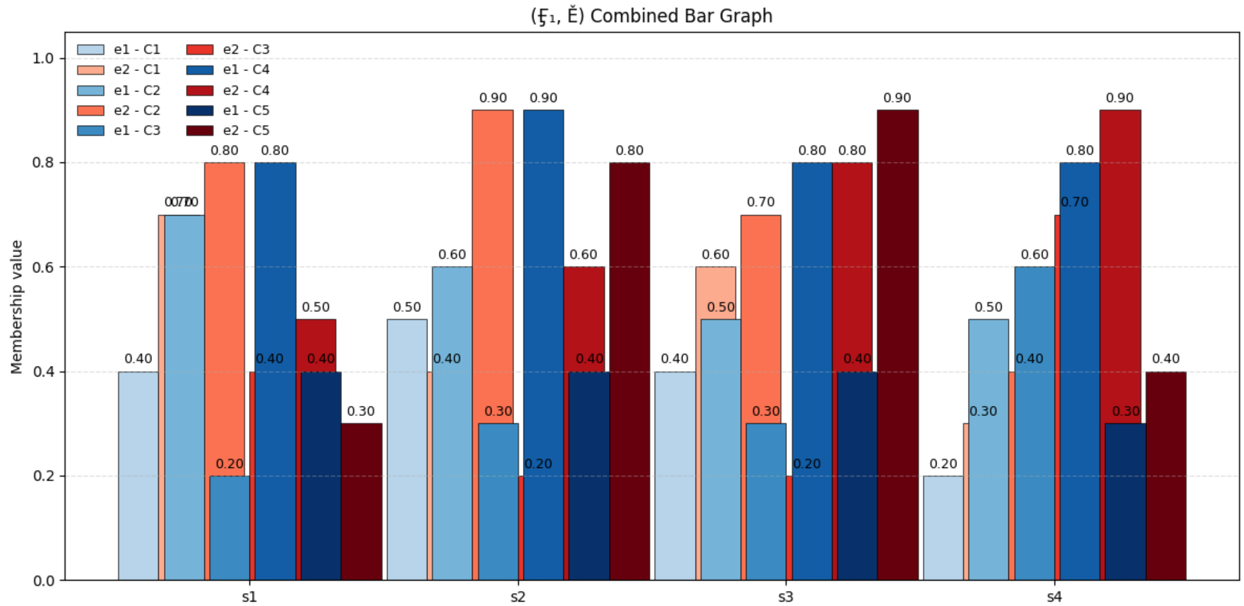

Fig 3.1

$$(\digamma_2, \breve{E}) = \begin{cases} \breve{e}_1 = \begin{Bmatrix} (\text{ş}_1, 0.5, 0.6, 0.9, 0.2, 0.5), (\text{ş}_2, 0.6, 0.8, 0.3, 0.4, 0.5), \\ (\text{ş}_3, 0.7, 0.3, 0.1, 0.2, 0.8), (\text{ş}_4, 0.3, 0.4, 0.9, 0.4, 0.6) \end{Bmatrix} \\ \breve{e}_2 = \begin{Bmatrix} (\text{ş}_1, 0.6, 0.9, 0.3, 0.4, 0.6), (\text{ş}_2, 0.3, 0.6, 0.9, 0.3, 0.8), \\ (\text{ş}_3, 0.4, 0.2, 0.6, 0.8, 0.5), (\text{ş}_4, 0.6, 0.3, 0.7, 0.8, 0.4) \end{Bmatrix} \end{cases},$$

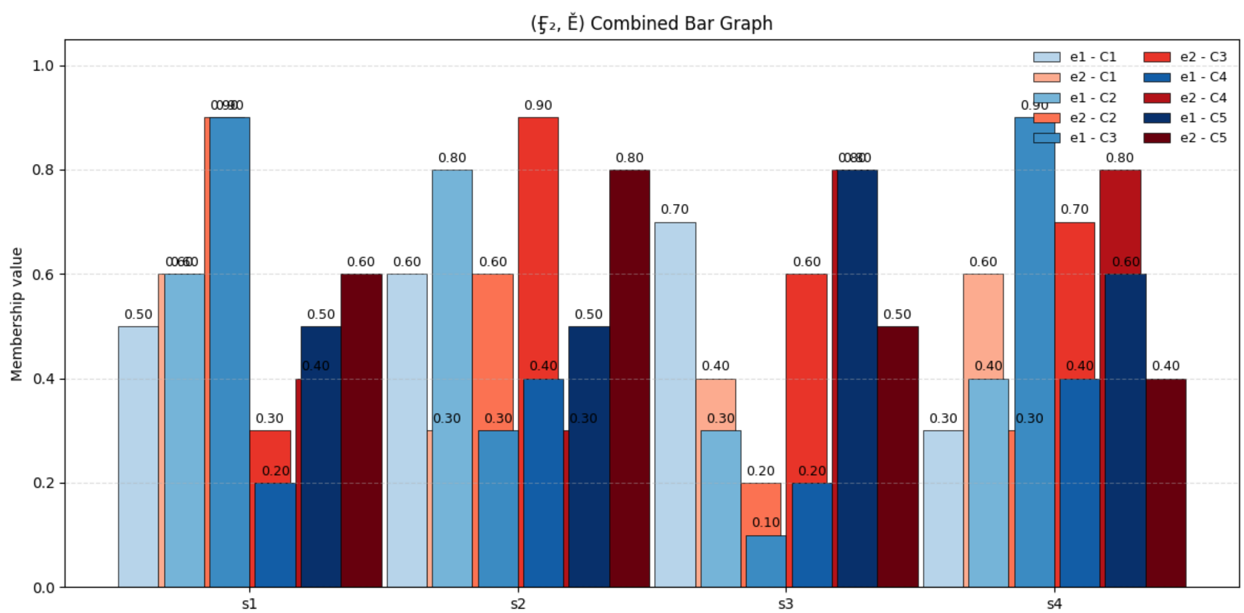

Fig 3.2

$$(\digamma_1, \breve{E}) \cup (\digamma_2, \breve{E}) = \begin{cases} \breve{e}_1 = \begin{Bmatrix} (\text{ş}_1, 0.5, 0.7, 0.9, 0.2, 0.4), (\text{ş}_2, 0.6, 0.8, 0.3, 0.4, 0.4), \\ (\text{ş}_3, 0.7, 0.5, 0.3, 0.2, 0.4), (\text{ş}_4, 0.3, 0.5, 0.9, 0.4, 0.3) \end{Bmatrix} \\ \breve{e}_2 = \begin{Bmatrix} (\text{ş}_1, 0.7, 0.9, 0.4, 0.4, 0.3), (\text{ş}_2, 0.4, 0.9, 0.9, 0.3, 0.8), \\ (\text{ş}_3, 0.6, 0.7, 0.6, 0.8, 0.5), (\text{ş}_4, 0.6, 0.4, 0.7, 0.8, 0.4) \end{Bmatrix} \end{cases},$$

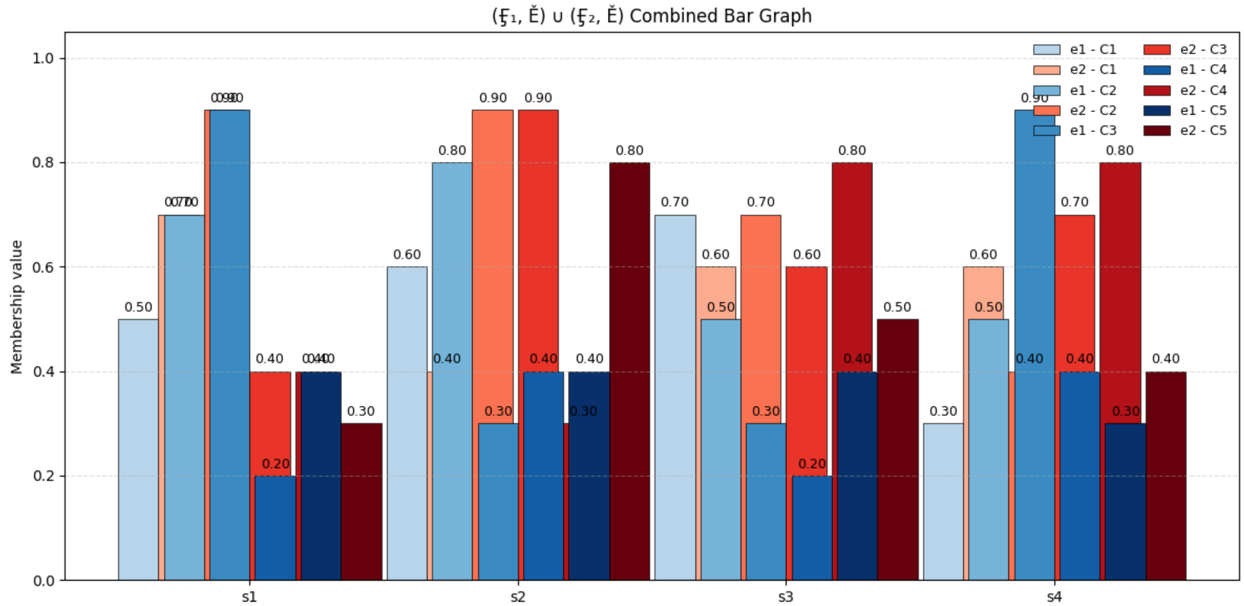

Fig 3.3

$$(\digamma_1, \breve{E}) \cap (\digamma_2, \breve{E}) = \left\{ \begin{array}{l} \breve{e}_1 = \left\{ \begin{array}{l} (\text{ş}_1, 0.4, 0.6, 0.2, 0.8, 0.5), (\text{ş}_2, 0.5, 0.6, 0.3, 0.9, 0.5), \\ (\text{ş}_3, 0.4, 0.3, 0.1, 0.8, 0.8), (\text{ş}_4, 0.2, 0.4, 0.6, 0.8, 0.6) \end{array} \right\} \\ \breve{e}_2 = \left\{ \begin{array}{l} (\text{ş}_1, 0.6, 0.8, 0.3, 0.5, 0.6), (\text{ş}_2, 0.3, 0.6, 0.2, 0.6, 0.8), \\ (\text{ş}_3, 0.4, 0.2, 0.2, 0.8, 0.9), (\text{ş}_4, 0.3, 0.3, 0.7, 0.9, 0.4) \end{array} \right\} \end{array} \right\},$$

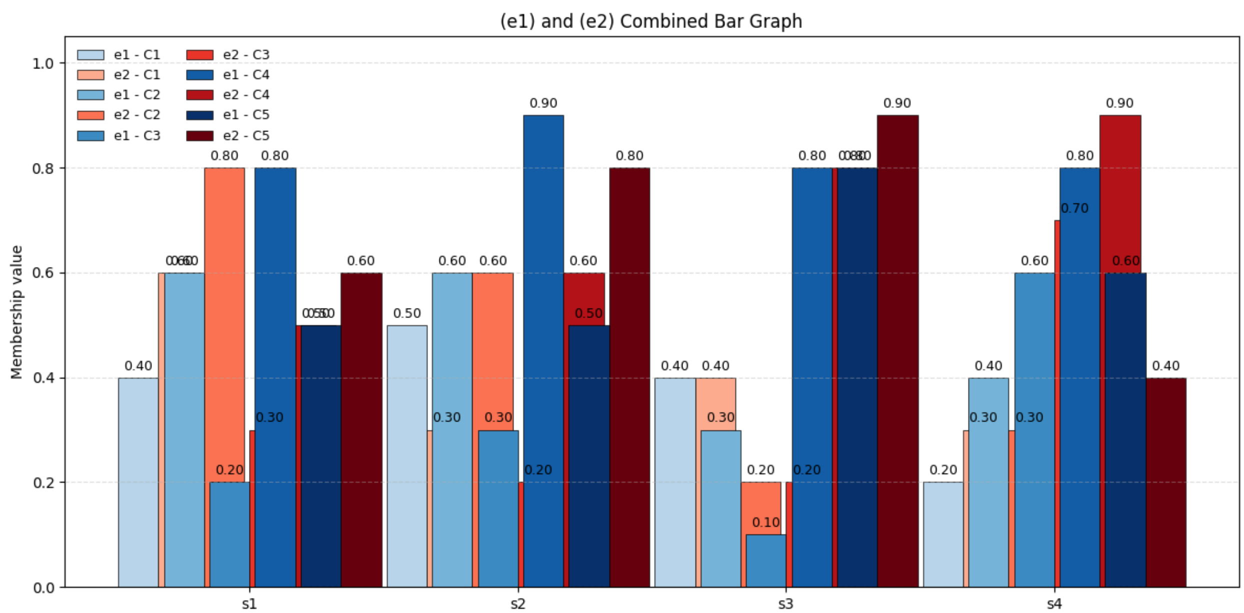

Fig 3.4

$$(\digamma_1, \breve{E})^c = \left\{ \begin{array}{l} \breve{e}_1 = \left\{ \begin{array}{l} (\text{ş}_1, 0.4, 0.8, 0.8, 0.7, 0.4), (\text{ş}_2, 0.4, 0.9, 0.7, 0.6, 0.5), \\ (\text{ş}_3, 0.4, 0.8, 0.7, 0.5, 0.4), (\text{ş}_4, 0.3, 0.8, 0.4, 0.5, 0.2) \end{array} \right\} \\ \breve{e}_2 = \left\{ \begin{array}{l} (\text{ş}_1, 0.3, 0.5, 0.6, 0.8, 0.7), (\text{ş}_2, 0.8, 0.6, 0.8, 0.9, 0.4), \\ (\text{ş}_3, 0.9, 0.8, 0.8, 0.7, 0.6), (\text{ş}_4, 0.4, 0.9, 0.3, 0.4, 0.3) \end{array} \right\} \end{array} \right\},$$

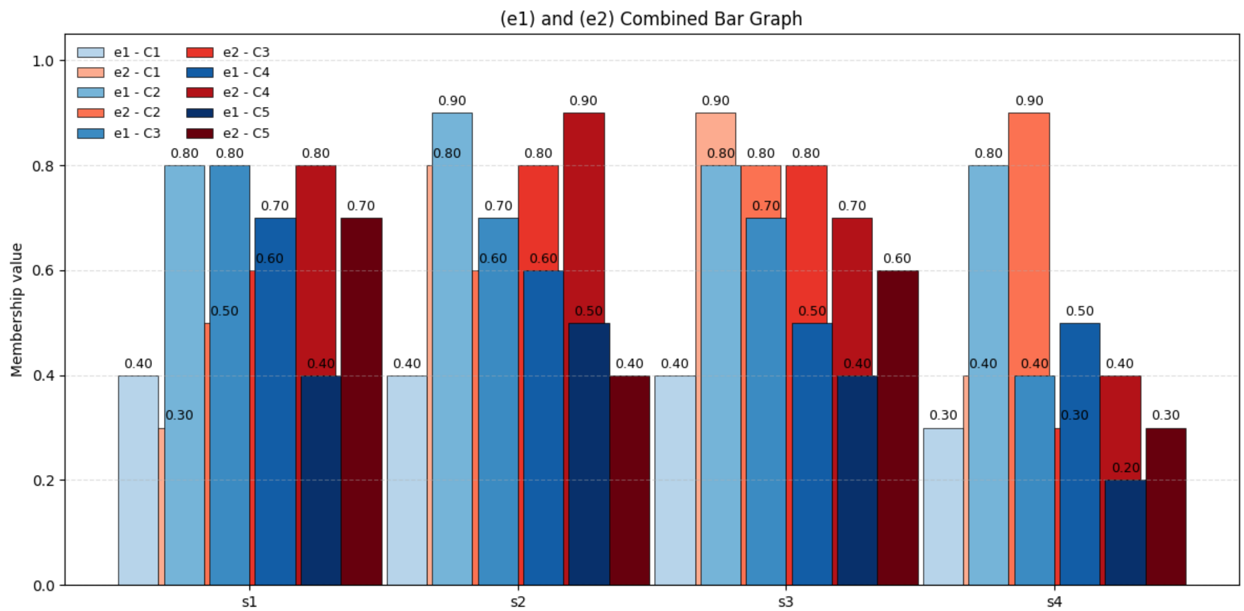

Fig 3.5

$$\left(\digamma_2,\check{E}\right)^c=\begin{cases}\check{e}_1=\begin{Bmatrix}(\S_1,0.5,0.2,0.1,0.6,0.5),(\S_2,0.5,0.4,0.7,0.8,0.6),\\(\S_3,0.8,0.2,0.9,0.3,0.7),(\S_4,0.6,0.4,0.1,0.4,0.3)\end{Bmatrix}\\\check{e}_2=\begin{Bmatrix}(\S_1,0.6,0.4,0.7,0.9,0.6),(\S_2,0.8,0.3,0.1,0.6,0.3),\\(\S_3,0.5,0.8,0.4,0.2,0.4),(\S_4,0.4,0.8,0.3,0.3,0.6)\end{Bmatrix}\end{cases},$$

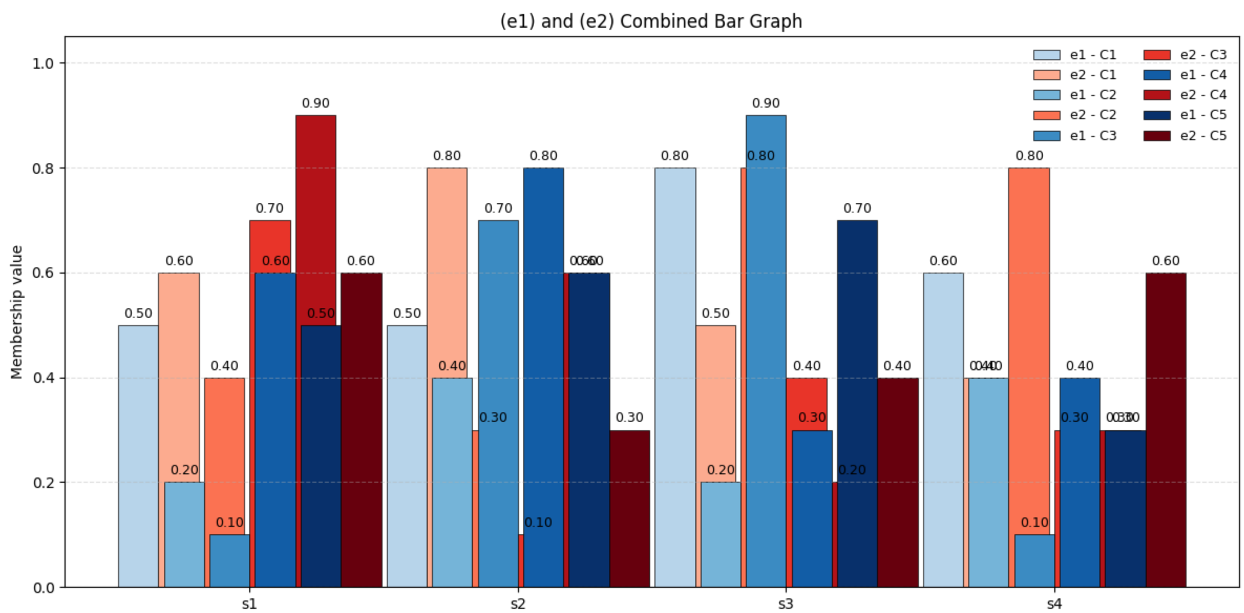

Fig 3.6

$$\left(\digamma_1,\check{E}\right)-\left(\digamma_2,\check{E}\right)=\left(\digamma_1,\check{E}\right)\cap\left(\digamma_2,\check{E}\right)^c$$

$$=\begin{cases}\check{e}_1=\begin{Bmatrix}(\S_1,0.4,0.2,0.1,0.8,0.5),(\S_2,0.5,0.4,0.3,0.9,0.6),\\(\S_3,0.4,0.2,0.3,0.8,0.7),(\S_4,0.2,0.4,0.1,0.8,0.3)\end{Bmatrix}\\\check{e}_2=\begin{Bmatrix}(\S_1,0.6,0.4,0.4,0.9,0.6),(\S_2,0.4,0.3,0.1,0.6,0.8),\\(\S_3,0.5,0.7,0.2,0.8,0.9),(\S_4,0.3,0.4,0.3,0.9,0.6)\end{Bmatrix}\end{cases},$$

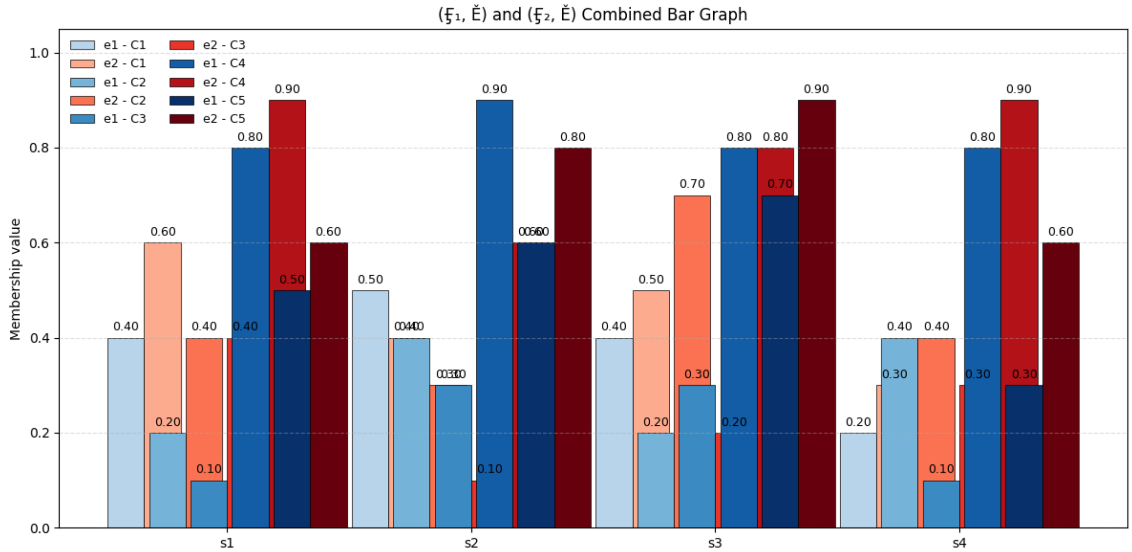

Fig 3.7

$$(ƒ_2, \breve{E}) - (ƒ_1, \breve{E}) = (ƒ_2, \breve{E}) \cap (ƒ_1, \breve{E})^c$$

$$= \left\{ \begin{array}{l} \breve{e}_1 = \left\{ \begin{array}{l} (\S_1, 0.4, 0.6, 0.8, 0.7, 0.5), (\S_2, 0.4, 0.8, 0.3, 0.6, 0.5), \\ (\S_3, 0.4, 0.3, 0.1, 0.5, 0.8), (\S_4, 0.3, 0.4, 0.4, 0.5, 0.6) \end{array} \right\} \\ \breve{e}_2 = \left\{ \begin{array}{l} (\S_1, 0.3, 0.5, 0.3, 0.8, 0.7), (\S_2, 0.3, 0.6, 0.8, 0.9, 0.8), \\ (\S_3, 0.4, 0.2, 0.6, 0.8, 0.6), (\S_4, 0.4, 0.3, 0.3, 0.8, 0.4) \end{array} \right\} \end{array} \right\}.$$

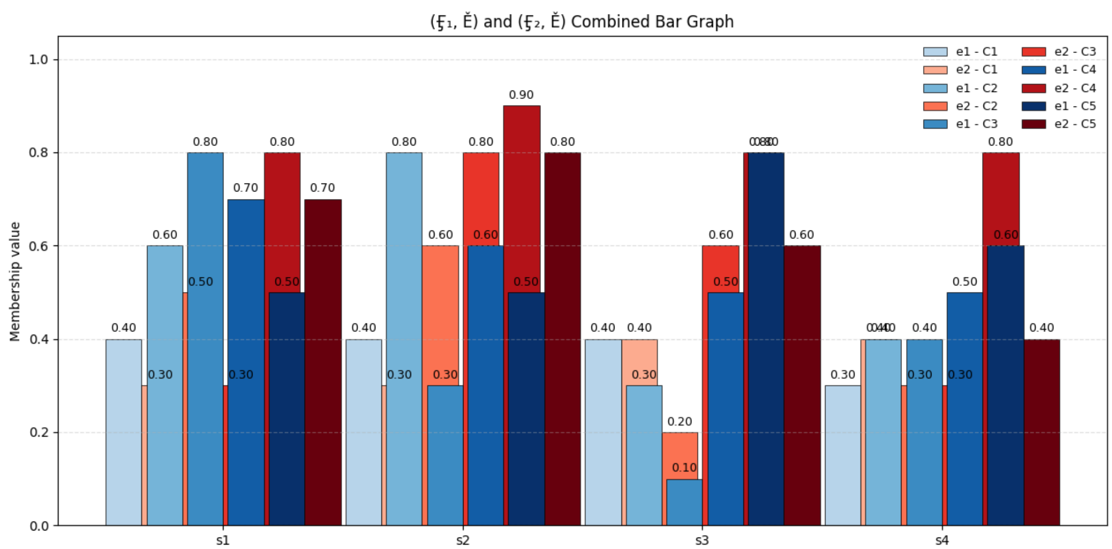

Fig 3.8

$$(ƒ_1, \breve{E}) \vee (ƒ_2, \breve{E}) = \left\{ \begin{array}{l} (\breve{e}_1, \breve{e}_1) = \left\{ \begin{array}{l} (\S_1, 0.5, 0.7, 0.9, 0.2, 0.4), (\S_2, 0.6, 0.8, 0.3, 0.4, 0.4), \\ (\S_3, 0.7, 0.5, 0.3, 0.2, 0.4), (\S_4, 0.3, 0.5, 0.9, 0.4, 0.3) \end{array} \right\} \\ (\breve{e}_1, \breve{e}_2) = \left\{ \begin{array}{l} (\S_1, 0.6, 0.9, 0.3, 0.4, 0.4), (\S_2, 0.5, 0.6, 0.9, 0.3, 0.4), \\ (\S_3, 0.4, 0.5, 0.6, 0.8, 0.4), (\S_4, 0.6, 0.5, 0.7, 0.8, 0.3) \end{array} \right\} \\ (\breve{e}_2, \breve{e}_1) = \left\{ \begin{array}{l} (\S_1, 0.7, 0.8, 0.9, 0.2, 0.3), (\S_2, 0.6, 0.9, 0.3, 0.4, 0.5), \\ (\S_3, 0.7, 0.7, 0.2, 0.2, 0.8), (\S_4, 0.3, 0.4, 0.9, 0.4, 0.4) \end{array} \right\} \\ (\breve{e}_2, \breve{e}_2) = \left\{ \begin{array}{l} (\S_1, 0.7, 0.9, 0.4, 0.4, 0.3), (\S_2, 0.4, 0.9, 0.9, 0.3, 0.8), \\ (\S_3, 0.6, 0.7, 0.6, 0.8, 0.5), (\S_4, 0.6, 0.4, 0.7, 0.8, 0.4) \end{array} \right\} \end{array} \right\},$$

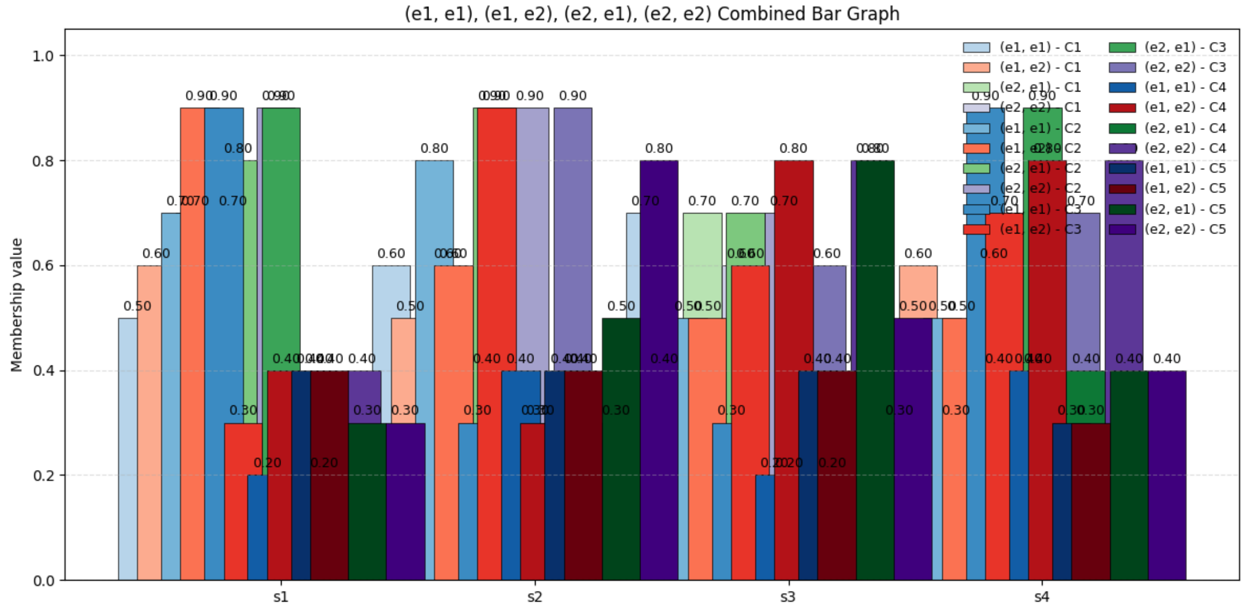

Fig 3.9

$$(\text{ƒ}_1,\breve{E}) \wedge (\text{ƒ}_2,\breve{E}) = \left\{\begin{array}{l} (\breve{e}_1,\breve{e}_1) = \left\{\begin{array}{l}(\S_1, 0.4, 0.6, 0.2, 0.8, 0.5), (\S_2, 0.5, 0.6, 0.3, 0.9, 0.5), \\ (\S_3, 0.4, 0.3, 0.1, 0.8, 0.8), (\S_4, 0.2, 0.4, 0.6, 0.8, 0.6)\end{array}\right\} \\ (\breve{e}_1,\breve{e}_2) = \left\{\begin{array}{l}(\S_1, 0.4, 0.7, 0.2, 0.8, 0.6), (\S_2, 0.3, 0.6, 0.3, 0.9, 0.8), \\ (\S_3, 0.4, 0.2, 0.3, 0.8, 0.5), (\S_4, 0.2, 0.3, 0.6, 0.8, 0.4)\end{array}\right\} \\ (\breve{e}_2,\breve{e}_1) = \left\{\begin{array}{l}(\S_1, 0.5, 0.6, 0.4, 0.5, 0.5), (\S_2, 0.4, 0.8, 0.2, 0.6\ 0.8), \\ (\S_3, 0.6, 0.3, 0.1, 0.8, 0.9), (\S_4, 0.3, 0.4, 0.7, 0.9, 0.6)\end{array}\right\} \\ (\breve{e}_2,\breve{e}_2) = \left\{\begin{array}{l}(\S_1, 0.6, 0.8, 0.3, 0.5, 0.6), (\S_2, 0.3, 0.6, 0.2, 0.6, 0.8), \\ (\S_3, 0.4, 0.2, 0.2, 0.8, 0.9), (\S_4, 0.3, 0.3, 0.7, 0.9, 0.4)\end{array}\right\} \end{array}\right\}.$$

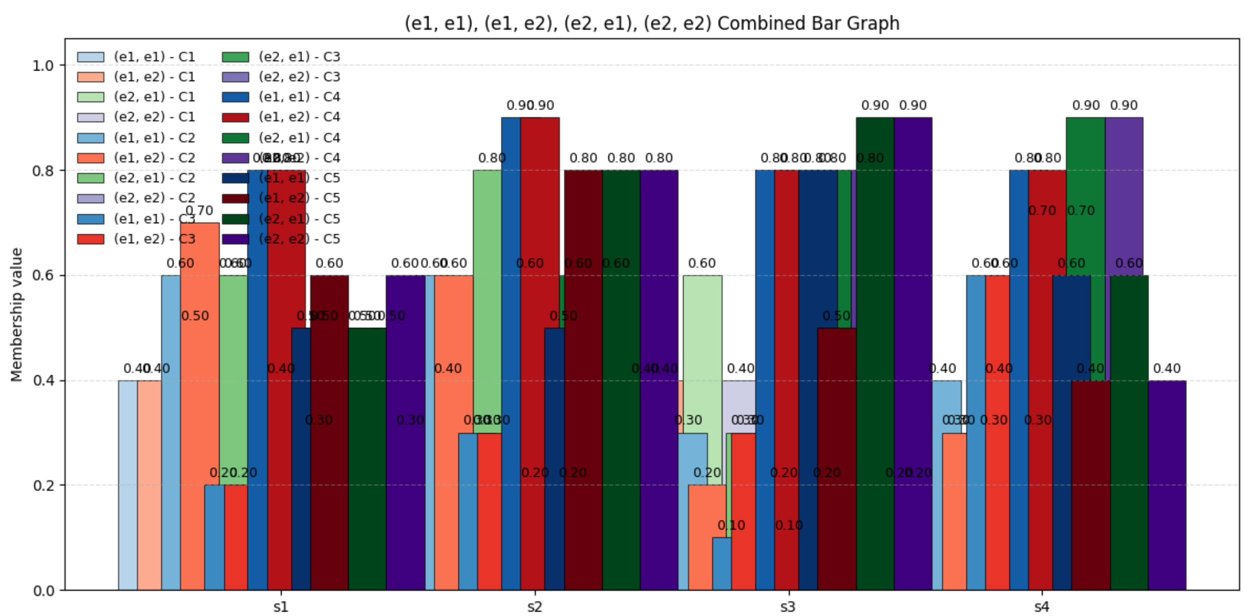

Fig 3.10

4. Tri-Valued Neutrosophic Soft Topological Space

This section is devoted to the family of TVNSSs, PNS closed sets, TVNSS interior, and TVNSS closure along with some basic theorems, propositions and examples.

Definition 4.1. Let TVNSS(Ú, Ě) *be family of all* TVNSS *on* Ú *and* $\tau^{\mathrm{TVNSS}} \subseteq$ TVNSS(Ú, Ě) *thěn* τ^{TVNSS} is *said to bě* TVNST *on* Ú, if

1. $0_{(\acute{U},\breve{E})}$ and $1_{(\acute{U},\breve{E})}$ belong to τ^{TVNSS},
2. The union of any number of PNSS in τ^{TVNSS} belong to τ^{TVNSS},
3. The intersection of finite number of PNSS in τ^{TVNSS} belong to τ^{TVNSS}.

Then (Ú, τ^{TVNSS}, Ě) *is said to bě* TVNSTS *on* Ú, each member of τ^{TVNSS} is TVNSS open set.

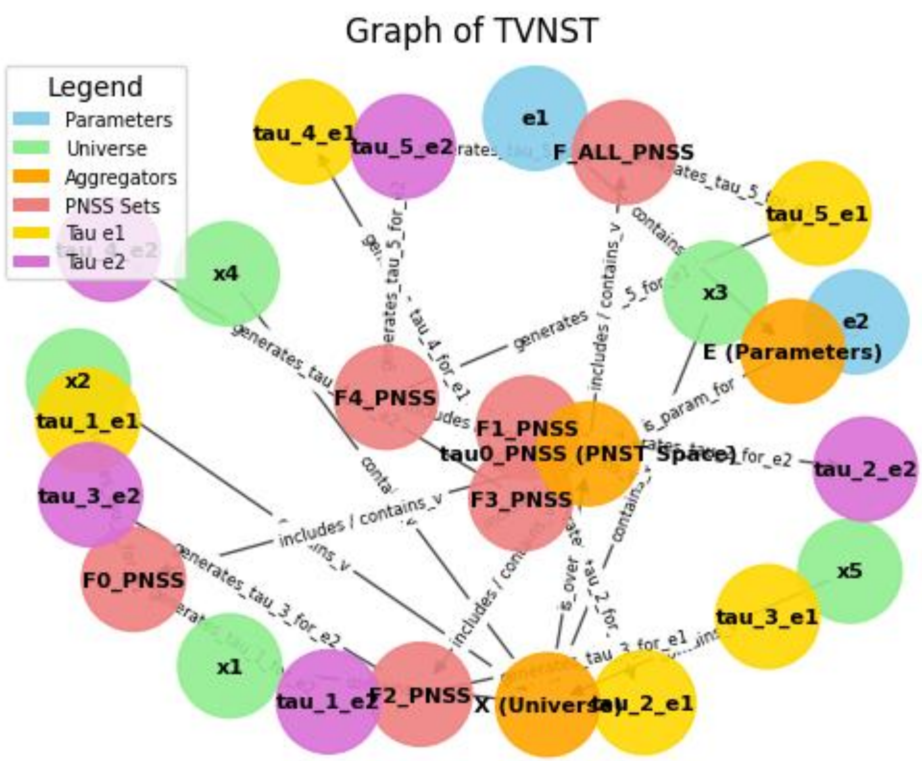

Fig 4.1

Definition 4.2. Assume that (Ú, τ^{TVNSS}, Ě) be PNST space over Ú and (Ƒ, Ě) be TVNSS over Ú, then (Ƒ, Ě) is said to be TVNS closed sets iff its complement is a TVNS open set.

Proposition 4.3. Let (Ú, τ_1^{TVNSS}, Ě) and (Ú, τ_2^{TVNSS}, Ě) be two TVNSTS spaces over Ú, then (Ú, $\tau_1^{\mathrm{TVNSS}} \cap \tau_2^{\mathrm{TVNSS}}$, Ě) is TVNSTS over Ú.

Proof. 1. Since $0_{(\acute{U},\check{E})}, 1_{(\acute{U},\check{E})} \in \tau_1^{\mathrm{TVNSS}}$ and $0_{(\acute{U},\check{E})}, 1_{(\acute{U},\check{E})} \in \tau_2^{\mathrm{TVNSS}}$ then $0_{(\acute{U},\check{E})}, 1_{(\acute{U},\check{E})} \in \tau_1^{\mathrm{TVNSS}} \cap \tau_2^{\mathrm{TVNSS}}$.

1. If $\{(ʄ_i, \breve{E}) : i \in I)\}$ *bĕ a family of* TVNSS *in* $\tau_1^{PNSS} \cap \tau_2^{\text{TVNSS}}$, *thĕn* $(ʄ_i, \breve{E}) \in \tau_1^{\text{TVNSS}}$ and $(ʄ_i, \breve{E}) \in \tau_2^{\text{TVNSS}}\ \forall\, i \in I$. So, $\cup_{i \in I}(ʄ_i, \breve{E}) \in \tau_1^{\text{TVNSS}}$ *and* $\cup_{i \in I}(ʄ_i, \breve{E}) \in \tau_2^{\text{TVNSS}}$. Thus $\cup_{i \in I}(ʄ_i, \breve{E}) \in \tau_1^{\text{TVNSS}} \cap \tau_2^{\text{TVNSS}}$.
2. *Lĕt* $\{(ʄ_i, \breve{E}) : i = 1,2,3 \dots n)\}$ *bĕ a family of thĕ finitĕ numbĕr of* TVNSS *in* $\tau_1^{\text{TVNSS}} \cap \tau_2^{PNSS}$, *thĕn* $(ʄ_i, \breve{E}) \in \tau_1^{\text{TVNSS}}$ *and* $(ʄ_i, \breve{E}) \in \tau_2^{PNSS}$, $\forall\, i \in 1,2,3 \dots n$, so $\cap_{i \in I}^{n}(ʄ_i, \breve{E}) \in \tau_1^{PNSS}$ and $\cap_{i \in I}^{n}(ʄ_i, \breve{E}) \in \tau_2^{\text{TVNSS}}$.
   Thus, $\cap_{i \in I}^{n}(ʄ_i, \breve{E}) \in \tau_1^{\text{TVNSS}} \cap \tau_2^{\text{TVNSS}}$.

Remark 4.4. The union of two TVNSTS over Ú may or may not always be TVNSTS on Ú.

Example 4.5. Assume that set $\acute{U} = \{§_1, §_2, §_3, §_4\}$ and $\breve{E} = [\breve{e}_1, \breve{e}_2\}$.
$\mathfrak{I}_1^{\text{TVNSS}} = \{0_{(\acute{U},\breve{E})}, 1_{(\acute{U},\breve{E})}, (ʄ_1, \breve{E}), (ʄ_2, \breve{E}), (ʄ_3, \breve{E})\}$ and $\mathfrak{I}_2^{\text{TVNSS}} = \{0_{(\acute{U},\breve{E})}, 1_{(\acute{U},\breve{E})}, (ʄ_2, \breve{E}), (ʄ_4, \breve{E})\}$ be TVNSSTS over Ú, here $(ʄ_1, \breve{E}), (ʄ_2, \breve{E}), (ʄ_3, \breve{E})$ and $(ʄ_4, \breve{E})$ are defined:

$$(ʄ_1, \breve{E}) = \left\{ \begin{array}{l} \breve{e}_1 = \left\{ \begin{array}{l} (§_1, 0.7, 0.8, 0.6, 0.4, 0.3), (§_2, 0.8, 0.7, 0.9, 0.5, 0.4), \\ (§_3, 0.6, 0.8, 0.9, 0.7, 0.4), (§_4, 0.9, 0.7, 0.6, 0.5, 0.4) \end{array} \right\} \\ \breve{e}_2 = \left\{ \begin{array}{l} (§_1, 0.8, 0.9, 0.8, 0.6, 0.4), (§_2, 0.9, 0.7, 0.6, 0.5, 0.6), \\ (§_3, 0.8, 0.9, 0.5, 0.4, 0.5), (§_4, 0.8, 0.5, 0.5, 0.4, 0.6) \end{array} \right\} \end{array} \right\},$$

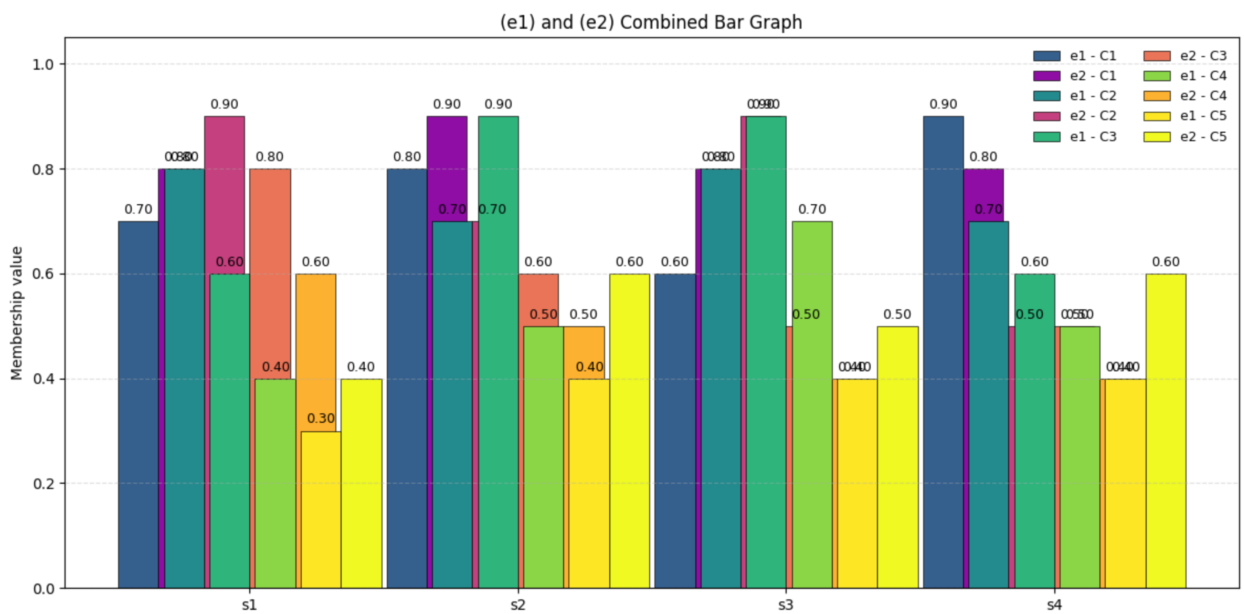

Fig 4.2

$$(ʄ_2, \breve{E}) = \left\{ \begin{array}{l} \breve{e}_1 = \left\{ \begin{array}{l} (§_1, 0.5, 0.6, 0.4, 0.4, 0.8), (§_2, 0.6, 0.7, 0.6, 0.8, 0.8), \\ (§_3, 0.6, 0.7, 0.9, 0.8, 0.6), (§_4, 0.8, 0.7, 0.6, 0.6, 0.8) \end{array} \right\} \\ \breve{e}_2 = \left\{ \begin{array}{l} (§_1, 0.7, 0.7, 0.6, 0.8, 0.4), (§_2, 0.8, 0.6, 0.5, 0.8, 0.6), \\ (§_3, 0.6, 0.8, 0.4, 0.4, 0.8), (§_4, 0.7, 0.5, 0.4, 0.6, 0.8) \end{array} \right\} \end{array} \right\},$$

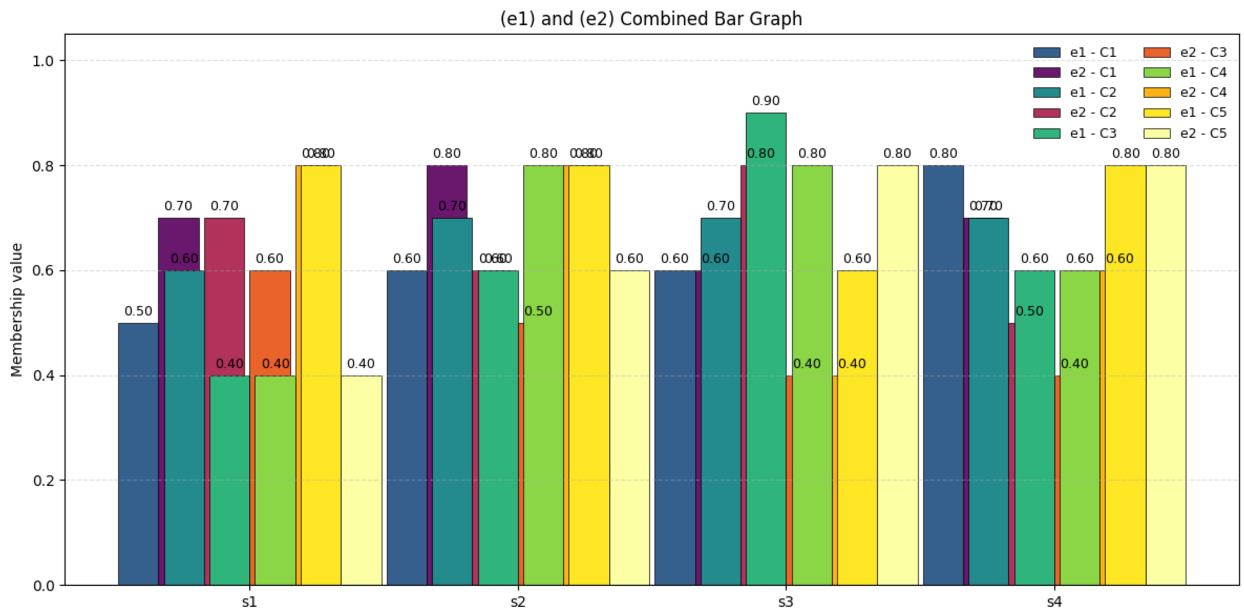

Fig 4.3

$$(\text{Ƒ}_3,\breve{E})=\begin{cases}\breve{e}_1=\begin{Bmatrix}(\text{ş}_1,0.4,0.5,0.4,0.5,0.8),(\text{ş}_2,0.5,0.6,0.5,0.9,0.8),\\(\text{ş}_3,0.5,0.6,0.5,0.8,0.7),(\text{ş}_4,0.7,0.5,0.4,0.8,0.9)\end{Bmatrix}\\ \breve{e}_2=\begin{Bmatrix}(\text{ş}_1,0.6,0.7,0.5,0.8,0.6),(\text{ş}_2,0.7,0.5,0.4,0.8,0.7),\\(\text{ş}_3,0.6,0.7,0.4,0.5,0.8),(\text{ş}_4,0.5,0.4,0.3,0.7,0.8)\end{Bmatrix}\end{cases},$$

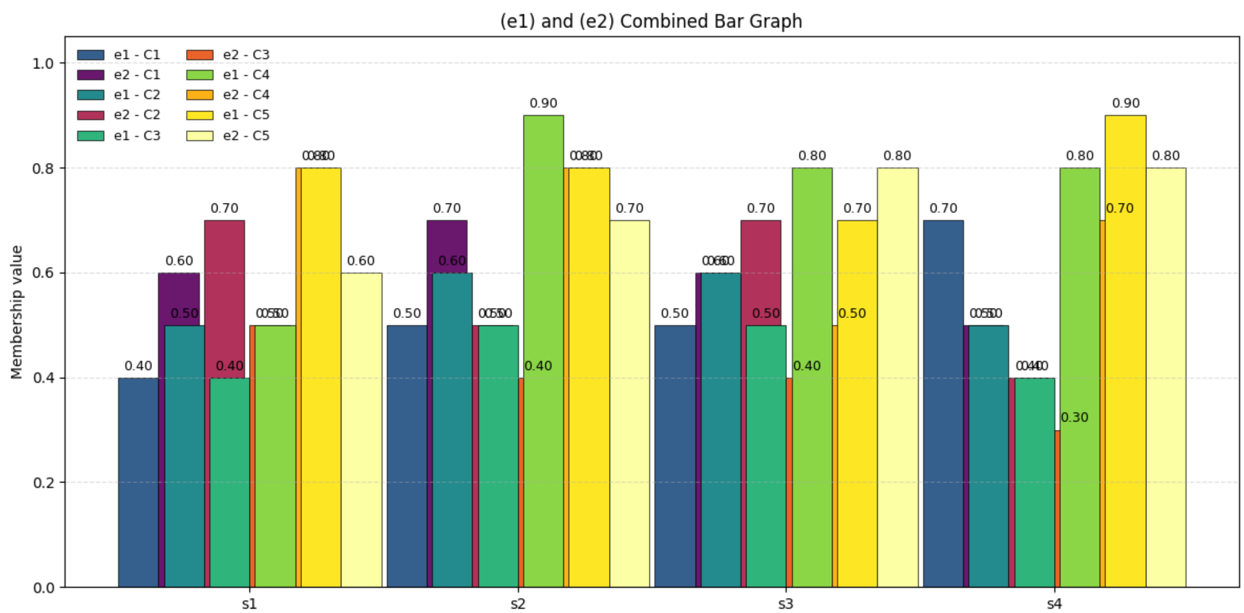

Fig 4.4

$$(\text{Ƒ}_4,\breve{E})=\begin{cases}\breve{e}_1=\begin{Bmatrix}(\text{ş}_1,0.4,0.3,0.2,0.8,0.9),(\text{ş}_2,0.4,0.5,0.3,0.9,0.9),\\(\text{ş}_3,0.3,0.1,0.4,0.9,0.8),(\text{ş}_4,0.5,0.3,0.2,0.8,0.9)\end{Bmatrix}\\ \breve{e}_2=\begin{Bmatrix}(\text{ş}_1,0.5,0.6,0.4,0.9,0.8),(\text{ş}_2,0.5,0.3,0.2,0.9,0.8),\\(\text{ş}_3,0.4,0.5,0.2,0.8,0.9),(\text{ş}_4,0.4,0.2,0.1,0.7,0.9)\end{Bmatrix}\end{cases},$$

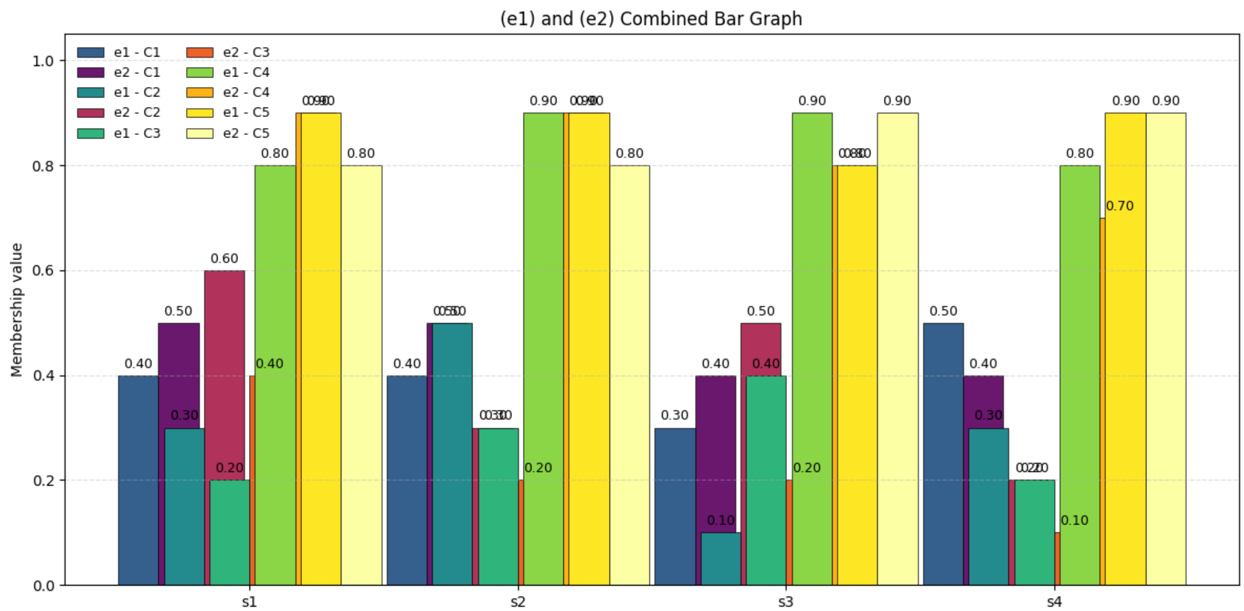

Fig 4.5

$$(\text{ƒ}_1,\breve{E})\cup(\text{ƒ}_2,\breve{E})=\left\{\begin{array}{l}\breve{e}_1\ =\left\{\begin{array}{l}(\text{ş}_1,0.7,0.8,0.6,0.4,0.3),(\text{ş}_2,0.8,0.7,0.9,0.5,0.4),\\(\text{ş}_3,0.6,0.8,0.9,0.7,0.4),(\text{ş}_4,0.9,0.7,0.6,0.5,0.4)\end{array}\right\}\\ \breve{e}_2\ =\left\{\begin{array}{l}(\text{ş}_1,0.8,0.9,0.8,0.6,0.4),(\text{ş}_2,0.9,0.7,0.6,0.5,0.6),\\(\text{ş}_3,0.8,0.9,0.5,0.4,0.5),(\text{ş}_4,0.8,0.5,0.5,0.4,0.6)\end{array}\right\}\end{array}\right\}=(\text{ƒ}_1,\breve{E})\in\Im_1,$$

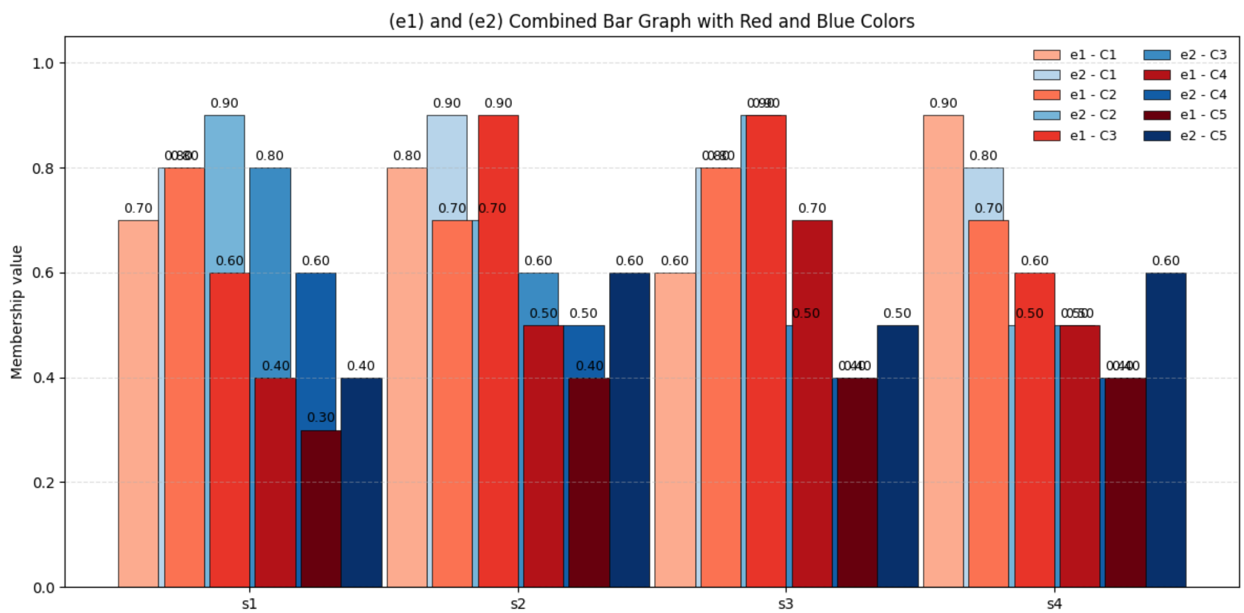

Fig 4.6

$$(\text{ƒ}_1,\breve{E})\cup(\text{ƒ}_3,\breve{E})=\left\{\begin{array}{l}\breve{e}_1\ =\left\{\begin{array}{l}(\text{ş}_1,0.7,0.8,0.6,0.4,0.3),(\text{ş}_2,0.8,0.7,0.9,0.5,0.4),\\(\text{ş}_3,0.6,0.8,0.9,0.7,0.4),(\text{ş}_4,0.9,0.7,0.6,0.5,0.4)\end{array}\right\}\\ \breve{e}_2\ =\left\{\begin{array}{l}(\text{ş}_1,0.8,0.9,0.8,0.6,0.4),(\text{ş}_2,0.9,0.7,0.6,0.5,0.6),\\(\text{ş}_3,0.8,0.9,0.5,0.4,0.5),(\text{ş}_4,0.8,0.5,0.5,0.4,0.6)\end{array}\right\}\end{array}\right\}=(\text{ƒ}_1,\breve{E})\in\Im_1,$$

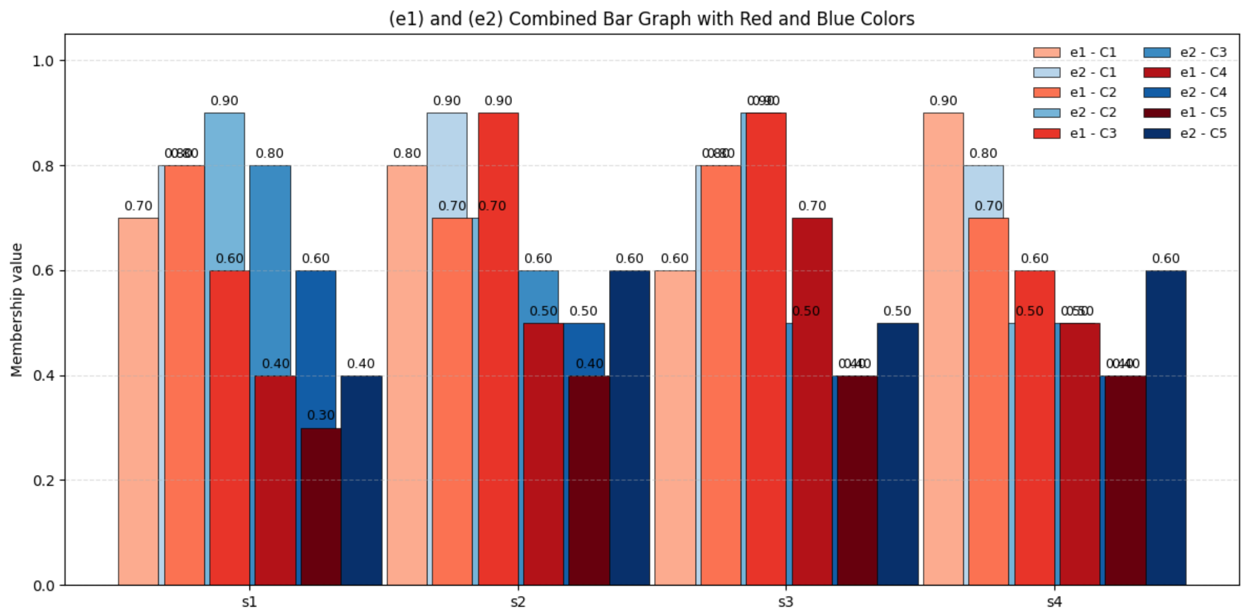

Fig 4.7

$$(\text{ʄ}_2,\check{E}) \cup (\text{ʄ}_3,\check{E}) = \left\{ \begin{array}{l} \check{e}_1 = \left\{ \begin{array}{l} (\text{ş}_1, 0.5, 0.6, 0.4, 0.4, 0.8), (\text{ş}_2, 0.6, 0.7, 0.6, 0.8, 0.8), \\ (\text{ş}_3, 0.6, 0.7, 0.9, 0.8, 0.6), (\text{ş}_4, 0.8, 0.7, 0.6, 0.6, 0.8) \end{array} \right\} \\ \check{e}_2 = \left\{ \begin{array}{l} (\text{ş}_1, 0.7, 0.7, 0.6, 0.8, 0.4), (\text{ş}_2, 0.8, 0.6, 0.5, 0.8, 0.6), \\ (\text{ş}_3, 0.6, 0.8, 0.4, 0.4, 0.8), (\text{ş}_4, 0.7, 0.5, 0.4, 0.6, 0.8) \end{array} \right\} \end{array} \right\} = (\text{ʄ}_2,\check{E}) \in \Im_1,$$

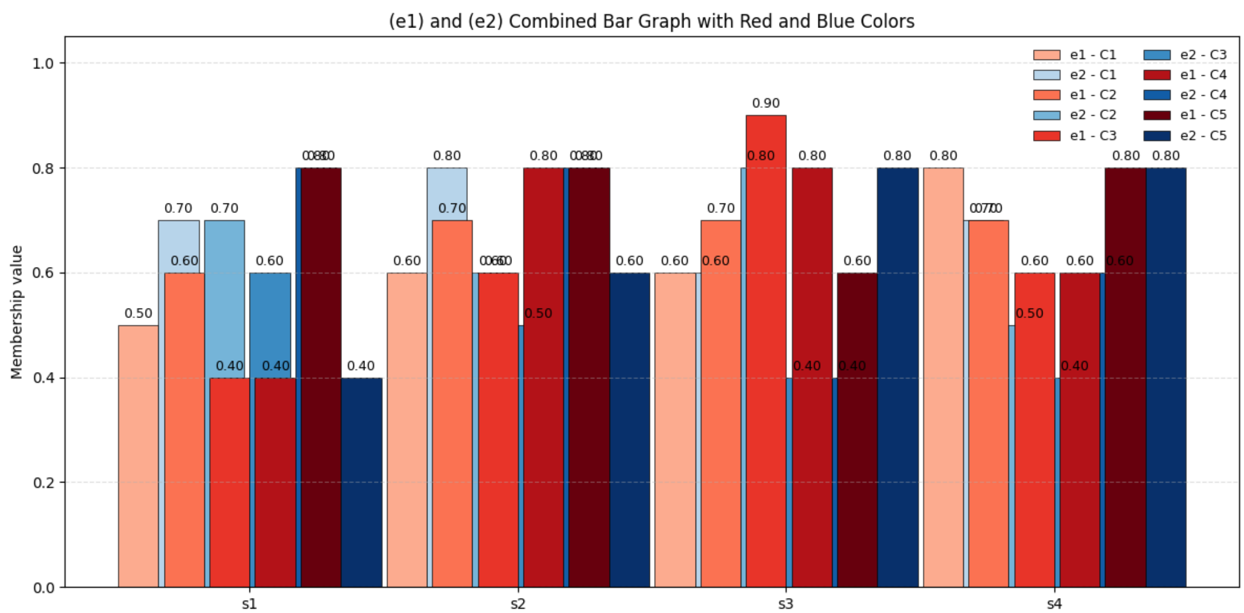

Fig 4.8

$$(\text{ʄ}_2,\check{E}) \cup (\text{ʄ}_4,\check{E}) = \left\{ \begin{array}{l} \check{e}_1 = \left\{ \begin{array}{l} (\text{ş}_1, 0.5, 0.6, 0.4, 0.4, 0.8), (\text{ş}_2, 0.6, 0.7, 0.6, 0.8, 0.8), \\ (\text{ş}_3, 0.6, 0.7, 0.9, 0.8, 0.6), (\text{ş}_4, 0.8, 0.7, 0.6, 0.6, 0.8) \end{array} \right\} \\ \check{e}_2 = \left\{ \begin{array}{l} (\text{ş}_1, 0.7, 0.7, 0.6, 0.8, 0.4), (\text{ş}_2, 0.8, 0.6, 0.5, 0.8, 0.6), \\ (\text{ş}_3, 0.6, 0.8, 0.4, 0.4, 0.8), (\text{ş}_4, 0.7, 0.5, 0.4, 0.6, 0.8) \end{array} \right\} \end{array} \right\} = (\text{ʄ}_2,\check{E}) \in \Im_2,$$

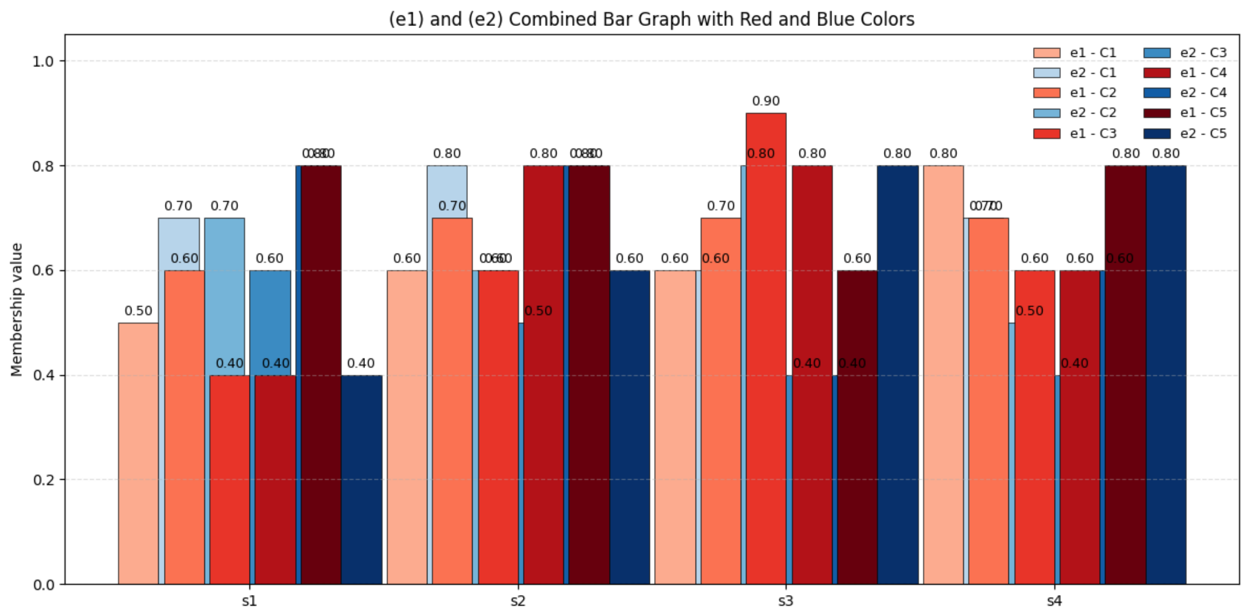

Fig 4.9

$$\left(\text{Ƒ}_1,\check{E}\right)\cap\left(\text{Ƒ}_2,\check{E}\right)=\left\{\begin{array}{l}\check{e}_1=\left\{\begin{array}{l}(\S_1,0.5,0.6,0.4,0.4,0.8),(\S_2,0.6,0.7,0.6,0.8,0.8),\\(\S_3,0.6,0.7,0.9,0.8,0.6),(\S_4,0.8,0.7,0.6,0.6,0.8)\end{array}\right\}\\\check{e}_2=\left\{\begin{array}{l}(\S_1,0.7,0.7,0.6,0.8,0.4),(\S_2,0.8,0.6,0.5,0.8,0.6),\\(\S_3,0.6,0.8,0.4,0.4,0.8),(\S_4,0.7,0.5,0.4,0.6,0.8)\end{array}\right\}\end{array}\right\}=\left(\text{Ƒ}_2,\check{E}\right)\in\mathfrak{I}_1,$$

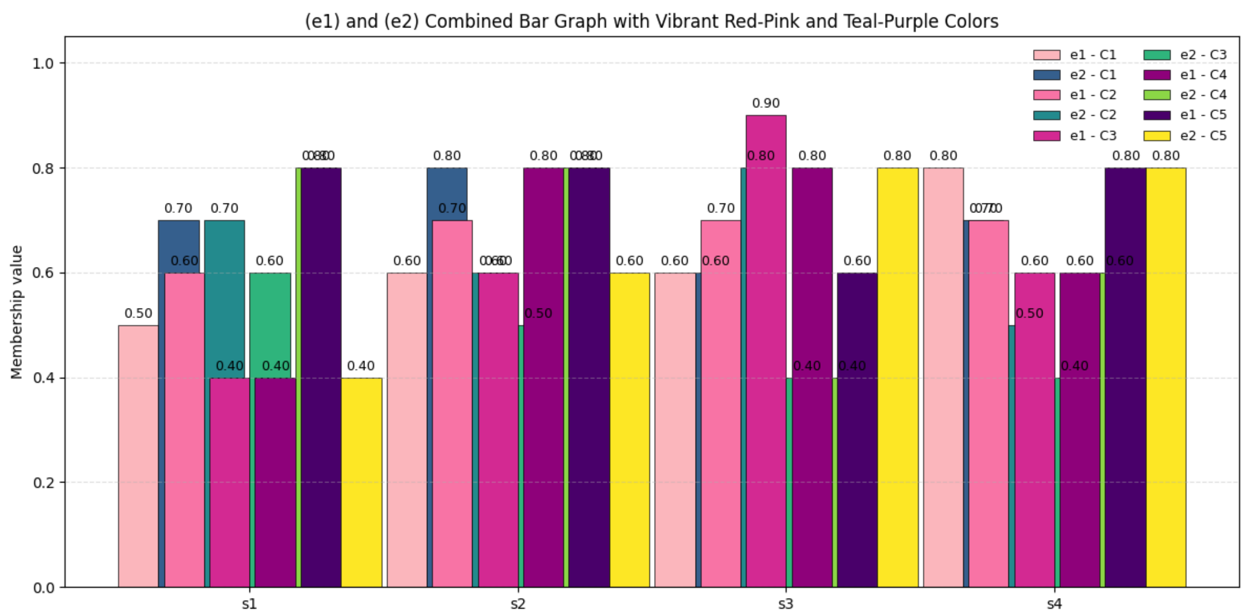

Fig 4.10

$$\left(\text{Ƒ}_1,\check{E}\right)\cap\left(\text{Ƒ}_3,\check{E}\right)=\left\{\begin{array}{l}\check{e}_1=\left\{\begin{array}{l}(\S_1,0.4,0.5,0.4,0.5,0.8),(\S_2,0.5,0.6,0.5,0.9,0.8),\\(\S_3,0.5,0.6,0.5,0.8,0.7),(\S_4,0.7,0.5,0.4,0.8,0.9)\end{array}\right\}\\\check{e}_2=\left\{\begin{array}{l}(\S_1,0.6,0.7,0.5,0.8,0.6),(\S_2,0.7,0.5,0.4,0.8,0.7),\\(\S_3,0.6,0.7,0.4,0.5,0.8),(\S_4,0.5,0.4,0.3,0.7,0.8)\end{array}\right\}\end{array}\right\}=\left(\text{Ƒ}_3,\check{E}\right)\in\mathfrak{I}_1,$$

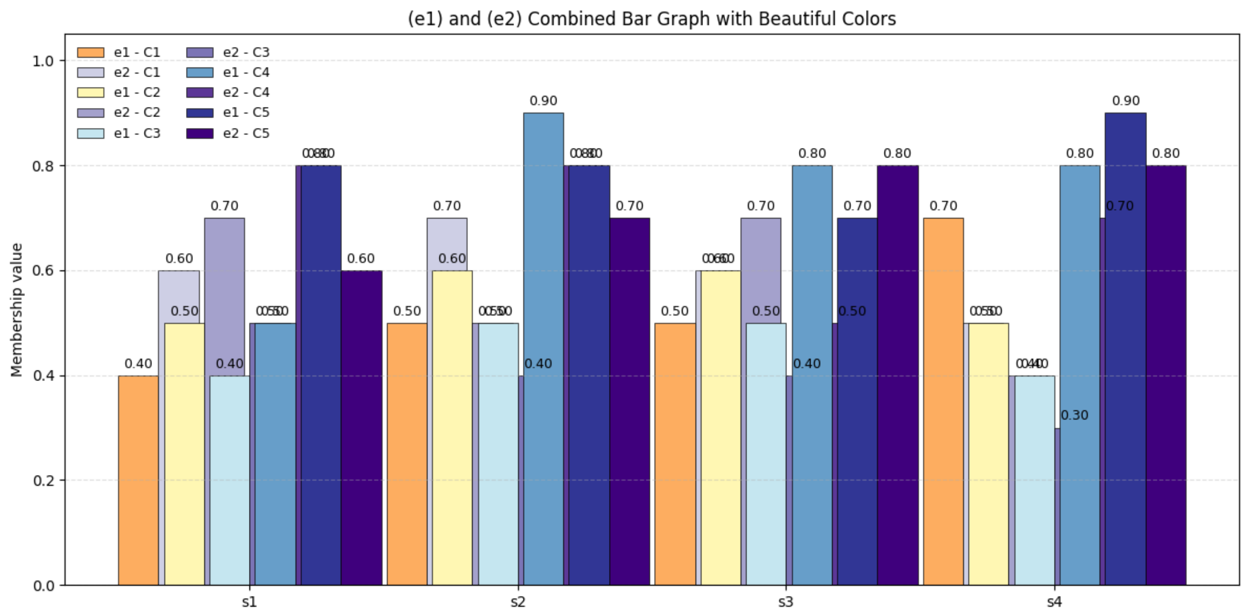

Fig 4.11

$$(\digamma_2,\breve{E})\cap(\digamma_3,\breve{E})=\left\{\begin{array}{l}\breve{e}_1=\left\{\begin{array}{l}(\varsigma_1,0.5,0.6,0.4,0.4,0.8),(\varsigma_2,0.6,0.7,0.6,0.8,0.8),\\(\varsigma_3,0.6,0.7,0.9,0.8,0.6),(\varsigma_4,0.8,0.7,0.6,0.6,0.8)\end{array}\right\}\\ \breve{e}_2=\left\{\begin{array}{l}(\varsigma_1,0.7,0.7,0.6,0.8,0.4),(\varsigma_2,0.8,0.6,0.5,0.8,0.6),\\(\varsigma_3,0.6,0.8,0.4,0.4,0.8),(\varsigma_4,0.7,0.5,0.4,0.6,0.8)\end{array}\right\}\end{array}\right\}=(\digamma_3,\breve{E})\in\mathfrak{I}_1,$$

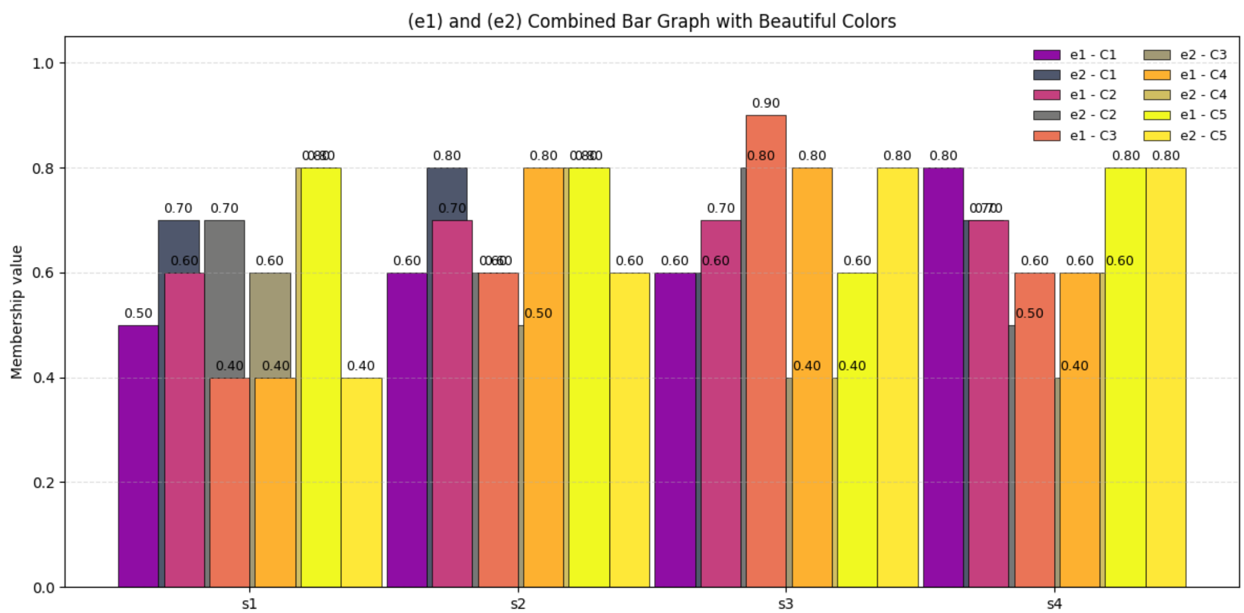

Fig 4.12

$$(\digamma_2,\breve{E})\cap(\digamma_4,\breve{E})=\left\{\begin{array}{l}\breve{e}_1=\left\{\begin{array}{l}(\varsigma_1,0.4,0.3,0.2,0.8,0.9),(\varsigma_2,0.4,0.5,0.3,0.9,0.9),\\(\varsigma_3,0.3,0.1,0.4,0.9,0.8),(\varsigma_4,0.5,0.3,0.2,0.8,0.9)\end{array}\right\}\\ \breve{e}_2=\left\{\begin{array}{l}(\varsigma_1,0.5,0.6,0.4,0.9,0.8),(\varsigma_2,0.5,0.3,0.2,0.9,0.8),\\(\varsigma_3,0.4,0.5,0.2,0.8,0.9),(\varsigma_4,0.4,0.2,0.1,0.7,0.9)\end{array}\right\}\end{array}\right\}=(\digamma_4,\breve{E})\in\mathfrak{I}_2.$$

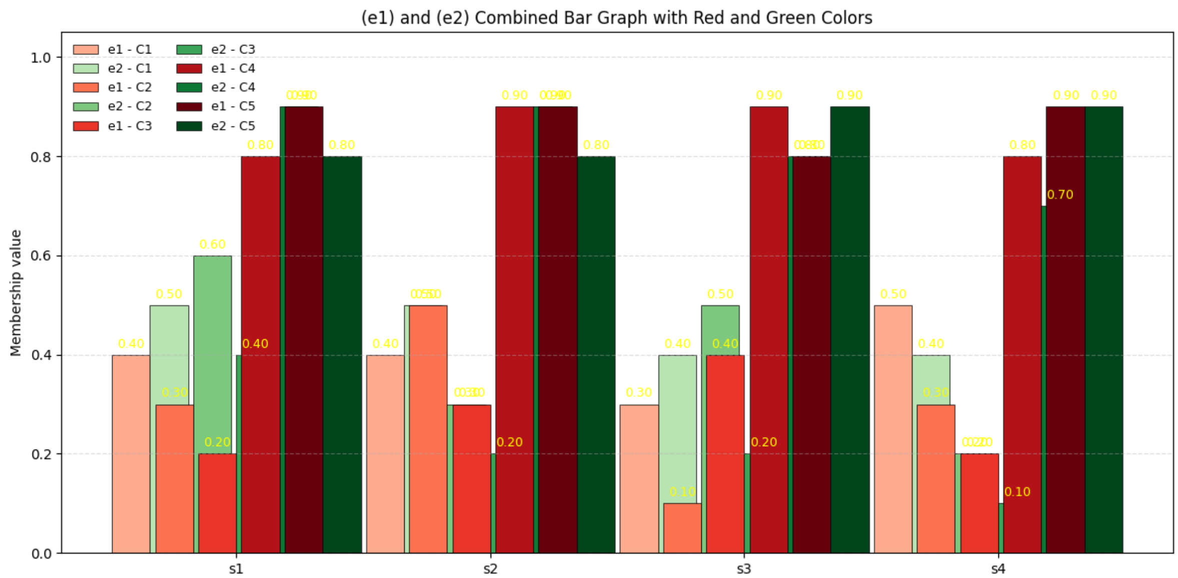

Fig 4.13

Hence, $\tau_1^{\mathrm{TVNSS}} \cup \tau_2^{\mathrm{TVNSS}}$ is a pentapartitioned neutrosophic soft topology over Ú. But, this is not possible always as given in the following example.

Example 4.6. Assume that set $Ú = \{ş_1, ş_2, ş_3, ş_4\}$ and $Ě = [ĕ_1, ĕ_2]$.

$\mathfrak{I}_1^{\mathrm{TVNSS}} = \left\{0_{(Ú,Ě)}, 1_{(Ú,Ě)}, (Ƒ_1, Ě), (Ƒ_2, Ě)\right\}$ and $\mathfrak{I}_2^{\mathrm{TVNSS}} = \left\{0_{(Ú,Ě)}, 1_{(Ú,Ě)}, (Ƒ_2, Ě), (Ƒ_3, Ě)\right\}$ be TVNSTS over Ú, here $(Ƒ_1, Ě), (Ƒ_2, Ě), (Ƒ_3, Ě)$ and $(Ƒ_4, Ě)$ are defined:

$$(Ƒ_1, Ě) = \begin{cases} ĕ_1 = \begin{Bmatrix} (ş_1, 0.7, 0.8, 0.6, 0.4, 0.3), (ş_2, 0.8, 0.7, 0.9, 0.5, 0.4), \\ (ş_3, 0.6, 0.8, 0.9, 0.7, 0.4), (ş_4, 0.9, 0.7, 0.6, 0.5, 0.4) \end{Bmatrix} \\ ĕ_2 = \begin{Bmatrix} (ş_1, 0.8, 0.9, 0.8, 0.6, 0.4), (ş_2, 0.9, 0.7, 0.6, 0.5, 0.6), \\ (ş_3, 0.8, 0.9, 0.5, 0.4, 0.5), (ş_4, 0.8, 0.5, 0.5, 0.4, 0.6) \end{Bmatrix} \end{cases},$$

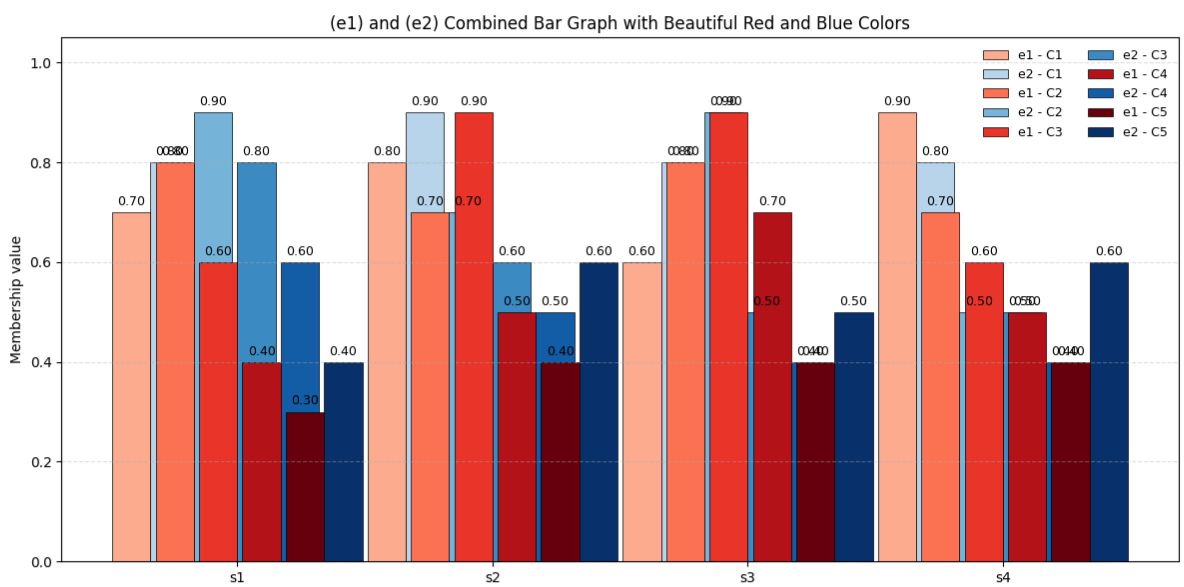

Fig 4.14

$$(ƒ_2, \breve{E}) = \begin{cases} \breve{e}_1 = \begin{Bmatrix} (ş_1, 0.5, 0.6, 0.4, 0.4, 0.8), (ş_2, 0.6, 0.7, 0.6, 0.8, 0.8), \\ (ş_3, 0.6, 0.7, 0.9, 0.8, 0.6), (ş_4, 0.8, 0.7, 0.6, 0.6, 0.8) \end{Bmatrix} \\ \breve{e}_2 = \begin{Bmatrix} (ş_1, 0.7, 0.7, 0.6, 0.8, 0.4), (ş_2, 0.8, 0.6, 0.5, 0.8, 0.6), \\ (ş_3, 0.6, 0.8, 0.4, 0.4, 0.8), (ş_4, 0.7, 0.5, 0.4, 0.6, 0.8) \end{Bmatrix} \end{cases},$$

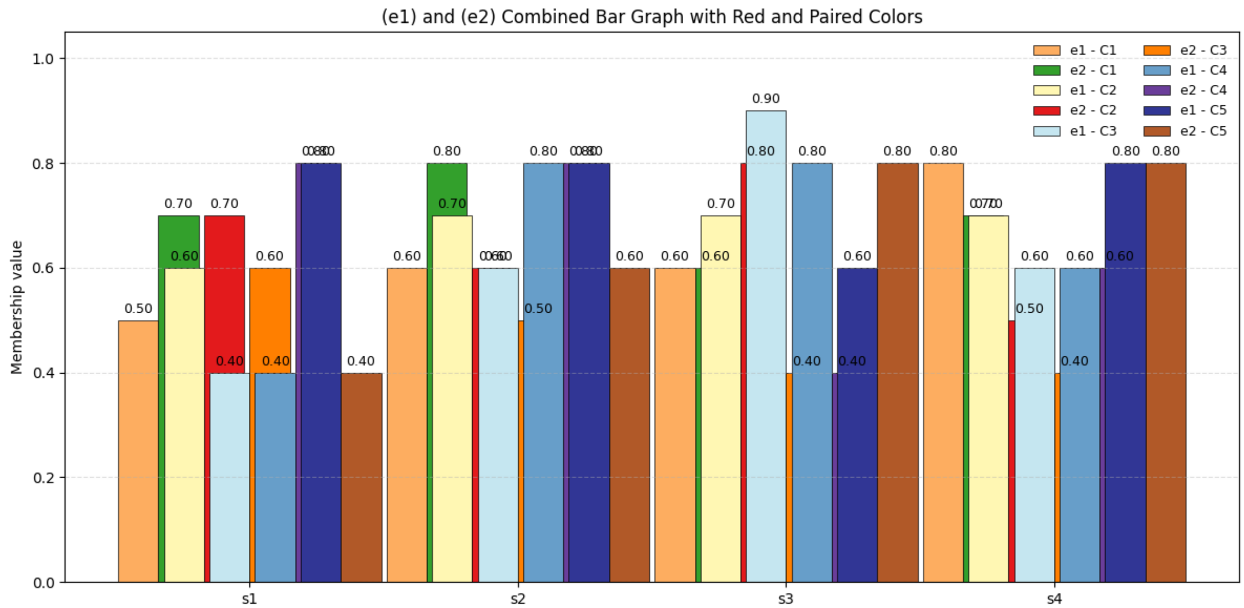

Fig 4.15

$$(ƒ_3, \breve{E}) = \begin{cases} \breve{e}_1 = \begin{Bmatrix} (ş_1, 0.8, 0.5, 0.4, 0.5, 0.7), (ş_2, 0.5, 0.6, 0.4, 0.3, 0.8), \\ (ş_3, 0.7, 0.6, 0.5, 0.4, 0.4), (ş_4, 0.9, 0.3, 0.4, 0.6, 0.7) \end{Bmatrix} \\ \breve{e}_2 = \begin{Bmatrix} (ş_1, 0.4, 0.5, 0.9, 0.3, 0.4), (ş_2, 0.3, 0.5, 0.7, 0.8, 0.4), \\ (ş_3, 0.6, 0.3, 0.6, 0.8, 0.9), (ş_4, 0.4, 0.5, 0.8, 0.4, 0.5) \end{Bmatrix} \end{cases},$$

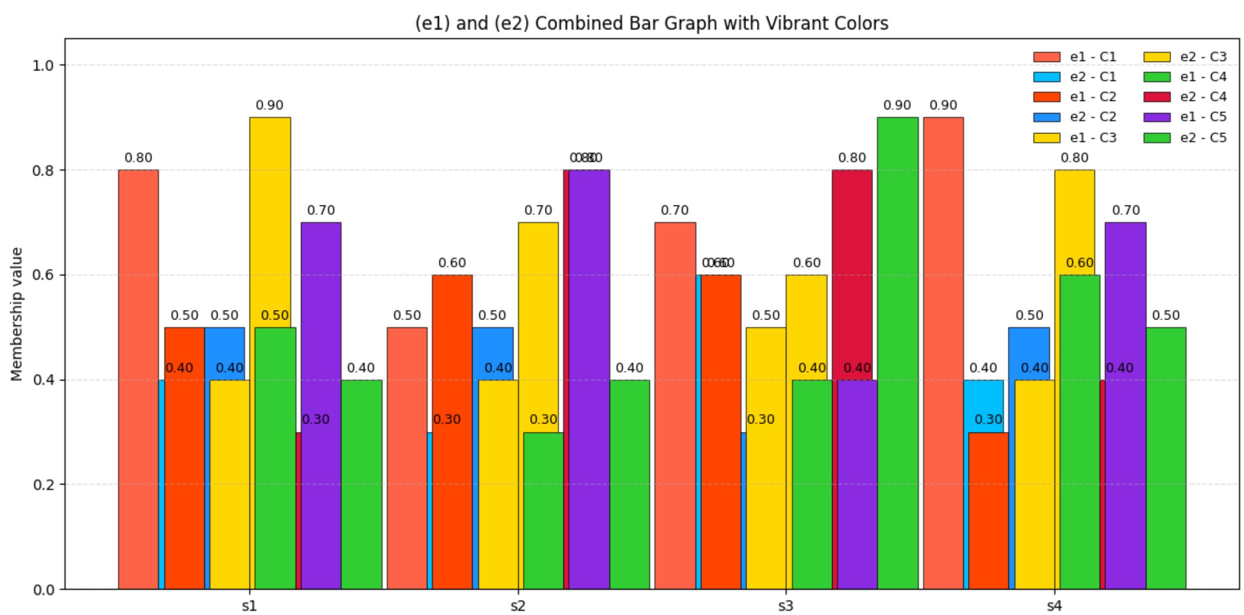

Fig 4.16

$$(ƒ_1,\breve{E})\cup(ƒ_2,\breve{E})=\left\{\begin{matrix}\breve{e}_1 &=\left\{\begin{matrix}(\varsigma_1,0.7,0.8,0.6,0.4,0.3),(\varsigma_2,0.8,0.7,0.9,0.5,0.4),\\(\varsigma_3,0.6,0.8,0.9,0.7,0.4),(\varsigma_4,0.9,0.7,0.6,0.5,0.4)\end{matrix}\right\}\\ \breve{e}_2 &=\left\{\begin{matrix}(\varsigma_1,0.8,0.9,0.8,0.6,0.4),(\varsigma_2,0.9,0.7,0.6,0.5,0.6),\\(\varsigma_3,0.8,0.9,0.5,0.4,0.5),(\varsigma_4,0.8,0.5,0.5,0.4,0.6)\end{matrix}\right\}\end{matrix}\right\}=(ƒ_1,\breve{E})\in\Im_1,$$

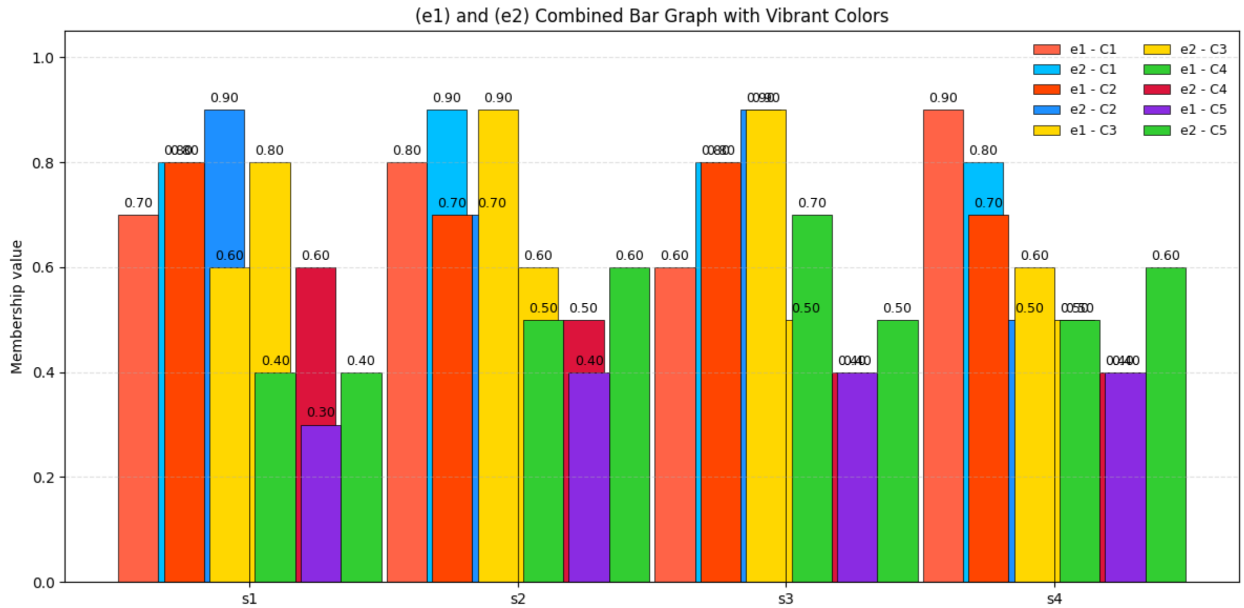

Fig 4.17

$$(ƒ_2,\breve{E})\cup(ƒ_3,\breve{E})=\left\{\begin{matrix}\breve{e}_1 &=\left\{\begin{matrix}(\varsigma_1,0.8,0.6,0.4,0.4,0.7),(\varsigma_2,0.6,0.7,0.6,0.3,0.8),\\(\varsigma_3,0.7,0.7,0.9,0.4,0.4),(\varsigma_4,0.9,0.7,0.6,0.6,0.7)\end{matrix}\right\}\\ \breve{e}_2 &=\left\{\begin{matrix}(\varsigma_1,0.7,0.7,0.9,0.3,0.4),(\varsigma_2,0.8,0.6,0.7,0.8,0.4),\\(\varsigma_3,0.6,0.8,0.6,0.4,0.8),(\varsigma_4,0.7,0.5,0.8,0.4,0.5)\end{matrix}\right\}\end{matrix}\right\}\neq(ƒ_2,\breve{E})\notin\Im_2,$$

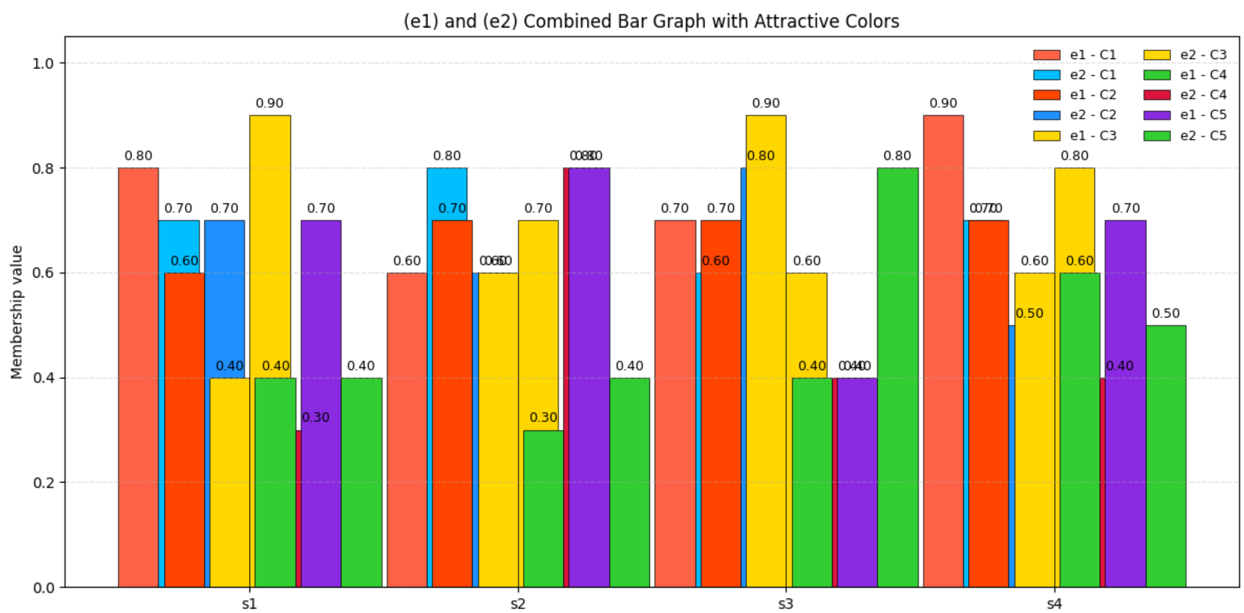

Fig 4.18

$$(\digamma_1, \check{\mathrm{E}}) \cap (\digamma_2, \check{\mathrm{E}}) = \begin{Bmatrix} \check{e}_1 = \begin{Bmatrix} (\S_1, 0.5, 0.6, 0.4, 0.4, 0.8), (\S_2, 0.6, 0.7, 0.6, 0.8, 0.8), \\ (\S_3, 0.6, 0.7, 0.9, 0.8, 0.6), (\S_4, 0.8, 0.7, 0.6, 0.6, 0.8) \end{Bmatrix} \\ \check{e}_2 = \begin{Bmatrix} (\S_1, 0.7, 0.7, 0.6, 0.8, 0.4), (\S_2, 0.8, 0.6, 0.5, 0.8, 0.6), \\ (\S_3, 0.6, 0.8, 0.4, 0.4, 0.8), (\S_4, 0.7, 0.5, 0.4, 0.6, 0.8) \end{Bmatrix} \end{Bmatrix} = (\digamma_2, \check{\mathrm{E}}) \in \Im_1,$$

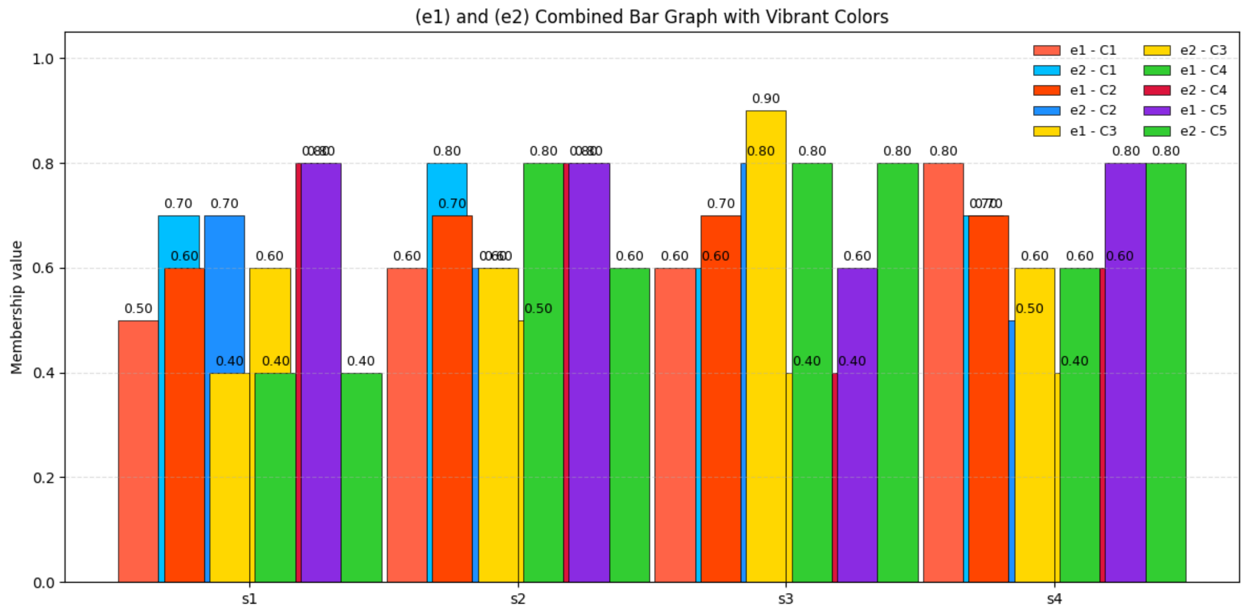

Fig 4.19

$$(\digamma_2, \check{\mathrm{E}}) \cap (\digamma_3, \check{\mathrm{E}}) = \begin{Bmatrix} \check{e}_1 = \begin{Bmatrix} (\S_1, 0.5, 0.5, 0.4, 0.5, 0.8), (\S_2, 0.5, 0.6, 0.4, 0.8, 0.8), \\ (\S_3, 0.6, 0.6, 0.5, 0.8, 0.6), (\S_4, 0.8, 0.3, 0.4, 0.6, 0.8) \end{Bmatrix} \\ \check{e}_2 = \begin{Bmatrix} (\S_1, 0.4, 0.5, 0.6, 0.8, 0.4), (\S_2, 0.3, 0.5, 0.5, 0.8, 0.6), \\ (\S_3, 0.6, 0.3, 0.4, 0.8, 0.9), (\S_4, 0.4, 0.5, 0.4, 0.6, 0.8) \end{Bmatrix} \end{Bmatrix} \neq (\digamma_3, \check{\mathrm{E}}) \notin \Im_2,$$

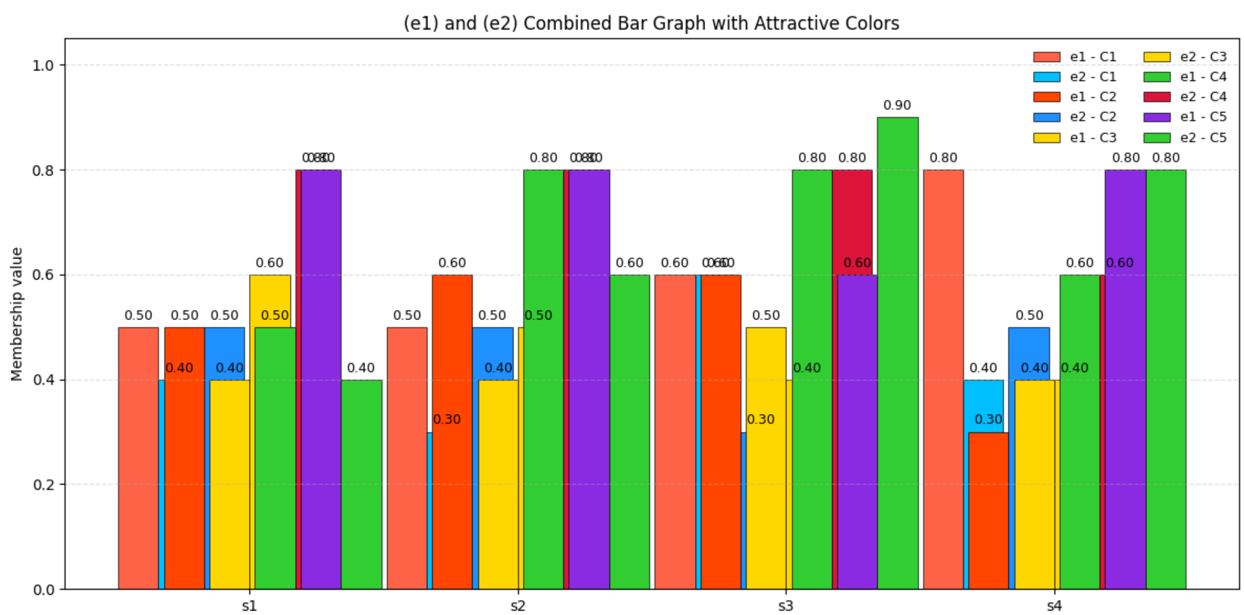

Fig 4.20

Hence, $(\digamma_2, \check{\mathrm{E}}) \cup (\digamma_3, \check{\mathrm{E}}) \neq \tau_1^{\mathrm{TVNSS}} \cup \tau_2^{\mathrm{TVNSS}}$,then $\tau_1^{\mathrm{TVNSS}} \cup \tau_2^{\mathrm{TVNSS}}$ *is not a* TVNST *on* Ú.

5. Application of Cosine Similarity Measure on Tri-valued Neutrosophic Softs Sets for Cancer Diagnosis

The recently developed tri-valued neutrosophic softs (TVNSS) similarity tests are as follows: The cosine similarity method will be used as the methodology. A crucial technique in medical diagnostics, especially when dealing with a complex disease like cancer, is cosine similarity, which shows how near data samples are to one another in high dimensional space. It is used to assess how well a patient's clinical profile matches the established diagnostic or therapy profile when it comes to cancer. One analytical technique for determining how similar two vectors (data) are to one another is the cosine similarity measure (CSM). It has numerous uses in a variety of settings related to machine learning, image processing, and data analysis. Taking into account the data points' geometrical orientation will enable CSM to spot some nuances in patterns and correlations that would have gone undetected without the use of only distance-based measurements.

It is frequently used in data analysis, machine learning, and image processing. It is feasible to employ CSM in military operations to classify potential targets based on surveillance data. The operating properties of a target and those of known categorized profiles are compared in order to accomplish this. The likelihood that threats will be compared and categorized appropriately is therefore increased by approximating the degree to which a target fits into pre-existing threat categories. The classification and pattern recognition tasks are made easier by a variety of machine learning and visualization technologies. Heatmaps, bar graphs, 3D plots, PCA, and other tools are used to analyze the signal-template relationship.

5.1. Cosine similarity measures

Let $T_i = (AbT_{ik}, ReT_{ik}, H_{ik}, RelF_{ik}, AbF_{ik})$, $C_j = \left(AbT_{jk}, ReT_{jk}, H_{jk}, RelF_{jk}, AbF_{jk}\right)$, are two PNSSs.

Each set is represented by four components for each feature k:

AbT_{ik}: Absolute truth membership of feature k for T_i.

ReT_{ik}: Relative truth value of feature k for T_i.

H_{ik}: Hesitation value of feature k for T_i.

$RelF_{ik}$: Relative false value of feature k for T_i.

AbF_{ik}: Absolute false value of feature k for T_i.

The values typically satisfy: $AbT_{ik}, ReT_{ik}, H_{ik}, RelF_{ik}, AbF_{ik} \in [0,1]$

Similarly, for object C_j:

AbT_{ik}: Absolute truth membership of feature k for C_j.

ReT_{ik}: Relative truth value of feature k for C_j.

H_{ik}: Hesitation value of feature k for C_j

$RelF_{ik}$: Relative false value of feature k for C_j.

AbF_{ik}: Absolute false value of feature k for C_j.

The values typically satisfy: $AbT_{ik}, ReT_{ik}, H_{ik}, RelF_{ik}, AbF_{ik} \in [0,1]$

The cosine similarity measure between T_i and C_j is defined as:

$Cosine_{PNSS}(T_i, C_j) =$

$$\frac{1}{n}\sum_{i=1}^{n}\left\{\frac{(AbT_{Mi})(AbT_{Ni})+(RelT_{Mi})(RelT_{Ni})+(H_{Mi})(H_{Ni}) + (RelF_{Mi})(RelF_{Ni})+(AbF_{Mi})(AbF_{Ni})}{\left(\sqrt{AbT_{M}{}^2+RelT_{M}{}^2+H_{M}{}^2+RelF_{M}{}^2+AbF_{M}{}^2} \times \sqrt{AbT_{N}{}^2+RelT_{N}{}^2+H_{N}{}^2+RelF_{N}{}^2+AbF_{N}{}^2}\right)}\right\}.$$

This calculation compares the comparable five-dimensional neutrosophic representation of T_i and $C_j$on feature k, calculating the average cosine similarity of all features.

5.2. Machine learning techniques

One way to visualize data is with a heat map, which shows the relationship between two variables as a matrix with a color for each value. Because it may be used to quickly identify groupings and patterns, it is especially effective when a large number of samples are involved. In terms of limited or sparse data, it may be less helpful and requires a careful selection of color scale. Rectangular forms are used in bar plots to display categorical data, with the height or length of the bar representing the value. When comparing quantities across classifications, such as in survey or sales data, they work best. They are simple to understand, have quick, low-number answers, get confounded by big numbers, and don't exhibit consistent patterns over time.

3D charts plot a three-axis on a two-dimensional graph to show the relationship between three data sets as continuous data. When applied to complicated data, such as 3D scatter plots or 3D surface plots, they offer greater depth; yet, they can also be challenging to understand and introduce an additional layer of complexity without enhancing clarity. Principal Component Analysis (PCA) converts a set of observations of variables that may theoretically be associated into a set of values of linearly independent variables known as principal components by using orthogonal transformation, which is similar to a change of basis. It is a frequently used statistical instrument.

5.3. Cancer diagnosis: Clinical use of Cosine Similarity in Patient–diagnosis Correlation

Let's say we have a dataset with different patients: $= \{P_1, P_2, P_3, P_4, P_5\}$: patients are represented. $D = \{D_1, D_2, D_3, D_4, D_5\}$: representing clinical indicators or diagnostic information (tumor size, HER 2, PSA level, etc.). The formula $= \{T_1, T_2, T_3, T_4, T_5\}$: denotes potential diagnoses or therapeutic approaches. Five terminologies—AbT (abnormal test value), RelT (relevant threshold), H (historical value), RelF (relative fluctuation), and AbF (abnormal fluctuation)—are used to express each diagnostic characteristic of a patient. Each patient's diagnosis or classification is created using the cosine similarity metric, which compares the parameters of the patient to those found in the current diagnostic profiles:

***Table 5.3.1**: Patient Diagnostic Parameter Matrix (P × D)*

	D_1	D_2	…	D_n
P_1	$AbT_{11}, RelT_{11}, H_{11}, RelF_{11}, AbF_{11}$	$AbT_{12}, RelT_{12}, H_{12}, RelF_{12}, AbF_{12}$	…	$AbT_{1n}, RelT_{1n}, H_{1n}, RelF_{1n}, AbF_{1n}$
P_2	$AbT_{21}, RelT_{21}, H_{21}, RelF_{21}, AbF_{21}$	$AbT_{22}, RelT_{22}, H_{22}, RelF_{21}, AbF_{22}$	…	$AbT_{2n}, RelT_{2n}, H_{2n}, RelF_{2n}, AbF_{2n}$
…	…	…	…	…
P_m	$AbT_{m1}, RelT_{m1}, H_{m1}, RelF_{m1}, AbF_{m1}$	$AbT_{m2}, RelT_{m2}, H_{m2}, RelF_{m2}, AbF_{m2}$	…	$AbT_{mn}, RelT_{mn}, H_{mn}, RelF_{mn}, AbF_{mn}$

This table represents each patient's diagnostic data across various diagnostic features (D_1 to D_5).

***Table 5.3.2:** Cosine Similarity Scores between Patients and Diagnostic Profiles* (**(P × D → T)**

Row - I	$\boldsymbol{D_1}$	$\boldsymbol{D_2}$	$\boldsymbol{D_3}$	$\boldsymbol{D_4}$	$\boldsymbol{D_5}$	**Row - II**	$\boldsymbol{T_1}$	$\boldsymbol{T_2}$	$\boldsymbol{T_3}$	$\boldsymbol{T_4}$	$\boldsymbol{T_5}$
$\boldsymbol{P_1}$	0.6	0.4	0.8	0.3	0.8	$\boldsymbol{D_1}$	0.8	0.3	0.8	0.7	0.6
	0.3	0.8	0.9	0.4	0.4		0.6	0.2	0.4	0.4	0.8
	0.8	0.7	0.3	0.6	0.6		0.4	0.9	0.6	0.3	0.7
	0.4	0.3	0.6	0.2	0.3		0.8	0.6	0.3	0.2	0.2
	0.8	0.2	0.4	0.8	0.2		0.2	0.8	0.5	0.6	0.4
$\boldsymbol{P_2}$	0.4	0.5	0.5	0.4	0.4	$\boldsymbol{D_2}$	0.5	0.6	0.4	0.8	0.5
	0.6	0.4	0.6	0.8	0.8		0.4	0.3	0.5	0.9	0.7
	0.4	0.8	0.8	0.9	0.9		0.8	0.9	0.6	0.6	0.6
	0.8	0.2	0.3	0.3	0.3		0.7	0.2	0.7	0.5	0.3
	0.3	0.6	0.9	0.4	0.6		0.6	0.8	0.4	0.4	0.2
$\boldsymbol{P_3}$	0.5	0.8	0.4	0.6	0.6	$\boldsymbol{D_3}$	0.2	0.9	0.4	0.7	0.8
	0.7	0.6	0.6	0.8	0.3		0.6	0.2	0.6	0.6	0.3
	0.3	0.4	0.3	0.3	0.4		0.7	0.8	0.7	0.7	0.4
	0.4	0.7	0.2	0.4	0.6		0.9	0.4	0.8	0.6	0.5
	0.8	0.5	0.6	0.2	0.7		0.8	0.6	0.5	0.3	0.4

$\boldsymbol{P_4}$	0.4	0.2	0.8	0.2	0.8	$\boldsymbol{D_4}$	0.9	0.3	0.3	0.3	0.6
	0.2	0.8	0.6	0.6	0.7		0.3	0.6	0.6	0.6	0.3
	0.3	0.3	0.4	0.4	0.3		0.6	0.4	0.9	0.8	0.4
	0.5	0.4	0.3	0.3	0.6		0.4	0.6	0.8	0.4	0.7
	0.9	0.4	0.6	0.2	0.4		0.2	0.9	0.4	0.2	0.8
$\boldsymbol{P_5}$	0.7	0.3	0.9	0.8	0.2	$\boldsymbol{D_5}$	0.3	0.3	0.2	0.1	0.6
	0.6	0.8	0.3	0.9	0.6		0.6	0.4	0.7	0.6	0.4
	0.8	0.9	0.2	0.3	0.5		0.8	0.5	0.4	0.7	0.1
	0.3	0.5	0.6	0.4	0.7		0.6	0.8	0.2	0.6	0.8
	0.1	0.4	0.8	0.3	0.8		0.4	0.9	0.8	0.4	0.3

This table displays the cosine similarity metric for both patient (P_1 to P_5) and diagnostic profile (D_1 to D_5) similarity. Each cell most likely represents the relationship between a particular parameter used in patient diagnosis (or a total measure of the five subcomponents) and a known profile of an ideal diagnosis or treatment plan.

As, $Cosine_{TVNSS}(T_i, C_j) =$

$$\frac{1}{n}\sum_{i=1}^{n}\left\{\frac{(AbT_{Mi})(AbT_{Ni})+(RelT_{Mi})(RelT_{Ni})+(H_{Mi})(H_{Ni}) + (RelF_{Mi})(RelF_{Ni})+(AbF_{Mi})(AbF_{Ni})}{\left(\sqrt{AbT_{M^2}+RelT_{M^2}+H_{M^2}+RelF_{M^2}+AbF_{M^2}}\times\sqrt{AbT_{N^2}+RelT_{N^2}+H_{N^2}+RelF_{N^2}+AbF_{N^2}}\right)}\right\}.$$

For $n = 5$ then $R_1 + C_1 \Rightarrow Cosine_{TVNSS}(T_i, C_j) =$

$$\frac{1}{5}\left\{\frac{(0.6)(0.8)+(0.3)(0.6)+(0.8)(0.4)+(0.4)(0.8)+(0.8)(0.2)}{\left(\sqrt{0.6^2+0.3^2+0.8^2+0.4^2+0.8^2}\times\sqrt{0.8^2+0.6^2+0.4^2+0.8^2+0.2^2}\right)}\right\}+$$
$$\frac{1}{5}\left\{\frac{(0.4)(0.5)+(0.8)(0.4)+(0.7)(0.8)+(0.3)(0.7)+(0.2)(0.6)}{\left(\sqrt{0.4^2+0.8^2+0.7^2+0.3^2+0.2^2}\times\sqrt{0.5^2+0.4^2+0.8^2+0.7^2+0.6^2}\right)}\right\}+$$
$$\frac{1}{5}\left\{\frac{(0.8)(0.2)+(0.9)(0.6)+(0.3)(0.7)+(0.6)(0.9)+(0.4)(0.8)}{\left(\sqrt{0.8^2+0.9^2+0.3^2+0.6^2+0.4^2}\times\sqrt{0.2^2+0.6^2+0.7^2+0.9^2+0.8^2}\right)}\right\}+$$
$$\frac{1}{5}\left\{\frac{(0.3)(0.9)+(0.4)(0.3)+(0.6)(0.6)+(0.2)(0.4)+(0.8)(0.2)}{\left(\sqrt{0.3^2+0.4^2+0.6^2+0.2^2+0.8^2}\times\sqrt{0.9^2+0.3^2+0.6^2+0.4^2+0.2^2}\right)}\right\}+$$
$$\frac{1}{5}\left\{\frac{(0.8)(0.3)+(0.4)(0.6)+(0.6)(0.8)+(0.3)(0.6)+(0.2)(0.4)}{\left(\sqrt{0.8^2+0.4^2+0.6^2+0.3^2+0.2^2}\times\sqrt{0.3^2+0.6^2+0.8^2+0.6^2+0.4^2}\right)}\right\}.$$

$= 0.1568 + 0.1716 + 0.1616 + 0.1311 + 0.1693 = 0.7904.$

For $n = 5$ then $R_1 + C_2 \Rightarrow Cosine_{TVNSS}(T_i, C_j) =$

$$\frac{1}{5}\left\{\frac{(0.6)(0.3)+(0.3)(0.2)+(0.8)(0.9)+(0.4)(0.6)+(0.8)(0.8)}{\left(\sqrt{0.6^2+0.3^2+0.8^2+0.4^2+0.8^2}\times\sqrt{0.3^2+0.2^2+0.9^2+0.6^2+0.8^2}\right)}\right\}+$$
$$\frac{1}{5}\left\{\frac{(0.4)(0.6)+(0.8)(0.3)+(0.7)(0.9)+(0.3)(0.2)+(0.2)(0.9)}{\left(\sqrt{0.4^2+0.8^2+0.7^2+0.3^2+0.2^2}\times\sqrt{0.6^2+0.3^2+0.9^2+0.2^2+0.8^2}\right)}\right\}+$$
$$\frac{1}{5}\left\{\frac{(0.8)(0.3)+(0.9)(0.6)+(0.3)(0.4)+(0.6)(0.6)+(0.4)(0.9)}{\left(\sqrt{0.8^2+0.9^2+0.3^2+0.6^2+0.4^2}\times\sqrt{0.3^2+0.6^2+0.4^2+0.6^2+0.9^2}\right)}\right\}+$$

$\frac{1}{5}\left\{\frac{(0.3)(0.9)+(0.4)(0.3)+(0.6)(0.6)+(0.2)(0.4)+(0.8)(0.2)}{\left(\sqrt{0.3^2+0.4^2+0.6^2+0.2^2+0.8^2}\times\sqrt{0.9^2+0.3^2+0.6^2+0.4^2+0.2^2}\right)}\right\}+$

$\frac{1}{5}\left\{\frac{(0.8)(0.3)+(0.4)(0.4)+(0.6)(0.5)+(0.3)(0.6)+(0.2)(0.8)}{\left(\sqrt{0.8^2+0.4^2+0.6^2+0.3^2+0.2^2}\times\sqrt{0.3^2+0.4^2+0.5^2+0.6^2+0.8^2}\right)}\right\}.$

$= 0.1926 + 0.1626 + 0.1692 + 0.1442 + 0.1410 = 0.8096.$

For $n = 5$ then $R_1 + C_3 \Rightarrow Cosine_{TVNSS}(T_i, C_j) =$

$\frac{1}{5}\left\{\frac{(0.6)(0.8)+(0.3)(0.4)+(0.8)(0.6)+(0.4)(0.3)+(0.8)(0.5)}{\left(\sqrt{0.6^2+0.3^2+0.8^2+0.4^2+0.8^2}\times\sqrt{0.8^2+0.4^2+0.6^2+0.3^2+0.5^2}\right)}\right\}+$

$\frac{1}{5}\left\{\frac{(0.4)(0.4)+(0.8)(0.5)+(0.7)(0.6)+(0.3)(0.7)+(0.2)(0.4)}{\left(\sqrt{0.4^2+0.8^2+0.7^2+0.3^2+0.2^2}\times\sqrt{0.4^2+0.5^2+0.6^2+0.7^2+0.4^2}\right)}\right\}+$

$\frac{1}{5}\left\{\frac{(0.8)(0.4)+(0.9)(0.6)+(0.3)(0.7)+(0.6)(0.8)+(0.4)(0.5)}{\left(\sqrt{0.8^2+0.9^2+0.3^2+0.6^2+0.4^2}\times\sqrt{0.4^2+0.6^2+0.7^2+0.8^2+0.5^2}\right)}\right\}+$

$\frac{1}{5}\left\{\frac{(0.3)(0.3)+(0.4)(0.6)+(0.6)(0.9)+(0.2)(0.8)+(0.8)(0.4)}{\left(\sqrt{0.3^2+0.4^2+0.6^2+0.2^2+0.8^2}\times\sqrt{0.3^2+0.6^2+0.9^2+0.8^2+0.4^2}\right)}\right\}+$

$\frac{1}{5}\left\{\frac{(0.8)(0.2)+(0.4)(0.7)+(0.6)(0.4)+(0.3)(0.2)+(0.2)(0.8)}{\left(\sqrt{0.8^2+0.4^2+0.6^2+0.3^2+0.2^2}\times\sqrt{0.2^2+0.7^2+0.4^2+0.2^2+0.8^2}\right)}\right\}.$

$= 0.1900 + 0.1788 + 0.1769 + 0.1656 + 0.1354 = 0.8467.$

For $n = 5$ then $R_1 + C_4 \Rightarrow Cosine_{TVNSS}(T_i, C_j) =$

$\frac{1}{5}\left\{\frac{(0.6)(0.7)+(0.3)(0.4)+(0.8)(0.3)+(0.4)(0.2)+(0.8)(0.6)}{\left(\sqrt{0.6^2+0.3^2+0.8^2+0.4^2+0.8^2}\times\sqrt{0.7^2+0.4^2+0.3^2+0.2^2+0.6^2}\right)}\right\}+$

$\frac{1}{5}\left\{\frac{(0.4)(0.8)+(0.8)(0.9)+(0.7)(0.6)+(0.3)(0.5)+(0.2)(0.4)}{\left(\sqrt{0.4^2+0.8^2+0.7^2+0.3^2+0.2^2}\times\sqrt{0.8^2+0.9^2+0.6^2+0.5^2+0.4^2}\right)}\right\}+$

$\frac{1}{5}\left\{\frac{(0.8)(0.7)+(0.9)(0.6)+(0.3)(0.7)+(0.6)(0.6)+(0.4)(0.3)}{\left(\sqrt{0.8^2+0.9^2+0.3^2+0.6^2+0.4^2}\times\sqrt{0.7^2+0.6^2+0.7^2+0.6^2+0.3^2}\right)}\right\}+$

$\frac{1}{5}\left\{\frac{(0.3)(0.3)+(0.4)(0.6)+(0.6)(0.8)+(0.2)(0.4)+(0.8)(0.2)}{\left(\sqrt{0.3^2+0.4^2+0.6^2+0.2^2+0.8^2}\times\sqrt{0.3^2+0.6^2+0.8^2+0.4^2+0.2^2}\right)}\right\}+$

$\frac{1}{5}\left\{\frac{(0.8)(0.1)+(0.4)(0.6)+(0.6)(0.7)+(0.3)(0.6)+(0.2)(0.4)}{\left(\sqrt{0.8^2+0.4^2+0.6^2+0.3^2+0.2^2}\times\times\sqrt{0.1^2+0.6^2+0.7^2+0.6^2+0.4^2}\right)}\right\}.$

$= 0.1825 + 0.1909 + 0.1864 + 0.1627 + 0.1499 = 0.8724.$

For $n = 5$ then $R_1 + C_5 \Rightarrow Cosine_{TVNSS}(T_i, C_j) =$

$\frac{1}{5}\left\{\frac{(0.6)(0.6)+(0.3)(0.8)+(0.8)(0.7)+(0.4)(0.2)+(0.8)(0.4)}{\left(\sqrt{0.6^2+0.3^2+0.8^2+0.4^2+0.8^2}\times\sqrt{0.6^2+0.8^2+0.7^2+0.2^2+0.4^2}\right)}\right\}+$

$\frac{1}{5}\left\{\frac{(0.4)(0.5)+(0.8)(0.7)+(0.7)(0.6)+(0.3)(0.3)+(0.2)(0.2)}{\left(\sqrt{0.4^2+0.8^2+0.7^2+0.3^2+0.2^2}\times\sqrt{0.5^2+0.7^2+0.6^2+0.3^2+0.2^2}\right)}\right\}+$

$\frac{1}{5}\left\{\frac{(0.8)(0.8)+(0.9)(0.3)+(0.3)(0.4)+(0.6)(0.5)+(0.4)(0.4)}{\left(\sqrt{0.8^2+0.9^2+0.3^2+0.6^2+0.4^2}\times\sqrt{0.8^2+0.3^2+0.4^2+0.5^2+0.4^2}\right)}\right\}+$

$\frac{1}{5}\left\{\frac{(0.3)(0.6)+(0.4)(0.3)+(0.6)(0.4)+(0.2)(0.7)+(0.8)(0.8)}{\left(\sqrt{0.3^2+0.4^2+0.6^2+0.2^2+0.8^2}\times\sqrt{0.6^2+0.3^2+0.4^2+0.7^2+0.8^2}\right)}\right\}+$

$\frac{1}{5}\left\{\frac{(0.8)(0.6)+(0.4)(0.4)+(0.6)(0.1)+(0.3)(0.8)+(0.2)(0.3)}{\left(\sqrt{0.8^2+0.4^2+0.6^2+0.3^2+0.2^2}\times\sqrt{0.6^2+0.4^2+0.1^2+0.8^2+0.3^2}\right)}\right\}.$

$= 0.1745 + 0.1982 + 0.1821 + 0.1762 + 0.1568 = 0.8878.$

For $n = 5$ then $R_2 + C_1 \Rightarrow Cosine_{TVNSS}(T_i, C_j) =$

$\frac{1}{5}\left\{\frac{(0.4)(0.8)+(0.6)(0.6)+(0.4)(0.4)+(0.8)(0.8)+(0.3)(0.2)}{\left(\sqrt{0.4^2+0.6^2+0.4^2+0.8^2+0.3^2}\times\sqrt{0.8^2+0.6^2+0.4^2+0.8^2+0.2^2}\right)}\right\}+$
$\frac{1}{5}\left\{\frac{(0.5)(0.5)+(0.4)(0.4)+(0.8)(0.8)+(0.2)(0.7)+(0.6)(0.6)}{\left(\sqrt{0.5^2+0.4^2+0.8^2+0.2^2+0.6^2}\times\sqrt{0.5^2+0.4^2+0.8^2+0.7^2+0.6^2}\right)}\right\}+$
$\frac{1}{5}\left\{\frac{(0.5)(0.2)+(0.6)(0.6)+(0.8)(0.7)+(0.3)(0.9)+(0.9)(0.8)}{\left(\sqrt{0.5^2+0.6^2+0.8^2+0.3^2+0.9^2}\times\sqrt{0.2^2+0.6^2+0.7^2+0.9^2+0.8^2}\right)}\right\}+$
$\frac{1}{5}\left\{\frac{(0.4)(0.9)+(0.8)(0.3)+(0.9)(0.6)+(0.3)(0.4)+(0.4)(0.2)}{\left(\sqrt{0.4^2+0.8^2+0.9^2+0.3^2+0.4^2}\times\sqrt{0.9^2+0.3^2+0.6^2+0.4^2+0.2^2}\right)}\right\}+$
$\frac{1}{5}\left\{\frac{(0.4)(0.3)+(0.8)(0.6)+(0.9)(0.8)+(0.3)(0.6)+(0.6)(0.4)}{\left(\sqrt{0.4^2+0.8^2+0.9^2+0.3^2+0.6^2}\times\sqrt{0.3^2+0.6^2+0.8^2+0.6^2+0.4^2}\right)}\right\}.$
$= 0.1912 + 0.1867 + 0.1792 + 0.1626 + 0.1910 = 0.9107.$

For $n = 5$ then $R_2 + C_2 \Rightarrow Cosine_{TVNSS}(T_i, C_j) =$

$\frac{1}{5}\left\{\frac{(0.4)(0.3)+(0.6)(0.2)+(0.4)(0.9)+(0.8)(0.6)+(0.3)(0.8)}{\left(\sqrt{0.4^2+0.6^2+0.4^2+0.8^2+0.3^2}\times\sqrt{0.3^2+0.2^2+0.9^2+0.6^2+0.8^2}\right)}\right\}+$
$\frac{1}{5}\left\{\frac{(0.5)(0.6)+(0.4)(0.3)+(0.8)(0.9)+(0.2)(0.2)+(0.6)(0.8)}{\left(\sqrt{0.5^2+0.4^2+0.8^2+0.2^2+0.6^2}\times\sqrt{0.6^2+0.3^2+0.9^2+0.2^2+0.8^2}\right)}\right\}+$
$\frac{1}{5}\left\{\frac{(0.5)(0.9)+(0.6)(0.2)+(0.8)(0.8)+(0.3)(0.4)+(0.9)(0.6)}{\left(\sqrt{0.5^2+0.6^2+0.8^2+0.3^2+0.9^2}\times\sqrt{0.9^2+0.2^2+0.8^2+0.4^2+0.6^2}\right)}\right\}+$
$\frac{1}{5}\left\{\frac{(0.4)(0.3)+(0.8)(0.6)+(0.9)(0.4)+(0.3)(0.6)+(0.4)(0.9)}{\left(\sqrt{0.4^2+0.8^2+0.9^2+0.3^2+0.4^2}\times\sqrt{0.3^2+0.6^2+0.4^2+0.6^2+0.9^2}\right)}\right\}+$
$\frac{1}{5}\left\{\frac{(0.4)(0.3)+(0.8)(0.4)+(0.9)(0.5)+(0.3)(0.8)+(0.6)(0.6)}{\left(\sqrt{0.4^2+0.8^2+0.9^2+0.3^2+0.6^2}\times\sqrt{0.3^2+0.4^2+0.5^2+0.8^2+0.6^2}\right)}\right\}.$
$= 0.1596 + 0.1979 + 0.1799 + 0.1648 + 0.1695 = 0.8717.$

For $n = 5$ then $R_2 + C_3 \Rightarrow Cosine_{TVNSS}(T_i, C_j) =$

$\frac{1}{5}\left\{\frac{(0.4)(0.8)+(0.6)(0.4)+(0.4)(0.6)+(0.8)(0.3)+(0.3)(0.5)}{\left(\sqrt{0.4^2+0.6^2+0.4^2+0.8^2+0.3^2}\times\sqrt{0.8^2+0.4^2+0.6^2+0.3^2+0.5^2}\right)}\right\}+$
$\frac{1}{5}\left\{\frac{(0.5)(0.4)+(0.4)(0.5)+(0.8)(0.6)+(0.2)(0.7)+(0.6)(0.4)}{\left(\sqrt{0.5^2+0.4^2+0.8^2+0.2^2+0.6^2}\times\sqrt{0.4^2+0.5^2+0.6^2+0.7^2+0.4^2}\right)}\right\}+$
$\frac{1}{5}\left\{\frac{(0.5)(0.4)+(0.6)(0.6)+(0.8)(0.7)+(0.3)(0.8)+(0.9)(0.5)}{\left(\sqrt{0.5^2+0.6^2+0.8^2+0.3^2+0.9^2}\times\sqrt{0.4^2+0.6^2+0.7^2+0.8^2+0.5^2}\right)}\right\}+$
$\frac{1}{5}\left\{\frac{(0.4)(0.3)+(0.8)(0.6)+(0.9)(0.9)+(0.3)(0.8)+(0.4)(0.4)}{\left(\sqrt{0.4^2+0.8^2+0.9^2+0.3^2+0.4^2}\times\sqrt{0.3^2+0.6^2+0.9^2+0.8^2+0.4^2}\right)}\right\}+$
$\frac{1}{5}\left\{\frac{(0.4)(0.2)+(0.8)(0.7)+(0.9)(0.4)+(0.3)(0.2)+(0.6)(0.8)}{\left(\sqrt{0.4^2+0.8^2+0.9^2+0.3^2+0.6^2}\times\sqrt{0.2^2+0.7^2+0.4^2+0.2^2+0.8^2}\right)}\right\}.$
$= 0.1636 + 0.1895 + 0.1791 + 0.1849 + 0.1833 = 0.9004.$

For $n = 5$ then $R_2 + C_4 \Rightarrow Cosine_{TVNSS}(T_i, C_j) =$

$\frac{1}{5}\left\{\frac{(0.4)(0.7)+(0.6)(0.4)+(0.4)(0.3)+(0.8)(0.2)+(0.3)(0.6)}{\left(\sqrt{0.4^2+0.6^2+0.4^2+0.8^2+0.3^2}\times\sqrt{0.7^2+0.4^2+0.3^2+0.2^2+0.6^2}\right)}\right\}+$
$\frac{1}{5}\left\{\frac{(0.5)(0.8)+(0.4)(0.9)+(0.8)(0.6)+(0.2)(0.5)+(0.6)(0.4)}{\left(\sqrt{0.5^2+0.4^2+0.8^2+0.2^2+0.6^2}\times\sqrt{0.8^2+0.9^2+0.6^2+0.5^2+0.4^2}\right)}\right\}+$
$\frac{1}{5}\left\{\frac{(0.5)(0.7)+(0.6)(0.6)+(0.8)(0.7)+(0.3)(0.6)+(0.9)(0.3)}{\left(\sqrt{0.5^2+0.6^2+0.8^2+0.3^2+0.9^2}\times\sqrt{0.7^2+0.6^2+0.7^2+0.6^2+0.3^2}\right)}\right\}+$
$\frac{1}{5}\left\{\frac{(0.4)(0.3)+(0.8)(0.6)+(0.9)(0.8)+(0.3)(0.4)+(0.4)(0.2)}{\left(\sqrt{0.4^2+0.8^2+0.9^2+0.3^2+0.4^2}\times\sqrt{0.3^2+0.6^2+0.8^2+0.4^2+0.2^2}\right)}\right\}+$
$\frac{1}{5}\left\{\frac{(0.4)(0.1)+(0.8)(0.6)+(0.9)(0.7)+(0.3)(0.6)+(0.6)(0.4)}{\left(\sqrt{0.4^2+0.8^2+0.9^2+0.3^2+0.6^2}\times\sqrt{0.1^2+0.6^2+0.7^2+0.6^2+0.4^2}\right)}\right\}.$

$= 0.1545 + 0.1761 + 0.1753 + 0.1962 + 0.1862 = 0.8883.$

For $n = 5$ then $R_2 + C_5 \Rightarrow Cosine_{TVNSS}(T_i, C_j) =$

$$\frac{1}{5}\left\{\frac{(0.4)(0.6)+(0.6)(0.8)+(0.4)(0.7)+(0.8)(0.2)+(0.3)(0.4)}{\left(\sqrt{0.4^2+0.6^2+0.4^2+0.8^2+0.3^2}\times\sqrt{0.6^2+0.8^2+0.7^2+0.2^2+0.4^2}\right)}\right\}+$$

$$\frac{1}{5}\left\{\frac{(0.5)(0.5)+(0.4)(0.7)+(0.8)(0.6)+(0.2)(0.3)+(0.6)(0.2)}{\left(\sqrt{0.5^2+0.4^2+0.8^2+0.2^2+0.6^2}\times\sqrt{0.5^2+0.7^2+0.6^2+0.3^2+0.2^2}\right)}\right\}+$$

$$\frac{1}{5}\left\{\frac{(0.5)(0.8)+(0.6)(0.3)+(0.8)(0.4)+(0.3)(0.5)+(0.9)(0.4)}{\left(\sqrt{0.5^2+0.6^2+0.8^2+0.3^2+0.9^2}\times\sqrt{0.8^2+0.3^2+0.4^2+0.5^2+0.4^2}\right)}\right\}+$$

$$\frac{1}{5}\left\{\frac{(0.4)(0.6)+(0.8)(0.3)+(0.9)(0.4)+(0.3)(0.7)+(0.4)(0.8)}{\left(\sqrt{0.4^2+0.8^2+0.9^2+0.3^2+0.4^2}\times\sqrt{0.6^2+0.3^2+0.4^2+0.7^2+0.8^2}\right)}\right\}+$$

$$\frac{1}{5}\left\{\frac{(0.4)(0.6)+(0.8)(0.4)+(0.9)(0.1)+(0.3)(0.8)+(0.6)(0.3)}{\left(\sqrt{0.4^2+0.8^2+0.9^2+0.3^2+0.6^2}\times\sqrt{0.6^2+0.4^2+0.1^2+0.8^2+0.3^2}\right)}\right\}.$$

$= 0.1658 + 0.1782 + 0.1686 + 0.1747 + 0.1328 = 0.8201.$

For $n = 5$ then $R_3 + C_1 \Rightarrow Cosine_{TVNSS}(T_i, C_j) =$

$$\frac{1}{5}\left\{\frac{(0.5)(0.8)+(0.7)(0.6)+(0.3)(0.4)+(0.4)(0.8)+(0.8)(0.2)}{\left(\sqrt{0.5^2+0.7^2+0.3^2+0.4^2+0.8^2}\times\sqrt{0.8^2+0.6^2+0.4^2+0.8^2+0.2^2}\right)}\right\}+$$

$$\frac{1}{5}\left\{\frac{(0.8)(0.5)+(0.6)(0.4)+(0.4)(0.8)+(0.7)(0.7)+(0.5)(0.6)}{\left(\sqrt{0.8^2+0.6^2+0.4^2+0.7^2+0.5^2}\times\sqrt{0.5^2+0.4^2+0.8^2+0.7^2+0.6^2}\right)}\right\}+$$

$$\frac{1}{5}\left\{\frac{(0.4)(0.2)+(0.6)(0.6)+(0.3)(0.7)+(0.2)(0.9)+(0.6)(0.8)}{\left(\sqrt{0.4^2+0.6^2+0.3^2+0.2^2+0.6^2}\times\sqrt{0.2^2+0.6^2+0.7^2+0.9^2+0.8^2}\right)}\right\}+$$

$$\frac{1}{5}\left\{\frac{(0.6)(0.9)+(0.8)(0.3)+(0.3)(0.6)+(0.4)(0.4)+(0.2)(0.2)}{\left(\sqrt{0.6^2+0.8^2+0.3^2+0.4^2+0.2^2}\times\sqrt{0.9^2+0.3^2+0.6^2+0.4^2+0.2^2}\right)}\right\}+$$

$$\frac{1}{5}\left\{\frac{(0.6)(0.3)+(0.3)(0.6)+(0.4)(0.8)+(0.6)(0.6)+(0.7)(0.4)}{\left(\sqrt{0.6^2+0.3^2+0.4^2+0.6^2+0.7^2}\times\sqrt{0.3^2+0.6^2+0.8^2+0.6^2+0.4^2}\right)}\right\}.$$

$= 0.1639 + 0.1842 + 0.1704 + 0.1690 + 0.1722 = 0.8597.$

For $n = 5$ then $R_3 + C_2 \Rightarrow Cosine_{TVNSS}(T_i, C_j) =$

$$\frac{1}{5}\left\{\frac{(0.5)(0.3)+(0.7)(0.2)+(0.3)(0.9)+(0.4)(0.6)+(0.8)(0.8)}{\left(\sqrt{0.5^2+0.7^2+0.3^2+0.4^2+0.8^2}\times\sqrt{0.3^2+0.2^2+0.9^2+0.6^2+0.8^2}\right)}\right\}+$$

$$\frac{1}{5}\left\{\frac{(0.8)(0.6)+(0.6)(0.3)+(0.4)(0.9)+(0.7)(0.2)+(0.5)(0.8)}{\left(\sqrt{0.8^2+0.6^2+0.4^2+0.7^2+0.5^2}\times\sqrt{0.6^2+0.3^2+0.9^2+0.2^2+0.8^2}\right)}\right\}+$$

$$\frac{1}{5}\left\{\frac{(0.4)(0.9)+(0.6)(0.2)+(0.3)(0.8)+(0.2)(0.4)+(0.6)(0.6)}{\left(\sqrt{0.4^2+0.6^2+0.3^2+0.2^2+0.6^2}\times\sqrt{0.9^2+0.2^2+0.8^2+0.4^2+0.6^2}\right)}\right\}+$$

$$\frac{1}{5}\left\{\frac{(0.6)(0.3)+(0.8)(0.6)+(0.3)(0.4)+(0.4)(0.6)+(0.2)(0.9)}{\left(\sqrt{0.6^2+0.8^2+0.3^2+0.4^2+0.2^2}\times\sqrt{0.3^2+0.6^2+0.4^2+0.6^2+0.9^2}\right)}\right\}+$$

$$\frac{1}{5}\left\{\frac{(0.6)(0.3)+(0.3)(0.4)+(0.4)(0.5)+(0.6)(0.8)+(0.7)(0.6)}{\left(\sqrt{0.6^2+0.3^2+0.4^2+0.6^2+0.7^2}\times\sqrt{0.3^2+0.4^2+0.5^2+0.8^2+0.6^2}\right)}\right\}.$$

$= 0.1619 + 0.1625 + 0.1628 + 0.1583 + 0.1892 = 0.8347.$

For $n = 5$ then $R_3 + C_3 \Rightarrow Cosine_{TVNSS}(T_i, C_j) =$

$$\frac{1}{5}\left\{\frac{(0.5)(0.8)+(0.7)(0.4)+(0.3)(0.6)+(0.4)(0.3)+(0.8)(0.5)}{\left(\sqrt{0.5^2+0.7^2+0.3^2+0.4^2+0.8^2}\times\sqrt{0.8^2+0.4^2+0.6^2+0.3^2+0.5^2}\right)}\right\}+$$

$$\frac{1}{5}\left\{\frac{(0.8)(0.4)+(0.6)(0.5)+(0.4)(0.6)+(0.7)(0.7)+(0.5)(0.4)}{\left(\sqrt{0.8^2+0.6^2+0.4^2+0.7^2+0.5^2}\times\sqrt{0.4^2+0.5^2+0.6^2+0.7^2+0.4^2}\right)}\right\}+$$

$$\frac{1}{5}\left\{\frac{(0.4)(0.4)+(0.6)(0.6)+(0.3)(0.7)+(0.2)(0.8)+(0.6)(0.5)}{\left(\sqrt{0.4^2+0.6^2+0.3^2+0.2^2+0.6^2}\times\sqrt{0.4^2+0.6^2+0.7^2+0.8^2+0.5^2}\right)}\right\}+$$

$\frac{1}{5}\left\{\frac{(0.6)(0.3)+(0.8)(0.6)+(0.3)(0.9)+(0.4)(0.8)+(0.2)(0.4)}{\left(\sqrt{0.6^2+0.8^2+0.3^2+0.4^2+0.2^2}\times\sqrt{0.3^2+0.6^2+0.9^2+0.8^2+0.4^2}\right)}\right\}+$

$\frac{1}{5}\left\{\frac{(0.6)(0.2)+(0.3)(0.7)+(0.4)(0.4)+(0.6)(0.2)+(0.7)(0.8)}{\left(\sqrt{0.6^2+0.3^2+0.4^2+0.6^2+0.7^2}\times\sqrt{0.2^2+0.7^2+0.4^2+0.2^2+0.8^2}\right)}\right\}.$

$= 0.1765 + 0.1887 + 0.1709 + 0.1631 + 0.1583 = 0.8575.$

For $n = 5$ then $R_3 + C_4 \Rightarrow Cosine_{TVNSS}(T_i, C_j) =$

$\frac{1}{5}\left\{\frac{(0.5)(0.7)+(0.7)(0.4)+(0.3)(0.3)+(0.4)(0.2)+(0.8)(0.6)}{\left(\sqrt{0.5^2+0.7^2+0.3^2+0.4^2+0.8^2}\times\sqrt{0.7^2+0.4^2+0.3^2+0.2^2+0.6^2}\right)}\right\}+$

$\frac{1}{5}\left\{\frac{(0.8)(0.8)+(0.6)(0.9)+(0.4)(0.6)+(0.7)(0.5)+(0.5)(0.4)}{\left(\sqrt{0.8^2+0.6^2+0.4^2+0.7^2+0.5^2}\times\sqrt{0.8^2+0.9^2+0.6^2+0.5^2+0.4^2}\right)}\right\}+$

$\frac{1}{5}\left\{\frac{(0.4)(0.7)+(0.6)(0.6)+(0.3)(0.7)+(0.2)(0.6)+(0.6)(0.3)}{\left(\sqrt{0.4^2+0.6^2+0.3^2+0.2^2+0.6^2}\times\sqrt{0.7^2+0.6^2+0.7^2+0.6^2+0.3^2}\right)}\right\}+$

$\frac{1}{5}\left\{\frac{(0.6)(0.3)+(0.8)(0.6)+(0.3)(0.8)+(0.4)(0.4)+(0.2)(0.2)}{\left(\sqrt{0.6^2+0.8^2+0.3^2+0.4^2+0.2^2}\times\sqrt{0.3^2+0.6^2+0.8^2+0.4^2+0.2^2}\right)}\right\}+$

$\frac{1}{5}\left\{\frac{(0.6)(0.1)+(0.3)(0.6)+(0.4)(0.7)+(0.6)(0.6)+(0.7)(0.4)}{\left(\sqrt{0.6^2+0.3^2+0.4^2+0.6^2+0.7^2}\times\sqrt{0.1^2+0.6^2+0.7^2+0.6^2+0.4^2}\right)}\right\}.$

$= 0.1878 + 0.1918 + 0.1710 + 0.1705 + 0.1634 = 0.8845.$

For $n = 5$ then $R_3 + C_5 \Rightarrow Cosine_{TVNSS}(T_i, C_j) =$

$\frac{1}{5}\left\{\frac{(0.5)(0.6)+(0.7)(0.8)+(0.3)(0.7)+(0.4)(0.2)+(0.8)(0.4)}{\left(\sqrt{0.5^2+0.7^2+0.3^2+0.4^2+0.8^2}\times\sqrt{0.6^2+0.8^2+0.7^2+0.2^2+0.4^2}\right)}\right\}+$

$\frac{1}{5}\left\{\frac{(0.8)(0.5)+(0.6)(0.7)+(0.4)(0.6)+(0.7)(0.3)+(0.5)(0.2)}{\left(\sqrt{0.8^2+0.6^2+0.4^2+0.7^2+0.5^2}\times\sqrt{0.5^2+0.7^2+0.6^2+0.3^2+0.2^2}\right)}\right\}+$

$\frac{1}{5}\left\{\frac{(0.4)(0.8)+(0.6)(0.3)+(0.3)(0.4)+(0.2)(0.5)+(0.6)(0.4)}{\left(\sqrt{0.4^2+0.6^2+0.3^2+0.2^2+0.6^2}\times\sqrt{0.8^2+0.3^2+0.4^2+0.5^2+0.4^2}\right)}\right\}+$

$\frac{1}{5}\left\{\frac{(0.6)(0.6)+(0.8)(0.3)+(0.3)(0.4)+(0.4)(0.7)+(0.2)(0.8)}{\left(\sqrt{0.6^2+0.8^2+0.3^2+0.4^2+0.2^2}\times\sqrt{0.6^2+0.3^2+0.4^2+0.7^2+0.8^2}\right)}\right\}+$

$\frac{1}{5}\left\{\frac{(0.6)(0.6)+(0.3)(0.4)+(0.4)(0.1)+(0.6)(0.8)+(0.7)(0.3)}{\left(\sqrt{0.6^2+0.3^2+0.4^2+0.6^2+0.7^2}\times\sqrt{0.6^2+0.4^2+0.1^2+0.8^2+0.3^2}\right)}\right\}.$

$= 0.1771 + 0.1792 + 0.1675 + 0.1548 + 0.1784 = 0.8570.$

For $n = 5$ then $R_4 + C_1 \Rightarrow Cosine_{TVNSS}(T_i, C_j) =$

$\frac{1}{5}\left\{\frac{(0.4)(0.8)+(0.2)(0.6)+(0.3)(0.4)+(0.5)(0.8)+(0.9)(0.2)}{\left(\sqrt{0.4^2+0.2^2+0.3^2+0.5^2+0.9^2}\times\sqrt{0.8^2+0.6^2+0.4^2+0.8^2+0.2^2}\right)}\right\}+$

$\frac{1}{5}\left\{\frac{(0.2)(0.5)+(0.8)(0.4)+(0.3)(0.8)+(0.4)(0.7)+(0.4)(0.6)}{\left(\sqrt{0.2^2+0.8^2+0.3^2+0.4^2+0.4^2}\times\sqrt{0.5^2+0.4^2+0.8^2+0.7^2+0.6^2}\right)}\right\}+$

$\frac{1}{5}\left\{\frac{(0.8)(0.2)+(0.6)(0.6)+(0.4)(0.7)+(0.3)(0.9)+(0.6)(0.8)}{\left(\sqrt{0.8^2+0.6^2+0.4^2+0.3^2+0.6^2}\times\sqrt{0.2^2+0.6^2+0.7^2+0.9^2+0.8^2}\right)}\right\}+$

$\frac{1}{5}\left\{\frac{(0.2)(0.9)+(0.6)(0.3)+(0.4)(0.6)+(0.3)(0.4)+(0.2)(0.2)}{\left(\sqrt{0.2^2+0.6^2+0.4^2+0.3^2+0.2^2}\times\sqrt{0.9^2+0.3^2+0.6^2+0.4^2+0.2^2}\right)}\right\}+$

$\frac{1}{5}\left\{\frac{(0.8)(0.3)+(0.7)(0.6)+(0.3)(0.8)+(0.6)(0.6)+(0.4)(0.4)}{\left(\sqrt{0.8^2+0.7^2+0.3^2+0.6^2+0.4^2}\times\sqrt{0.3^2+0.6^2+0.8^2+0.6^2+0.4^2}\right)}\right\}.$

$= 0.1446 + 0.1306 + 0.1597 + 0.1514 + 0.1694 = 0.7557.$

For $n = 5$ then $R_4 + C_2 \Rightarrow Cosine_{TVNSS}(T_i, C_j) =$

$\frac{1}{5}\left\{\frac{(0.4)(0.3)+(0.2)(0.2)+(0.3)(0.9)+(0.5)(0.6)+(0.9)(0.8)}{\left(\sqrt{0.4^2+0.2^2+0.3^2+0.5^2+0.9^2}\times\sqrt{0.3^2+0.2^2+0.9^2+0.6^2+0.8^2}\right)}\right\}+$

$\frac{1}{5}\left\{\frac{(0.2)(0.6)+(0.8)(0.3)+(0.3)(0.9)+(0.4)(0.2)+(0.4)(0.8)}{\left(\sqrt{0.2^2+0.8^2+0.3^2+0.4^2+0.4^2}\times\sqrt{0.6^2+0.3^2+0.9^2+0.2^2+0.8^2}\right)}\right\}+$

$\frac{1}{5}\left\{\frac{(0.8)(0.9)+(0.6)(0.2)+(0.4)(0.8)+(0.3)(0.4)+(0.6)(0.6)}{\left(\sqrt{0.8^2+0.6^2+0.4^2+0.3^2+0.6^2}\times\sqrt{0.9^2+0.2^2+0.8^2+0.4^2+0.6^2}\right)}\right\}+$

$\frac{1}{5}\left\{\frac{(0.2)(0.3)+(0.6)(0.6)+(0.4)(0.4)+(0.3)(0.6)+(0.2)(0.9)}{\left(\sqrt{0.2^2+0.6^2+0.4^2+0.3^2+0.2^2}\times\sqrt{0.3^2+0.6^2+0.4^2+0.6^2+0.9^2}\right)}\right\}+$

$\frac{1}{5}\left\{\frac{(0.8)(0.3)+(0.7)(0.4)+(0.3)(0.5)+(0.6)(0.8)+(0.4)(0.6)}{\left(\sqrt{0.8^2+0.7^2+0.3^2+0.6^2+0.4^2}\times\sqrt{0.3^2+0.4^2+0.5^2+0.8^2+0.6^2}\right)}\right\}.$

$= 0.1792 + 0.1416 + 0.1823 + 0.1696 + 0.1720 = 0.8447.$

For $n = 5$ then $R_4 + C_3 \Rightarrow Cosine_{TVNSS}(T_i, C_j) =$

$\frac{1}{5}\left\{\frac{(0.4)(0.8)+(0.2)(0.4)+(0.3)(0.6)+(0.5)(0.3)+(0.9)(0.5)}{\left(\sqrt{0.4^2+0.2^2+0.3^2+0.5^2+0.9^2}\times\sqrt{0.8^2+0.4^2+0.6^2+0.3^2+0.5^2}\right)}\right\}+$

$\frac{1}{5}\left\{\frac{(0.2)(0.4)+(0.8)(0.5)+(0.3)(0.6)+(0.4)(0.7)+(0.4)(0.4)}{\left(\sqrt{0.2^2+0.8^2+0.3^2+0.4^2+0.4^2}\times\sqrt{0.4^2+0.5^2+0.6^2+0.7^2+0.4^2}\right)}\right\}+$

$\frac{1}{5}\left\{\frac{(0.8)(0.4)+(0.6)(0.6)+(0.4)(0.7)+(0.3)(0.8)+(0.6)(0.5)}{\left(\sqrt{0.8^2+0.6^2+0.4^2+0.3^2+0.6^2}\times\sqrt{0.4^2+0.6^2+0.7^2+0.8^2+0.5^2}\right)}\right\}+$

$\frac{1}{5}\left\{\frac{(0.2)(0.3)+(0.6)(0.6)+(0.4)(0.9)+(0.3)(0.8)+(0.2)(0.4)}{\left(\sqrt{0.2^2+0.6^2+0.4^2+0.3^2+0.2^2}\times\sqrt{0.3^2+0.6^2+0.9^2+0.8^2+0.4^2}\right)}\right\}+$

$\frac{1}{5}\left\{\frac{(0.8)(0.2)+(0.7)(0.7)+(0.3)(0.4)+(0.6)(0.2)+(0.4)(0.8)}{\left(\sqrt{0.8^2+0.7^2+0.3^2+0.6^2+0.4^2}\times\sqrt{0.2^2+0.7^2+0.4^2+0.2^2+0.8^2}\right)}\right\}.$

$= 0.1658 + 0.1768 + 0.1715 + 0.1563 + 0.1567 = 0.8271.$

For $n = 5$ then $R_4 + C_4 \Rightarrow Cosine_{TVNSS}(T_i, C_j) =$

$\frac{1}{5}\left\{\frac{(0.4)(0.7)+(0.2)(0.4)+(0.3)(0.3)+(0.5)(0.2)+(0.9)(0.6)}{\left(\sqrt{0.4^2+0.2^2+0.3^2+0.5^2+0.9^2}\times\sqrt{0.7^2+0.4^2+0.3^2+0.2^2+0.6^2}\right)}\right\}+$

$\frac{1}{5}\left\{\frac{(0.2)(0.8)+(0.8)(0.9)+(0.3)(0.6)+(0.4)(0.5)+(0.4)(0.4)}{\left(\sqrt{0.2^2+0.8^2+0.3^2+0.4^2+0.4^2}\times\sqrt{0.8^2+0.9^2+0.6^2+0.5^2+0.4^2}\right)}\right\}+$

$\frac{1}{5}\left\{\frac{(0.8)(0.7)+(0.6)(0.6)+(0.4)(0.7)+(0.3)(0.6)+(0.6)(0.3)}{\left(\sqrt{0.8^2+0.6^2+0.4^2+0.3^2+0.6^2}\times\sqrt{0.7^2+0.6^2+0.7^2+0.6^2+0.3^2}\right)}\right\}+$

$\frac{1}{5}\left\{\frac{(0.2)(0.3)+(0.6)(0.6)+(0.4)(0.8)+(0.3)(0.4)+(0.2)(0.2)}{\left(\sqrt{0.2^2+0.6^2+0.4^2+0.3^2+0.2^2}\times\sqrt{0.3^2+0.6^2+0.8^2+0.4^2+0.2^2}\right)}\right\}+$

$\frac{1}{5}\left\{\frac{(0.8)(0.1)+(0.7)(0.6)+(0.3)(0.7)+(0.6)(0.6)+(0.4)(0.4)}{\left(\sqrt{0.8^2+0.7^2+0.3^2+0.6^2+0.4^2}\times\sqrt{0.1^2+0.6^2+0.7^2+0.6^2+0.4^2}\right)}\right\}.$

$= 0.1757 + 0.1825 + 0.1837 + 0.1907 + 0.1587 = 0.8913.$

For $n = 5$ then $R_4 + C_5 \Rightarrow Cosine_{TVNSS}(T_i, C_j) =$

$\frac{1}{5}\left\{\frac{(0.4)(0.6)+(0.2)(0.8)+(0.3)(0.7)+(0.5)(0.2)+(0.9)(0.4)}{\left(\sqrt{0.4^2+0.2^2+0.3^2+0.5^2+0.9^2}\times\sqrt{0.6^2+0.8^2+0.7^2+0.2^2+0.4^2}\right)}\right\}+$

$\frac{1}{5}\left\{\frac{(0.2)(0.5)+(0.8)(0.7)+(0.3)(0.6)+(0.4)(0.3)+(0.4)(0.2)}{\left(\sqrt{0.2^2+0.8^2+0.3^2+0.4^2+0.4^2}\times\sqrt{0.5^2+0.7^2+0.6^2+0.3^2+0.2^2}\right)}\right\}+$

$\frac{1}{5}\left\{\frac{(0.8)(0.8)+(0.6)(0.3)+(0.4)(0.4)+(0.3)(0.5)+(0.6)(0.4)}{\left(\sqrt{0.8^2+0.6^2+0.4^2+0.3^2+0.6^2}\times\sqrt{0.8^2+0.3^2+0.4^2+0.5^2+0.4^2}\right)}\right\}+$

$\frac{1}{5}\left\{\frac{(0.2)(0.6)+(0.6)(0.3)+(0.4)(0.4)+(0.3)(0.7)+(0.2)(0.8)}{\left(\sqrt{0.2^2+0.6^2+0.4^2+0.3^2+0.2^2}\times\sqrt{0.6^2+0.3^2+0.4^2+0.7^2+0.8^2}\right)}\right\}+$

$\frac{1}{5}\left\{\frac{(0.8)(0.6)+(0.7)(0.4)+(0.3)(0.1)+(0.6)(0.8)+(0.4)(0.3)}{\left(\sqrt{0.8^2+0.7^2+0.3^2+0.6^2+0.4^2}\times\sqrt{0.6^2+0.4^2+0.1^2+0.8^2+0.3^2}\right)}\right\}.$

$= 0.1416 + 0.1797 + 0.1893 + 0.1515 + 0.1877 = 0.8498.$

For $n = 5$ then $R_5 + C_1 \Rightarrow Cosine_{TVNSS}(T_i, C_j) =$

$\frac{1}{5}\left\{\frac{(0.7)(0.8)+(0.6)(0.6)+(0.8)(0.4)+(0.3)(0.8)+(0.1)(0.2)}{\left(\sqrt{0.7^2+0.6^2+0.8^2+0.3^2+0.1^2} \times \sqrt{0.8^2+0.6^2+0.4^2+0.8^2+0.2^2}\right)}\right\}+$

$\frac{1}{5}\left\{\frac{(0.3)(0.5)+(0.8)(0.4)+(0.9)(0.8)+(0.5)(0.7)+(0.4)(0.6)}{\left(\sqrt{0.3^2+0.8^2+0.9^2+0.5^2+0.4^2} \times \sqrt{0.5^2+0.4^2+0.8^2+0.7^2+0.6^2}\right)}\right\}+$

$\frac{1}{5}\left\{\frac{(0.9)(0.2)+(0.3)(0.6)+(0.2)(0.7)+(0.6)(0.9)+(0.8)(0.8)}{\left(\sqrt{0.9^2+0.3^2+0.2^2+0.6^2+0.8^2} \times \sqrt{0.2^2+0.6^2+0.7^2+0.9^2+0.8^2}\right)}\right\}+$

$\frac{1}{5}\left\{\frac{(0.8)(0.9)+(0.9)(0.3)+(0.3)(0.6)+(0.4)(0.4)+(0.3)(0.2)}{\left(\sqrt{0.8^2+0.9^2+0.3^2+0.4^2+0.3^2} \times \sqrt{0.9^2+0.3^2+0.6^2+0.4^2+0.2^2}\right)}\right\}+$

$\frac{1}{5}\left\{\frac{(0.2)(0.3)+(0.6)(0.6)+(0.5)(0.8)+(0.7)(0.6)+(0.8)(0.4)}{\left(\sqrt{0.2^2+0.6^2+0.5^2+0.7^2+0.8^2} \times \sqrt{0.3^2+0.6^2+0.8^2+0.6^2+0.4^2}\right)}\right\}.$

$= 0.1753 + 0.1849 + 0.1577 + 0.1720 + 0.1843 = 0.8742.$

For $n = 5$ then $R_5 + C_2 \Rightarrow Cosine_{TVNSS}(T_i, C_j) =$

$\frac{1}{5}\left\{\frac{(0.7)(0.3)+(0.6)(0.2)+(0.8)(0.9)+(0.3)(0.6)+(0.1)(0.8)}{\left(\sqrt{0.7^2+0.6^2+0.8^2+0.3^2+0.1^2} \times \sqrt{0.3^2+0.2^2+0.9^2+0.6^2+0.8^2}\right)}\right\}+$

$\frac{1}{5}\left\{\frac{(0.3)(0.6)+(0.8)(0.3)+(0.9)(0.9)+(0.5)(0.2)+(0.4)(0.8)}{\left(\sqrt{0.3^2+0.8^2+0.9^2+0.5^2+0.4^2} \times \sqrt{0.6^2+0.3^2+0.9^2+0.2^2+0.8^2}\right)}\right\}+$

$\frac{1}{5}\left\{\frac{(0.9)(0.9)+(0.3)(0.2)+(0.2)(0.8)+(0.6)(0.4)+(0.8)(0.6)}{\left(\sqrt{0.9^2+0.3^2+0.2^2+0.6^2+0.8^2} \times \sqrt{0.9^2+0.2^2+0.8^2+0.4^2+0.6^2}\right)}\right\}+$

$\frac{1}{5}\left\{\frac{(0.8)(0.3)+(0.9)(0.6)+(0.3)(0.4)+(0.4)(0.6)+(0.3)(0.9)}{\left(\sqrt{0.8^2+0.9^2+0.3^2+0.4^2+0.3^2} \times \sqrt{0.3^2+0.6^2+0.4^2+0.6^2+0.9^2}\right)}\right\}+$

$\frac{1}{5}\left\{\frac{(0.2)(0.3)+(0.6)(0.4)+(0.5)(0.5)+(0.7)(0.8)+(0.8)(0.6)}{\left(\sqrt{0.2^2+0.6^2+0.5^2+0.7^2+0.8^2} \times \sqrt{0.3^2+0.4^2+0.5^2+0.8^2+0.6^2}\right)}\right\}.$

$= 0.1491 + 0.1696 + 0.1772 + 0.1579 + 0.1946 = 0.8484.$

For $n = 5$ then $R_5 + C_3 \Rightarrow Cosine_{TVNSS}(T_i, C_j) =$

$\frac{1}{5}\left\{\frac{(0.7)(0.8)+(0.6)(0.4)+(0.8)(0.6)+(0.3)(0.3)+(0.1)(0.5)}{\left(\sqrt{0.7^2+0.6^2+0.8^2+0.3^2+0.1^2} \times \sqrt{0.8^2+0.4^2+0.6^2+0.3^2+0.5^2}\right)}\right\}+$

$\frac{1}{5}\left\{\frac{(0.3)(0.4)+(0.8)(0.5)+(0.9)(0.6)+(0.5)(0.7)+(0.4)(0.4)}{\left(\sqrt{0.3^2+0.8^2+0.9^2+0.5^2+0.4^2} \times \sqrt{0.4^2+0.5^2+0.6^2+0.7^2+0.4^2}\right)}\right\}+$

$\frac{1}{5}\left\{\frac{(0.9)(0.4)+(0.3)(0.6)+(0.2)(0.7)+(0.6)(0.8)+(0.8)(0.5)}{\left(\sqrt{0.9^2+0.3^2+0.2^2+0.6^2+0.8^2} \times \sqrt{0.4^2+0.6^2+0.7^2+0.8^2+0.5^2}\right)}\right\}+$

$\frac{1}{5}\left\{\frac{(0.8)(0.3)+(0.9)(0.6)+(0.3)(0.9)+(0.4)(0.8)+(0.3)(0.4)}{\left(\sqrt{0.8^2+0.9^2+0.3^2+0.4^2+0.3^2} \times \sqrt{0.3^2+0.6^2+0.9^2+0.8^2+0.4^2}\right)}\right\}+$

$\frac{1}{5}\left\{\frac{(0.2)(0.2)+(0.6)(0.7)+(0.5)(0.4)+(0.7)(0.2)+(0.8)(0.8)}{\left(\sqrt{0.2^2+0.6^2+0.5^2+0.7^2+0.8^2} \times \sqrt{0.2^2+0.7^2+0.4^2+0.2^2+0.8^2}\right)}\right\}.$

$= 0.1839 + 0.1887 + 0.1625 + 0.1551 + 0.1844 = 0.8746.$

For $n = 5$ then $R_5 + C_4 \Rightarrow Cosine_{TVNSS}(T_i, C_j) =$

$\frac{1}{5}\left\{\frac{(0.7)(0.7)+(0.6)(0.4)+(0.8)(0.3)+(0.3)(0.2)+(0.1)(0.6)}{\left(\sqrt{0.7^2+0.6^2+0.8^2+0.3^2+0.1^2} \times \sqrt{0.7^2+0.4^2+0.3^2+0.2^2+0.6^2}\right)}\right\}+$

$\frac{1}{5}\left\{\frac{(0.3)(0.8)+(0.8)(0.9)+(0.9)(0.6)+(0.5)(0.5)+(0.4)(0.4)}{\left(\sqrt{0.3^2+0.8^2+0.9^2+0.5^2+0.4^2} \times \sqrt{0.8^2+0.9^2+0.6^2+0.5^2+0.4^2}\right)}\right\}+$

$\frac{1}{5}\left\{\frac{(0.9)(0.7)+(0.3)(0.6)+(0.2)(0.7)+(0.6)(0.6)+(0.8)(0.3)}{\left(\sqrt{0.9^2+0.3^2+0.2^2+0.6^2+0.8^2} \times \sqrt{0.7^2+0.6^2+0.7^2+0.6^2+0.3^2}\right)}\right\}+$

$\frac{1}{5}\left\{\frac{(0.8)(0.3)+(0.9)(0.6)+(0.3)(0.8)+(0.4)(0.4)+(0.3)(0.2)}{\left(\sqrt{0.8^2+0.9^2+0.3^2+0.4^2+0.3^2} \times\sqrt{0.3^2+0.6^2+0.8^2+0.4^2+0.2^2}\right)}\right\}+$
$\frac{1}{5}\left\{\frac{(0.2)(0.1)+(0.6)(0.6)+(0.5)(0.7)+(0.7)(0.6)+(0.8)(0.4)}{\left(\sqrt{0.2^2+0.6^2+0.5^2+0.7^2+0.8^2} \times\sqrt{0.1^2+0.6^2+0.7^2+0.6^2+0.4^2}\right)}\right\}.$
$= 0.1619 + 0.1836 + 0.1663 + 0.1632 + 0.1875 = 0.8625.$

For $n = 5$ then $R_5 + C_5 \Rightarrow Cosine_{TVNSS}(T_i, C_j) =$
$\frac{1}{5}\left\{\frac{(0.7)(0.6)+(0.6)(0.8)+(0.8)(0.7)+(0.3)(0.2)+(0.1)(0.4)}{\left(\sqrt{0.7^2+0.6^2+0.8^2+0.3^2+0.1^2} \times\sqrt{0.6^2+0.8^2+0.7^2+0.2^2+0.4^2}\right)}\right\}+$
$\frac{1}{5}\left\{\frac{(0.3)(0.5)+(0.8)(0.7)+(0.9)(0.6)+(0.5)(0.3)+(0.4)(0.2)}{\left(\sqrt{0.3^2+0.8^2+0.9^2+0.5^2+0.4^2} \times\sqrt{0.5^2+0.7^2+0.6^2+0.3^2+0.2^2}\right)}\right\}+$
$\frac{1}{5}\left\{\frac{(0.9)(0.8)+(0.3)(0.3)+(0.2)(0.4)+(0.6)(0.5)+(0.8)(0.4)}{\left(\sqrt{0.9^2+0.3^2+0.2^2+0.6^2+0.8^2} \times\sqrt{0.8^2+0.3^2+0.4^2+0.5^2+0.4^2}\right)}\right\}+$
$\frac{1}{5}\left\{\frac{(0.8)(0.6)+(0.9)(0.3)+(0.3)(0.4)+(0.4)(0.7)+(0.3)(0.8)}{\left(\sqrt{0.8^2+0.9^2+0.3^2+0.4^2+0.3^2} \times\sqrt{0.6^2+0.3^2+0.4^2+0.7^2+0.8^2}\right)}\right\}+$
$\frac{1}{5}\left\{\frac{(0.2)(0.6)+(0.6)(0.4)+(0.5)(0.1)+(0.7)(0.8)+(0.8)(0.3)}{\left(\sqrt{0.2^2+0.6^2+0.5^2+0.7^2+0.8^2} \times\sqrt{0.6^2+0.4^2+0.1^2+0.8^2+0.3^2}\right)}\right\}.$
$= 0.1902 + 0.1911 + 0.1901 + 0.1575 + 0.1616 = 0.8905.$

Last but not least, the cosine similarity typically ranges from 0 to 1, where 0 indicates no resemblance and 1 indicates a perfect match. The fact that the distance value between 0 and 1 falls within this range suggests that the points are near to one another. As a result, for P_1, P_2, P_3, P_4 and P_5, the cosine similarity yields maximum values of 0.8878, 0.9107, 0.8845, 0.8913, and 0.8905. Regarding this, while we are making decisions for each patient, we should think about using the highest classification value.

Table 5.3.3: Cosine SM Results for P1 to P4 across D1 to D5

Cosine SM	D_1	D_2	D_3	D_4	D_5
P_1	0.7904	0.8096	0.8467	0.8724	**0.8878**
P_2	**0.9107**	0.8717	0.9004	0.8883	0.8201
P_3	0.8597	0.8347	0.8575	**0.8845**	0.8570
P_4	0.7557	0.8447	0.8271	**0.8913**	0.8498
P_5	0.8742	0.8484	0.8746	0.8625	**0.8905**

This table pertains to similarity values derived from tangents for comparing patients with decision alternatives and preconditions involved in utilizing maximum similarity levels.

6. Results and discussions

A 2D similarity matrix of the Cosine similarity of Patients (P1–P5) against Diseases (D1–D5) is visualized in **fig. 6.1** by plotting the cool-warm colormap, which has a range of deep blue to red. Red indicates a very high resemblance (0.89) to 0.91. The single cell with an encircling marker indicated is the most significant and robust match with P2–D1 (0.9107). P4-D4 (0.8913) and P5-D5 (0.8905) have warm reddish 0.89. Comparing cells like P1 D4 (0.8724) and P2 D4 (0.8883) reveals a high degree of similarity (≈ 0.87 0.89). The values between P1-D3 (0.8467) and P3-D5 (0.8570) are included in the moderate similarity (0.84–0.87). Reduced similarity is indicated by redder blues (c. 0.75–0.83), such as P4D1 (0.7557), P1D1 (0.7904), and P2D5 (0.8201). The map shows the single crucial match and gives a one-second visual indicator of the classification reliability in terms of color intensity.

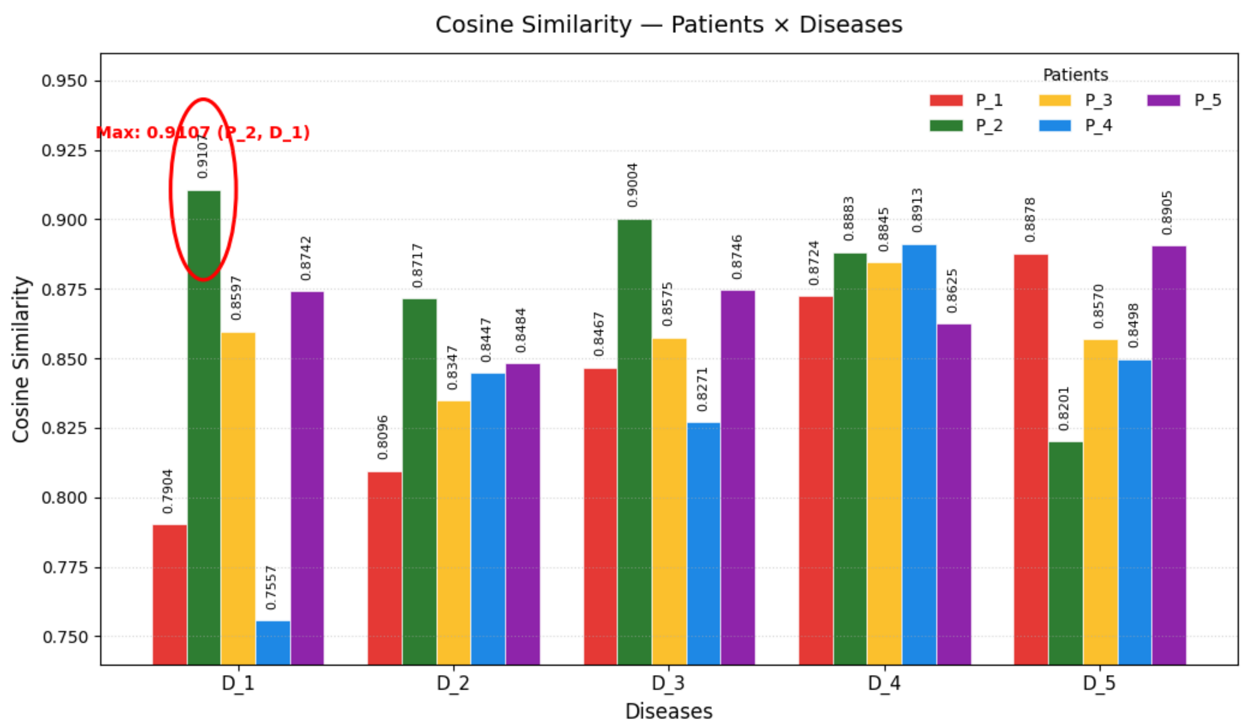

Fig 6.1

A 3D grouped bar chart showing the cosine similarity between diseases (D1-D5) and patients (P1-P5) is shown in **fig 2** below. According to the legend, the color of the ladders identifies the patient, and their height registers resemblance. On the plot, P2D1 (0.9107), the best and most important match, is indicated. P 2 - D3 (0.9004), P 4-D4 (0.8913), and P 5-D5 (0.8905) are further extremely high values with a range of 0.89-0.91. There is a strong resemblance (= 0.87-0.89) between P1-D4 (0.8724) and P2-D4 (0.8883). Cells like P1-D3 (= 0.8467), P3-D5 (= 0.8570), P3-D1 (= 0.8597), and P5-D4 (= 0.8625) are included in the moderate resemblance (= 0.84-0.87).P4 -D1 (0.7557), P1 -D1 (0.7904), P2 -D5 (0.8201), and P4 -D3 (0.8271) all exhibit lower similarity (= 0.75 -0.83). As there is just one peak that predominates in P2-D1 and a prominent ridge in D4 where the majority of patients score highly, classification reliability is generally immediately readable visually in the chart by the height of the bar.

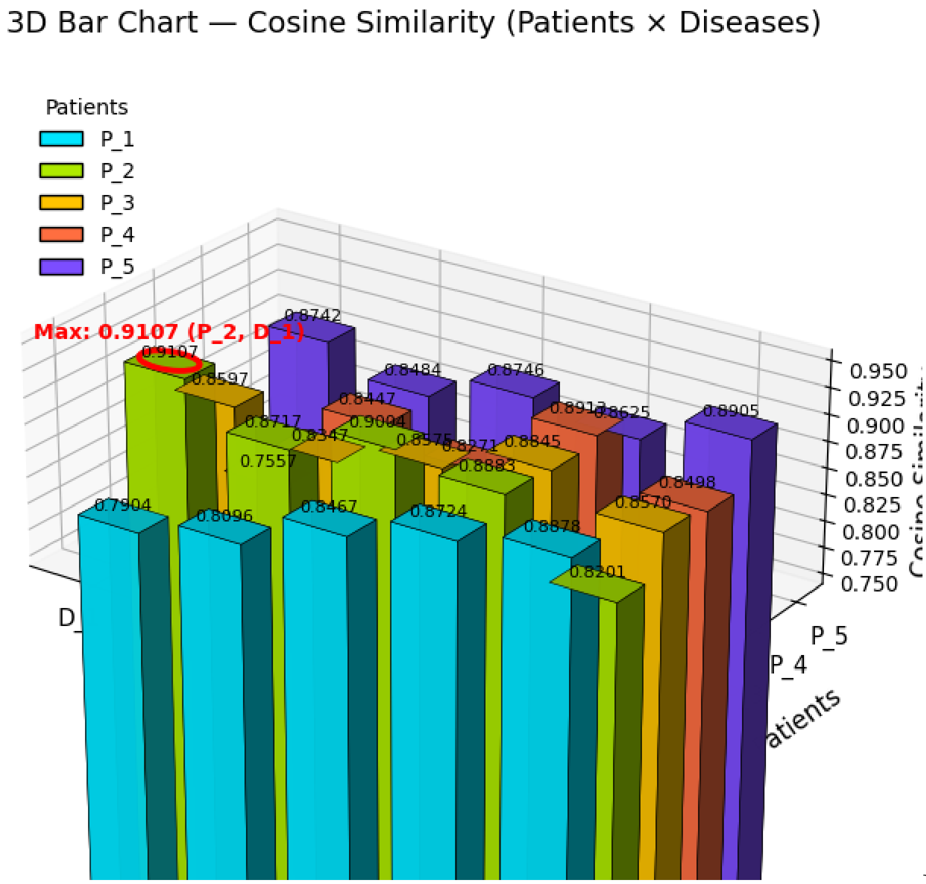

Fig6.2

Using a cool-warm colormap with deep-blue to red color ranges, **fig.6.3** shows the cosine similarity matrix of the Patients (P1-P5) across Diseases (D1-D5) in two dimensions. Red colors indicate very high similarities (≈ 0.89 - 0.91). P2D1 (0.9107), the single cell with an encircling marker, is the most important and definitive match. There are P45D4 (0.8913) and P55D5 (0.8905) in the warm reddish colorations about 0.89. Strong similarities (= 0.873-0.89) can be found between cells like P1-D4 (= 0.8724) and P2-D4 (= 0.8883). P1-D3 (= 0.8467) and P3-D5 (= 0.8570) are included in the moderate resemblance (= 0.84 -0.87). Cooler blue tones (0.7557, 0.7904, and 0.8201), specifically P4-D1 0.7557, P1-D1 0.7904, and P2-D5 0.8201, indicate lower similarity. The map indicates the one crucial match that was most noticeable and offers a condensed visual representation of categorization reliability through color intensity.

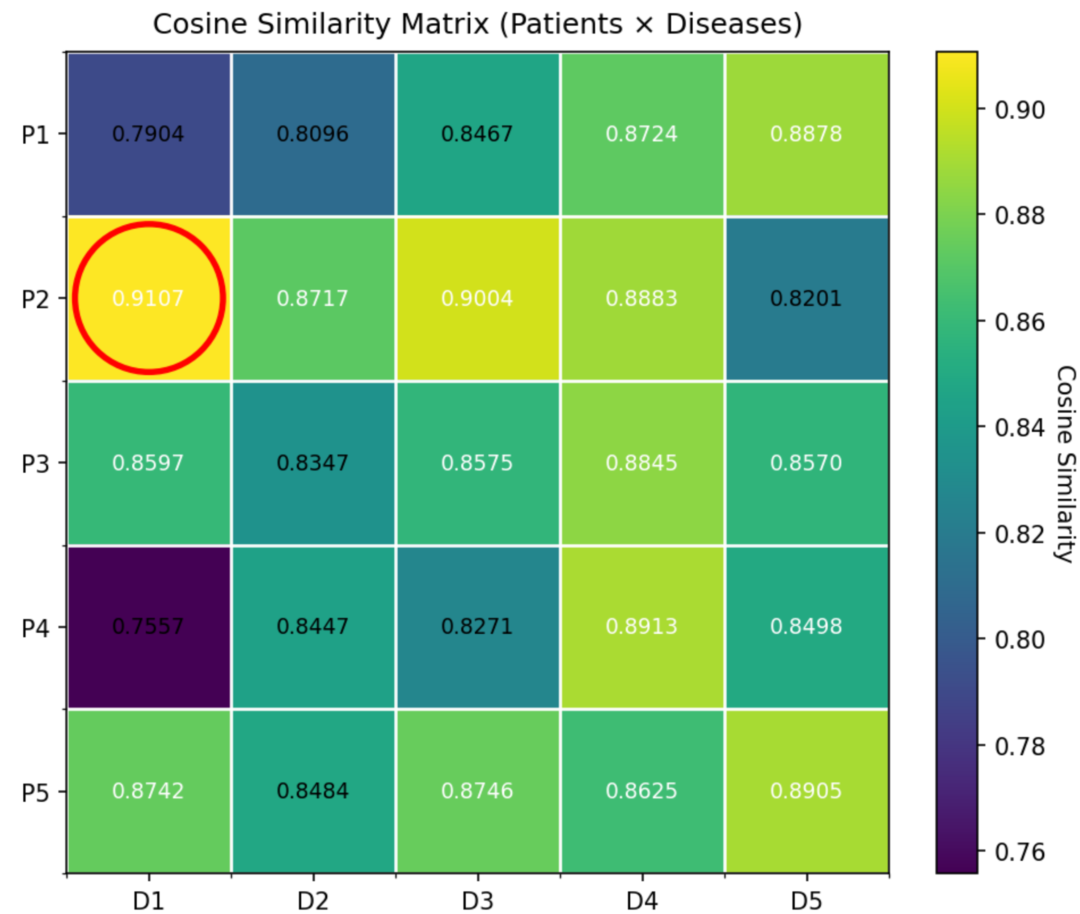

Fig 6.3

Fig 6.4 shows a normalized 2D similarity cosine matrix of Patients (P1-P5) by Diseases (D1-D5) using a cool-warm colormap that transitions from deep blue to red. Over the whole matrix, the values are min max normalized to the 0–1 range. Red indicates marked similarities (= -.93-1.00). The strongest and most decisive match of all is P2D1 (1.0000), which is merely indicated by an encircling mark. P2-D3(0.9335), P4-D4(0.8748), P5-D5(0.8697), and P2-D4(0.8555) are non-blue colors that are found in the 0.85–1.90 range.

Cells like P1 D5 (0.8523), P3 D4 (0.8310), P1 D4 (0.7529), P5 D1 (0.7645), and P5 D3 (0.7671) exhibit good similarity (≈ 0.70 0.85). P3-D1 (0.6710), P5-D4 (0.6890), P3-D3 (0.6568), P4-D5 (0.6071), and P1-D3 (0.5871) are all linked to moderate similarities (= 0.50-0.70). Cooler blue tones (= 0.00–0.50) indicate reduced similarity; they include P4D1 (0.0000), P2D5 (0.4155), P1D1 (0.2239), P1D2 (0.3477), and P4D3 (0.4606). The map offers a visual representation of the individual definitive match and the classification reliability on a normalized scale.

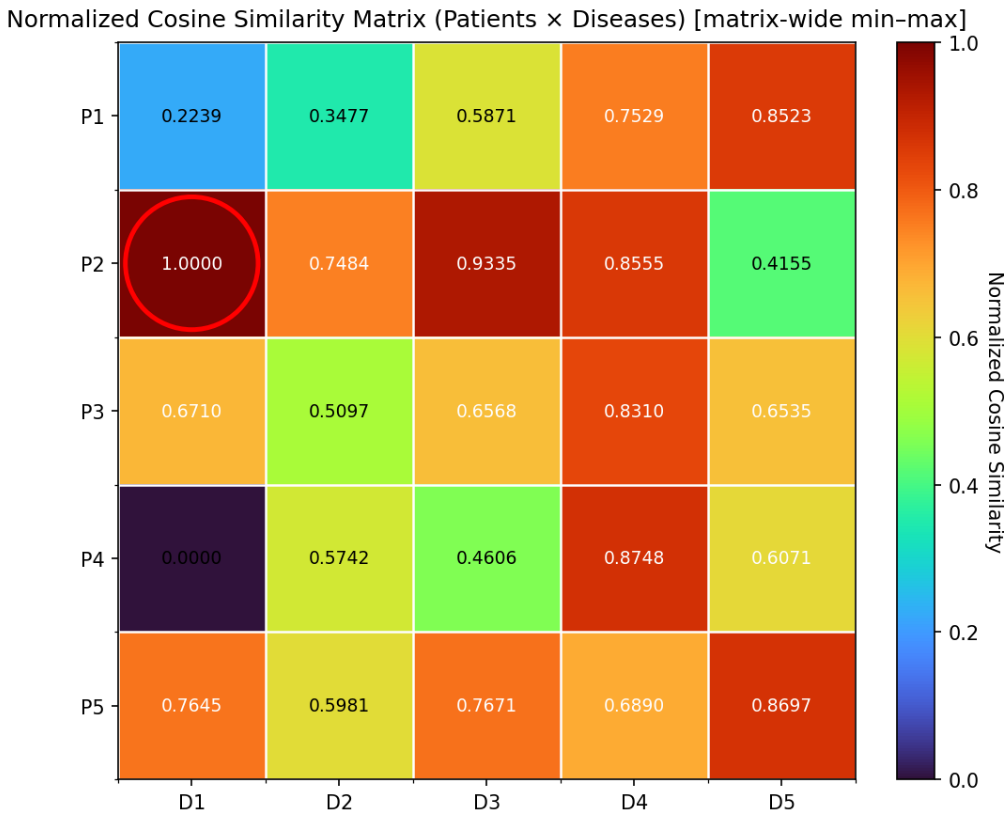

Fig 6.4

Fig 6.5 shows a Pearson Correlation Matrix of Patients (P1-P5) vs. Diseases (D1-D5) using a red yellow-green diverging colormap (green lower and red higher). Shades of red indicate very high similarities (≈ 0.89 - 0.91). The sole cell with an encircling marker highlighted is the most significant and overwhelming match (P2D1) (0.911). Warm reddish hues are present, with P4 (0.891) and P5 (0.890) at roughly 0.89.

Cells like P1D4 (0.872) and P2D4 (0.888) exhibit a considerable resemblance (~ 0.87 0.89). Values such as P1D3 (=0.847) and P3D5 (=0.857) are included in the moderate similarity (= 0.84087). Cooler greenish values (= -0.75-0.83), like P4D1 (= 0.756), P1D1 (= 0.790), and P2D5 (= 0.820), indicate lower similarity. The map highlights the most important match and offers a quick visual review of the classification's dependability based on color intensity.

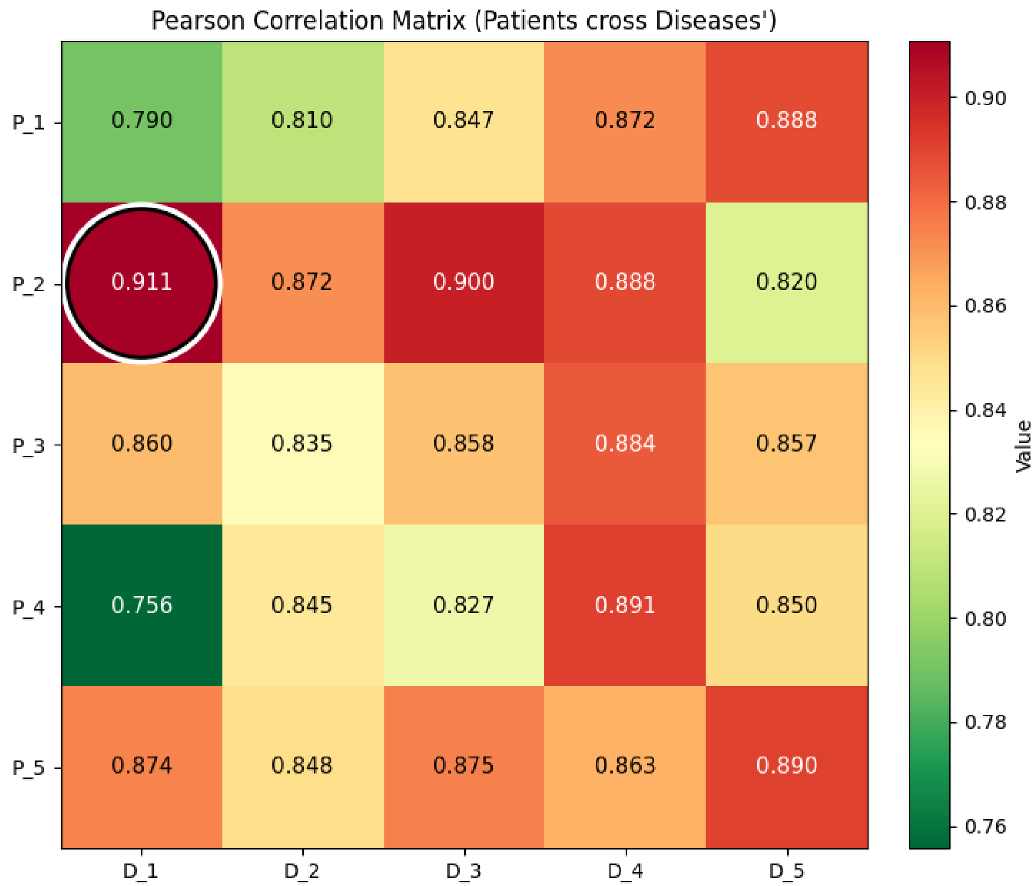

Fig 6.5

A normalized Pearson correlation matrix of Patients (P1-P5) by Diseases (D1-D5) is represented by a diverging colormap of red, yellow, and green that is normalized to 0-1 throughout the entire matrix in **Fig 6.6.** Green denotes a low correlation of almost 0.0, whereas deep red denotes a very strong correlation of nearly 1.0. The strongest matches—P2 one to D1, P1 to D5, P3 to D4, P4 to D4, and P5 to D5—are grouped together and are all on the 1.000 ceiling. Very strong but sub-maximal matches, such as P2-D3 (0.886), P1-D4 (0.842), P4-D2 (0.656), and P5-D3 (0.622), are reflected by warm tones. Cells with intermediate levels of association, such as P3-D3 (0.458), P4-D3 (0.527), and P3-D1 (0.502), exhibit mid values between 0.45 and 0.70. Cool greens between -0.35 and -0.00, such P4-D1 (0.000), P2-D5 (0.000), P3-D2 (0.000), P1-D1 (0.000), and P5-D4 (0.335), show weak alignment. The map provides a quick visual depiction of the classification's dependability after normalization, as well as the locations of the strongest matches made row-to-row.

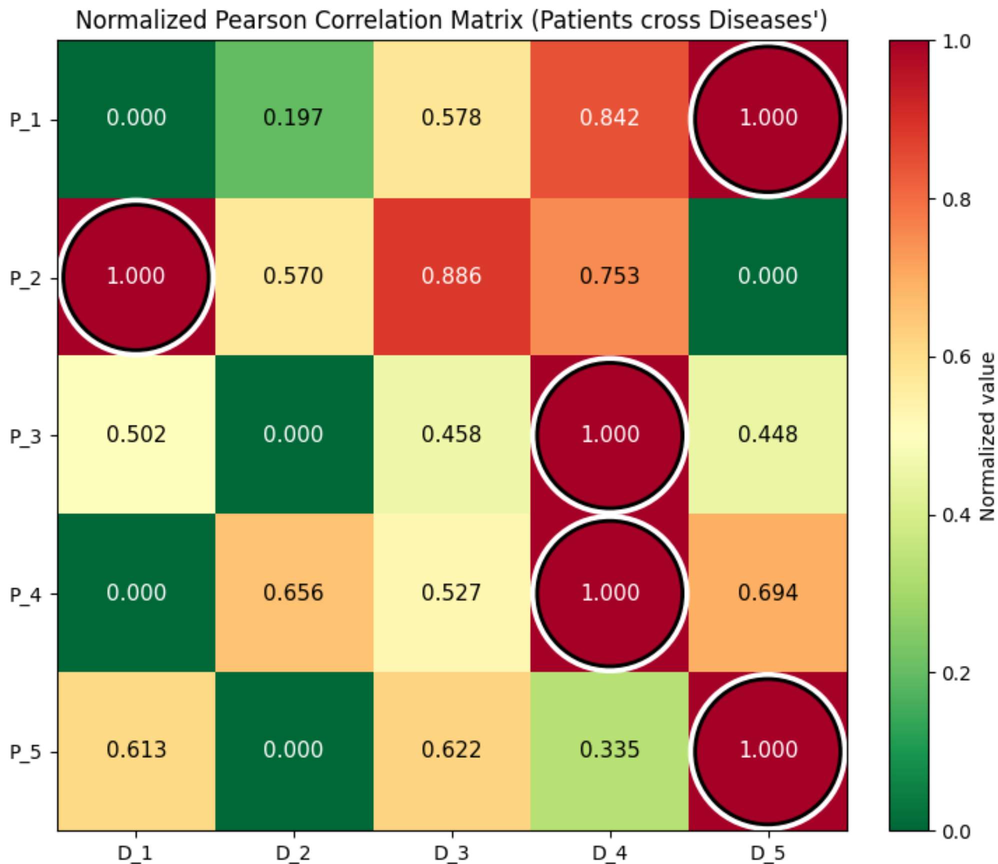

Fig 6.6.

The cool-to-warm perceptual colormap is used in **fig 6.7** to show a three-dimensional surface of the matrix of cosine similarity between Diseases (D1-D5) and Patients (P1-P5). Warm hues and height are more representative of similarity. The lowest valley (P4D1 0.7557) is shown after the highest peak (P2D1 0.9107). P2D1 (0.9107), P4D4 (0.8913), and P5D5 (0.8905) had very high (= 0.890.91) values. P1-D4 (= 0.8724), P2-D4 (= 0.8883), P3-D4 (= 0.8845), and P1-D5 (= 0.8878) make up the strong resemblance (= 0.87-0.89). Cells like P1-D3 (0.8467), P3-D5 (0.8570), P3-D1 (0.8597), and P5-D4 (0.8625) are included in the moderate similarity (0.84-0.87). The similarity between P4D1 (0.7557), P1D1 (0.7904), P2D5 (0.8201), and P4D3 (0.8271) is minimal (0.75-0.83). The entire scenery appears transparent due to the surface: the consistent elevation of D4, the strong angles of P1 and P5 at D5, and even one notable peak at P2-D1.

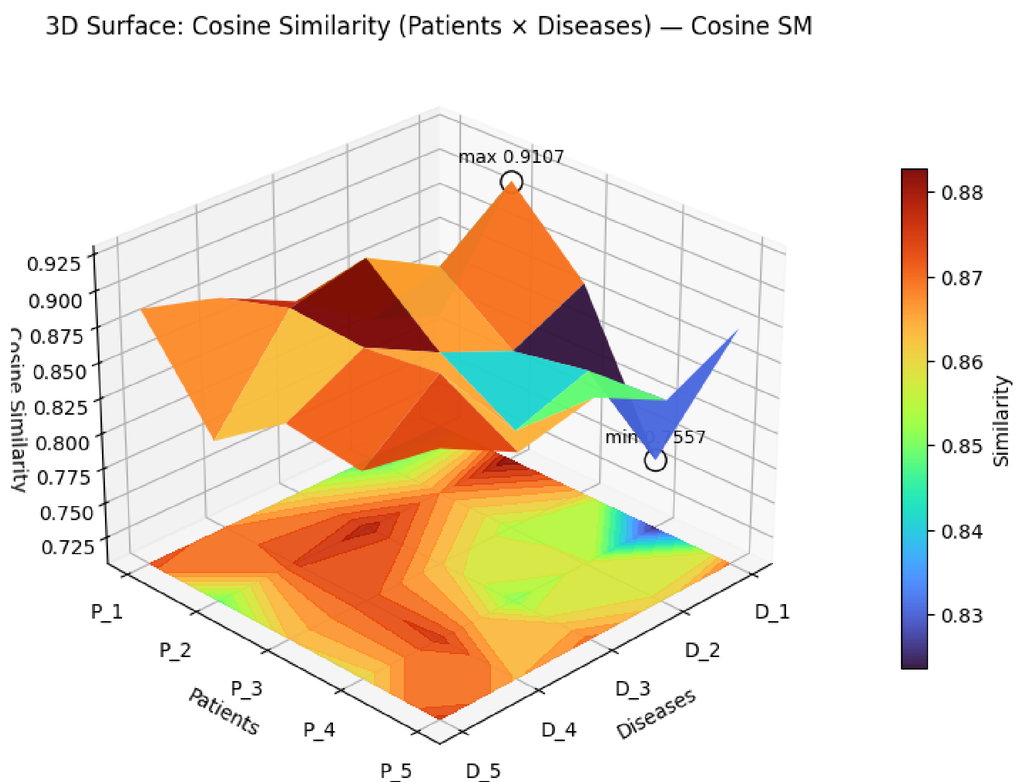

Fig 6.7

Fig 6.8 shows a 3D surface of the cosine similarity matrix of Patients (P1-P5) versus Diseases (D1-D5) with a cool-warm colormap and global min1-max1 normalization to 0-1. Warm hues and height indicate a very high normalized similarity (= 0.851.00). P2D1 (1.000), the biggest and most significant peak, is shown. P2D3 (0.9335), P4D4 (0.8748), P5D5 (0.8697), and P2D4 (0.8555) are the other noteworthy highs. At P1-D5 (0.8523), P3-D4 (0.8310), P1-D4 (0.7529), P5-D1 (0.7645), and P5-D3 (0.7671), there are strong but somewhat weaker ridges (= 0.700-0.85). P3-D1 (= 0.6710), P5-D4 (= 0.6890), P3-D3 (= 0.6568), P4-D5 (= 0.6071), and P1-D3 (= 0.5871) are moderate plateaus (= -0.50-0.70). Less similarity is indicated by cool troughs (= 0.000-0.500), such as P4D1 (= 0.000), P2D5 (= 0.4155), P1D1 (= 0.2239), P1D2 (= 0.3477), and P4D3 (= 0.4606). The surface highlights the individual most important summit and offers a quick global picture of the classification's dependability when in a normalization condition.

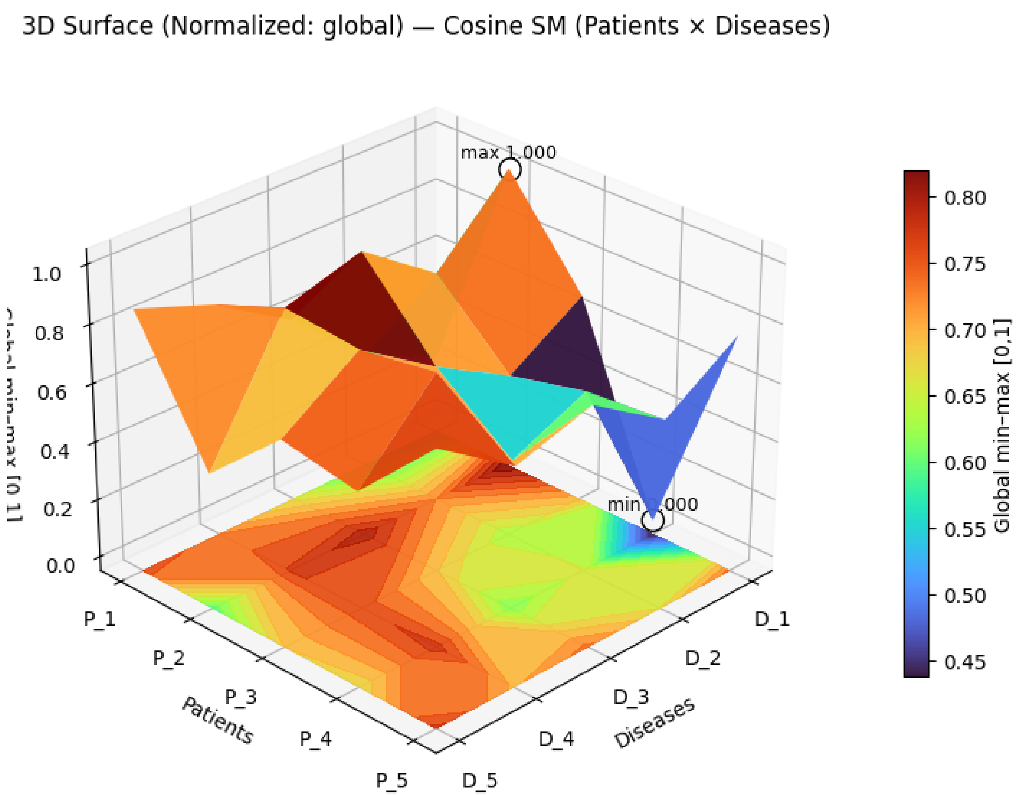

Fig 6.8

A 3D PCA clustering of the cosine similarity matrix of the diseases (D1 to D5) versus the patients (P1 to P5) is shown in **Fig 6.9**. The points are colored by the k-means labels; Cluster 0 is purple, while Cluster 1 is yellow. The PC1PC2 perspective already accounts for 96.9 percent of the structure, with PC1 explaining 80.7 percent of the variance, PC2 explaining 16.2 percent, and PC3 explaining 3.1 percent. There are two clear clusters: Cluster 1 = P1, P4, and Cluster 0 = P2, P3, and P5. P2 and P5 are on the positive side, P1 and P4 are on the negative side, and P3 is closer to Cluster 0. Separation mostly takes place along PC1. PC3 is not noteworthy, and PC2 shows a small dispersion across each group's members. The figure reads the similarity structure quickly, and the two-cluster division is stable.

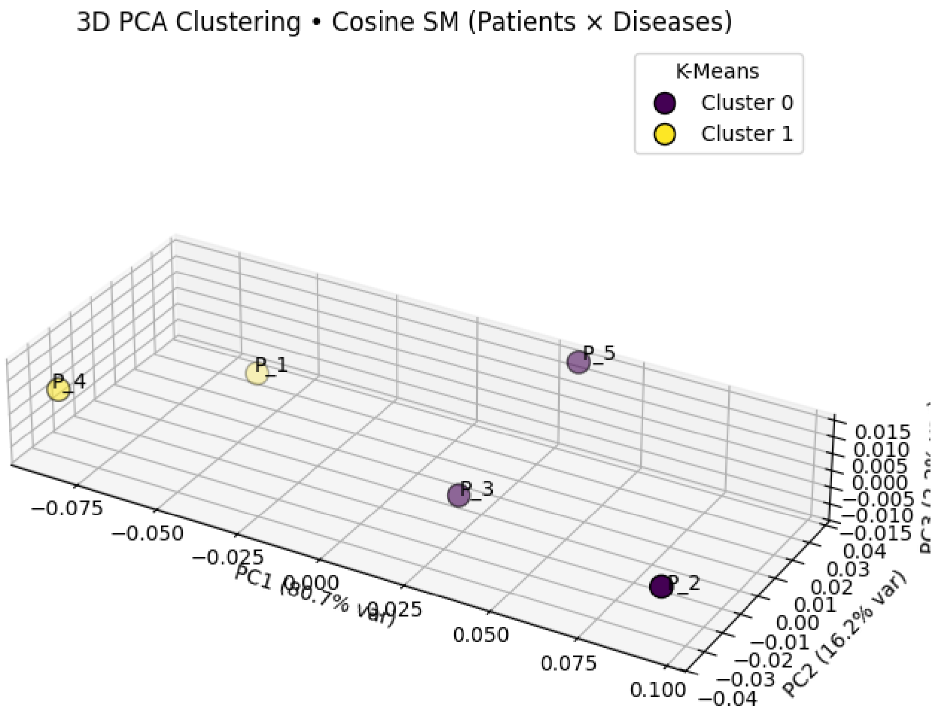

Fig 6.9.

A 3D PCA grouping of the normalized cosine similarity table of patients (P1-P5) versus diseases (D1-D5) is shown in **Fig. 6.10.** The points are colored with labels made using k-means (yellow = Cluster 1, purple = Cluster 0). The PC1-PC2 approach explains almost 94% of the structure since PC1 explains 58.6% of the variance and PC2 explains 35.4%. In contrast to P1, 3, 4, and 5, which cluster up as Cluster 0, P2 is distinct and forms its own cluster, indicating its own profile in the matrix. PC1 and P2 on the positive and P1/P5 on the negative carry the majority of the separation; PC2 further divides the group by positioning P4 and P1 higher and lower, respectively.

A quick summary of the post-normalization structure is given by the plot, which includes one clustered patient population and one conspicuous outlier (P2).

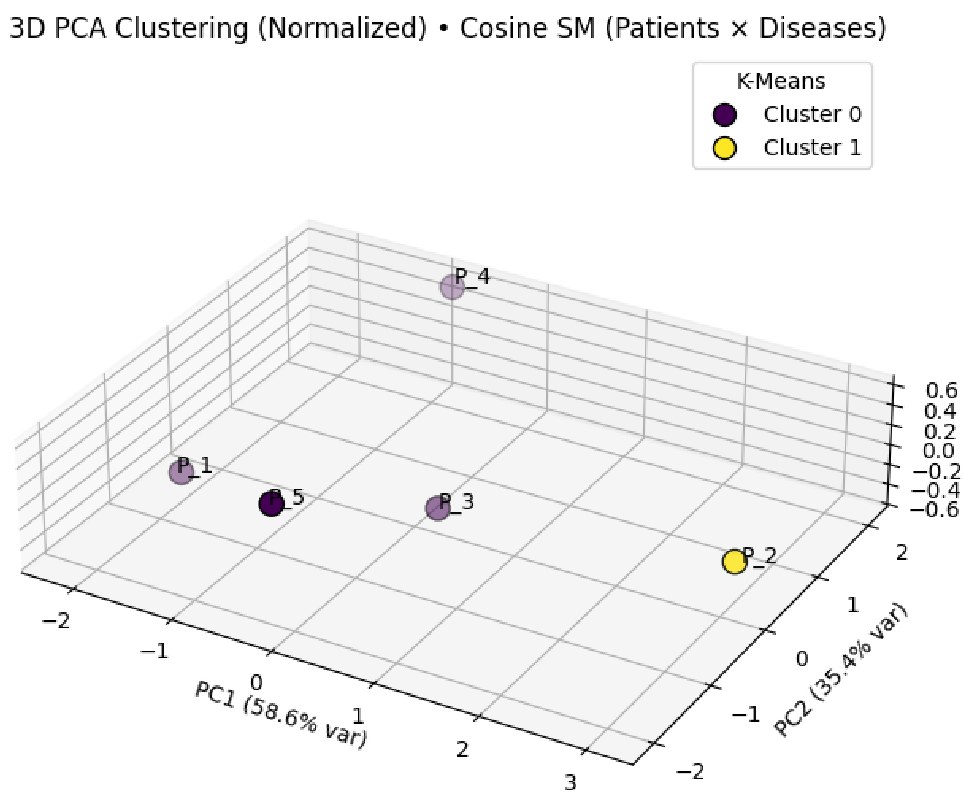

Fig. 6.10

7. Aspect- and Method-Based Analysis of Similarity Patterns

Two types of analysis are covered in this section: 7.1 Aspect-based Analysis and 7.2 Method-based Analysis. A review of the findings about the similarities between patients and diseases is given in Section 7.1, along with a list of the most striking parallels and near alternatives. Cool-warm Heatmaps, grouped 3D bar charts, normalization, Pearson correlation, 3D surfaces, and PCA are some of the techniques used that produce the same result and help make logical judgments (see Section 7.2). Below are detailed findings and supporting documentation.

7.1 Aspect-based analysis

With the strongest matches falling between 0.89 and 0.91 and the global magnitude falling between 0.7557 and 0.9107, the similarity between the patient profile and the available options was consistently high. Because these cosine scores are tangent-based, they emphasize directional congruence between patient patterns and illness alternatives. Warm colors are prominent at a glance, and the results of Figures 6.1 and 6.3 (cool-warm Heatmaps) and Table 6.4 (score-color mapping) support the conclusion that P 2 D 1 (0.9107) has the strongest relationship, closely followed by P 2 D 3 (0.9004), P 4 D 4 (0.8913), and P 5 D 5 (0.8905). As may be observed in P_4–D 1(0.7557), P 1-D 1(0.7904), and P 2-D 5(0.8201), the lighter hues suggest a weaker match, while the deep reds emphasize exceptionally high likeness, making it straightforward to read off the best cells. With the largest bar at P 2 D 1 and a clear ridge descending D 4 (P 2 D 4 = 0.8724, P 3 D 4 = 0.8883, P 4 D 4 = 0.8913, P 5 D 4 = 0.8625), the repurposed 3D bar chart in Figure 6.2 lends greater credence to this story. While patients with flatter profiles, like P 5, are always asked to make a ranked short-list rather than a single, definitive choice, those with sharp-peaked profiles, like P 2, can be categorized with high confidence.

Because P 2 D 1 is mapped to 1.000 and the low points are drawn to 0.000, the structure is still preserved even after normalizing to 01 (Figure 6.4 and 6.8). In particular, this standardizes the contrast at rows and columns without changing the outcome. The D 4 ridge and the strong corners at D 5 in P 1 and P 5 are once again indicated by the identical hotspots, which are replicated in Pearson correlation heatmaps (Figures 6.5 and 6.6), confirming the validity of the cosine view. The 3D surface (Figure 6.7) can show marginal situations (i.e. the best two are almost equal) and score plateaus (i.e., numerous possibilities are similarly good), such as along D 4, where the value distribution is closely packed, making it easier to visualize uncertain judgments. P1, where D 5 = 0.8878 and D 4 = 0.8724 (divider 0.0154), and P5, where D 5 = 0.8905 and D 4 = 0.8746 (divider 0.0159), are two good examples. Additionally, the structure can be preserved in PCA clustering (Figure 6.9 and Figure 6.10): with two separate clusters {P 2, P 3, P 5} and {P 1, P 4, P 5, P 6 } before normalization and a single cluster of four points P 2 after, PC1, PC2, and PC3 explain roughly 80.7, 16.2, and 3.1, respectively, prior to normalization.

In actuality, this favors ranking based on similarity rather than rigid cut-offs. Instead of being thrown away, case duplicates are organized or saved, which helps clinical support when there are minor variations and time limits. Operationally, the decisive pairings (P_2–D 1, P 2 -D 3, P 4 - D 4, and P 5 -D 5) are separated using a high-confidence filter of around 0.89, and P1 -D 4, P 1 -D 5, P 2 -D 4, and P 3 -D 4 are added by a strong band at a frequency that approaches 0.87. This offers a robust, comprehensible ranking that is consistent with the visual proof found in PCA, surfaces, bar charts, and Heatmaps.

7.2 Method-Based Analysis

The cool-warm Heatmaps (Figs. 6.1 and 6.3) give a clear picture of a match's advantages and disadvantages. They confirm that the D4 ridge is seen in patients (P1 D4 = 0.8724, P2 D4 = 0.8883, P3 D4 = 0.8845, P4 D4 = 0.8913, P5 D4 = 0.8625), the single top pair P2 D1 = 0.9107, and the low regions, like P4 D1 = 0.7557. Since Table 6.4 is the key to score and color, this keeps the visual scan and the numbers parallel and ensures that the same warmth is at the same band in every figure. The 3D grouped bar chart (Fig 6.2) converts the height of similarity into height, making P2D1 the tallest bar and the D4 ridge a continuous line of tall bars. Row shapes are also shown, including flat rows like P5 that are ranked shortlist rather than hard select, or sharp peaks like P2 that are decisive. Without changing the order of rank, the normalized cosine map (Fig. 6.4) adjusts the values to fall between 0 and 1, making P2D1 1.000 and the rest spread out in the same proportion. This makes cross-row or cross-column comparisons clearer and improves contrast in situations when the raw scores are closely packed. Pearson correlation, which examines the linear relationship between symptom patterns, also reaches the similar hotspots (Fig 6.5). The cosine and Pearson's agreement reduces the likelihood that outcomes are the product of one metric's bias. In a row-wise assignment with optional losers, the normalized Pearson display (Fig. 6.6) keeps credible losers visible while moving the winner of each row to the roof.

The matrix is a terrain since the surfaces (Figs. 6.7 and 6.8) are three-dimensional. The D4 ridge is shown as a line of high spine, whereas the highest and lowest points are P2 to P3 and P4 to P3, respectively. Minor gaps and plateaus can be better observed after 01 scaling of a similar area is no longer required. When two options are similar, such P1 having D5 = 0.8878 and D4 = 0.8724 and P5 having D5 = 0.8905 and D3 = 0.8746, it is helpful since the gaps around 0.016 are sufficiently tiny to indicate that the ranks are higher than the cut line. In a smaller space, PCA clustering preserves the structure. Taking into account the raw data (Fig 6.9), PC1, PC2, and PC3 represent roughly 80.7, 16.2, and 3.1 percent of the variance, respectively, and draw a line between P1 and P4 and between two patient groups {P2, P3, P5}. PC1 and PC2 capture roughly 58.6% and 35.4% as it normalizes (Fig 6.10), and P2 moves off as a distinct profile, while the gap between P1, P3, P4, and P5 converges into a small group. This shows that using cluster-aware rules makes sense and that the uniqueness of P2 is not a scaling phenomenon. A crude decision pipeline is produced by combining these techniques. A Heatmaps or bar chart can be used to identify the top cell per patient in seconds. The robustness can be checked using the normalized and Pearson views, and surfaces or PCA can be utilized if the two top cells are close to one another. P1 D5, P2 D1, P3 D4, P4 D4, and P5 D5 are the assignments that show up on this table. P2D1 is the world champion, and the high ridge along D4 is a reliable source of other good alternatives.

Conclusion

The tri-valued neutrosophic soft set, its elementary operations, and the creation of a tri-valued neutrosophic topological space are all proposed in this study. Algebra is held accountable by using crisp figures and illustrated labor to bring the principles into the actual world. The 5x5 patient-disease matrix offers a cohesive explanation of the applied side's perspectives.

Cosine similarity, min-max normalization, Pearson correlation, PCA using k-means are all directed to the the same anchor is the focus of cosine similarity, min-max normalization, Pearson correlation, and PCA using k-means. P2D1 has the highest similarity, the D4 column has a repeated high ridge, and the other structure divides into two sets of values that are consistently stable. The second cluster consists of P1 and P4 along the first main component, while P5, P3, and

P2 are in one sitting prior to normalization. Following normalization, P2 emerges as a distinct point, while the remaining points form a close cluster, with the first two components accounting for the majority of the variance. The assurance that the signal is not a result of the method's one-way choice is provided by the convergence of metrics and scales. The theoretical foundation, the example-driven algebra, and the corresponding visualizations form a single pipeline that defines, calculates, visualizes, and explains why the same cells keep winning.

Limitations

The work still has a number of limitations. This is because cluster validation is challenging and statistical power is limited due to the matrix's tiny size. Decisions on similarity are specific and may not be valid based on information or rank. While k-means are built on roughly spherical groups and depend on scaling and initialization, min-max scaling can stretch extremes and is sensitive to outliers. The visualizations presume that the inputs are fixed because the tri-valved components of uncertainty are not transmitted. There is no objective clinical ground truth that can confirm the strongest matches. Instead of being a formal relationship, the relationship between the topological definitions and the patterns in the observed data is more suggestive.

Future Work

Test the peaks, ridges, and clusters using subsampling, bootstraps, and permutation tests to determine the degree to which the results are stable before extrapolating to bigger, longitudinal data in the future. To determine when P 2 D1 peak and D4 ridge persist, compare Pearson and cosine with Spearman, Kendall, Mahalanobis, and Jensen Sharon ridge. To be able to see the differences in scaling local maxima and clusters, have test z-score and robust variants, quantile transforms, and mixed row and column schemes. Include clustering based on hierarchical, spectral, density-based, and mixture models with consensus or stability paths that indicate the number of groups available for selection. Use ellipses for PCA scores, error bars for peaks, and intervals for Heatmaps to illustrate the uncertainty of the tri-valued procedures. designs that demonstrate the improvement in separation on labeled information and designs that respect the neutrosophic topology. Semi-supervised and supervised models that have been trained to generate illness classifications based on TVNSS features and explain the factors that contribute to the match, such as P2-D1. Contrast with general clinical norms and professional opinion. Promote the complete, replicable process, which includes data versioning, seeded instances, and a small dashboard that allows users to switch between metrics, scaling, and clustering. Repeat measurements can be used to assess if a dynamic or structural ridge, like D4, is dynamic by seeing them as curves on the tri-valued space.

Acknowledgement: We extend our sincere appreciation to Mindanao State University – Tawi-Tawi College of Technology and Oceanography (MSU-TCTO) for their generous financial support of this work.

Author Contributions: All authors read and approved the final manuscript.

Funding: This research received no external funding.

Conflicts of Interest: The author(s) declare that there are no conflicts of interest regarding the publication of this paper.

References

[1] F. Smarandache, Neutrosophy: Neutrosophic Probability, Set, and Logic: Analytic Synthesis & Synthetic Analysis, American Research Press, 1998.

[2] F. Smarandache, A Unifying Field in Logics. Neutrosophy: Neutrosophic Probability, Set, and Logic, American Research Press, Rehoboth, 1999.

[3] H. Wang, F. Smarandache, Y.Q. Zhang, R. Sunderraman, Single valued neutrosophic sets, in: F. Smarandache (Ed.), Multispace & Multistructure. Neutrosophic Transdisciplinarity, Vol. 4, North-European Scientific Publishers, Hanko, Finland, 2010, pp. 410–413.

[4] S. Alkhazaleh, B. Batiha, A. Al-khateeb, H. Zureigat, A. Al-shboul, K. Batiha, Possibility Fermatean Neutrosophic Soft Set, Int. J. Neutrosophic Sci. 24 (2024), 105-125. https://doi.org/10.54216/IJNS.240408.

[5] R.K. Mohanty, B.K. Tripathy, A New Approach to Neutrosophic Soft Sets and Their Application in Decision Making, Neutrosophic Sets Syst. 60 (2023), 159-174.

[6] M. Parimala, M. Karthika, F. Smarandache, A Review of Fuzzy Soft Topological Spaces, Intuitionistic Fuzzy Soft Topological Spaces and Neutrosophic Soft Topological Spaces, Int. J. Neutrosophic Sci. 10 (2020), 96–104.

[7] P. Liu, L. Shi, The Generalized Hybrid Weighted Average Operator Based on Interval Neutrosophic Hesitant Set and Its Application to Multiple Attribute Decision Making, Neural Comput. Appl. 26 (2014), 457-471. https://doi.org/10.1007/s00521-014-1736-4.

[8] C. Kahraman, I. Otay, Eds., Fuzzy Multi-Criteria Decision-Making Using Neutrosophic Sets, Springer, 2019. https://doi.org/10.1007/978-3-030-00045-5.

[9] Y. Guo, H. Cheng, New Neutrosophic Approach to Image Segmentation, Pattern Recognit. 42 (2009), 587-595. https://doi.org/10.1016/j.patcog.2008.10.002.

[10] M. Abdel-Basset, M. Saleh, A. Gamal, F. Smarandache, An Approach of TOPSIS Technique for Developing Supplier Selection with Group Decision Making Under Type-2 Neutrosophic Number, Appl. Soft Comput. 77 (2019), 438-452. https://doi.org/10.1016/j.asoc.2019.01.035.

[11] F. Smarandache, Refined Literal Indeterminacy and the Multiplication Law of Sub-Indeterminacies, Neutrosophic Sets Syst. 9 (2015), 58–63.

[12] I. Deli, Refined Neutrosophic Sets and Refined Neutrosophic Soft Sets: Theory and Applications, in: Handbook of Research on Generalized and Hybrid Set Structures and Applications for Soft Computing, IGI Global, 2016: pp. 321--343. https://doi.org/10.4018/978-1-4666-9798-0.ch016.

[13] U. Solang, J. Ye, Refined Simplified Neutrosophic Similarity Measures Based on Trigonometric Function and Their Application in Construction Project Decision-Making, J. Soft Comput. Civ. Eng. 2 (2018), 1-12. https://doi.org/10.22115/scce.2018.126129.1056.

[14] R. Sahin, M. Yigider, A Multi-Criteria Neutrosophic Group Decision Making Method Based TOPSIS for Supplier Selection, Appl. Math. Inf. Sci. 10 (2016), 1843-1852. https://doi.org/10.18576/amis/100525.

[15] M. Teodorescu, D. Ionescu, Florentin Smarandache & Ştefan Vlăduțescu: Neutrosophic Emergences and Incidences in Communication and Information - Book Review, Int. Lett. Soc. Humanist. Sci. 38 (2014), 94-99. https://doi.org/10.18052/www.scipress.com/ILSHS.38.94.

[16] M.M. Saeed, R.H. Hatamleh, A.M.A. El-latif, A. Al-Husban, T. Fujita, et al., Separation Axioms in Quadri-Partition Neutrosophic Soft Topological Spaces, Eur. J. Pure Appl. Math. 18 (2025), 6324. https://doi.org/10.29020/nybg.ejpam.v18i3.6324.

[17] F. Smarandache, Neutrosophic Set – A Generalization of the Intuitionistic Fuzzy Sets, J. Pure Appl. Math. 24 (2005), 287-297.

[18] D. Molodtsov, Soft Set Theory—First Results, Comput. Math. Appl. 37 (1999), 19-31. https://doi.org/10.1016/S0898-1221(99)00056-5.

[19] P.K. Maji, Neutrosophic Soft Set, Ann. Fuzzy Math. Inform. 5 (2013), 157–168.

[20] T. Bera, N.K. Mahapatra, Introduction to Neutrosophic Soft Topological Space, OPSEARCH 54 (2017), 841-867. https://doi.org/10.1007/s12597-017-0308-7.

[21] T.Y. Ozturk, C.G. Aras, S. Bayramov, A New Approach to Operations on Neutrosophic Soft Sets and to Neutrosophic Soft Topological Spaces, Commun. Math. Appl. 10 (2019), 481–493. https://doi.org/10.26713/cma.v10i3.1068.

[22] T. Fujita, The Hyperfuzzy VIKOR and Hyperfuzzy DEMATEL Methods for Multi-Criteria Decision-Making, Spectr. Decis. Mak. Appl. 3 (2026), 292-315. https://doi.org/10.31181/sdmap31202654.

[23] M.E.M. Abdalla, A. Uzair, A. Ishtiaq, M. Tahir, M. Kamran, Algebraic Structures and Practical Implications of Interval-Valued Fermatean Neutrosophic Super HyperSoft Sets in Healthcare, Spectr. Oper. Res. 2 (2025), 240-259. https://doi.org/10.31181/sor21202523.

[24] R. Gul, An Extension of VIKOR Approach for MCDM Using Bipolar Fuzzy Preference Δ-Covering Based Bipolar Fuzzy Rough Set Model, Spectr. Oper. Res. 2 (2025), 72-91. https://doi.org/10.31181/sor21202511.

[25] A. Jaleel, T. Mahmood, D. Pamucar, M. Iftikhar, Optimizing Computer Engineering Problems Using CODAS Method with Bipolar Complex Fuzzy Soft Frank Aggregation Operators, Contemp. Math. 6 (2025), 5145–5171.

[26] S. Goswami, D. Pamucar, Application of Fuzzy MCDM in Selecting Eco-Friendly Materials for Electric Vehicle Interiors, J. Appl. Eng. Sci. 23 (2025), 504-522. https://doi.org/10.5937/jaes0-57423.

[27] A. Tarafdar, A. Shaikh, D. Bhowmik, P. Majumder, D. Pamucar, et al., Integration of Data-Driven T-Spherical Fuzzy Mathematical Models for Evaluation of Electric Vehicles: Response to Electric Vehicle Market Demands, Renew. Sustain. Energy Rev. 223 (2025), 116008. https://doi.org/10.1016/j.rser.2025.116008.

[28] M. Palanikumar, N. Kausar, D. Pamucar, V. Simic, Optimizing Industrial Robot Selection Using Novel Trigonometric Pythagorean Fuzzy Normal Aggregation Operators, Complex Intell. Syst. 11 (2025), 453. https://doi.org/10.1007/s40747-025-02083-5.

[29] F. Lilik, L. Solecki, B. Sziová, L.T. Kóczy, S. Nagy, On Wavelet Based Enhancing Possibilities of Fuzzy Classification Methods, in: P. Kulczycki, J. Kacprzyk, L.T. Kóczy, R. Mesiar, R. Wisniewski (Eds.), Information Technology, Systems Research, and Computational Physics, Springer, Cham, 2020: pp. 56–73. https://doi.org/10.1007/978-3-030-18058-4_5.

[30] A. Tormási, L.T. Kóczy, Comparing the Efficiency of a Fuzzy Single-Stroke Character Recognizer with Various Parameter Values, in: S. Greco, B. Bouchon-Meunier, G. Coletti, M. Fedrizzi, B. Matarazzo, R.R. Yager (Eds.), Advances on Computational Intelligence, Springer, Berlin, Heidelberg, 2012: pp. 260–269. https://doi.org/10.1007/978-3-642-31709-5_27.

[31] D. Göndöcs, V. Dörfler, AI in Medical Diagnosis: AI Prediction & Human Judgment, Artif. Intell. Med. 149 (2024), 102769. https://doi.org/10.1016/j.artmed.2024.102769.

[32] A. Ballagi, L.T. Koczy, Decision Making in Multi-Robot Cooperation by Fuzzy Signature Sets, in: International Conference on Fuzzy Systems, IEEE, 2010, pp. 1-8. https://doi.org/10.1109/FUZZY.2010.5584821.

[33] A.A. Abubaker, R. Hatamleh, K. Matarneh, A. Al-Husban, On the Numerical Solutions for Some Neutrosophic Singular Boundary Value Problems by Using (LPM) Polynomials, Int. J. Neutrosophic Sci. 25 (2025), 197-205. https://doi.org/10.54216/IJNS.250217.

[34] A. Ahmad, R. Hatamleh, K. Matarneh, A. Al-Husban, On the Irreversible K-Threshold Conversion Number for Some Graph Products and Neutrosophic Graphs, Int. J. Neutrosophic Sci. 25 (2025), 183–196. https://doi.org/10.54216/IJNS.250216.

[35] R. Hatamleh, A. Al-Husban, K. Sundareswari, G. Balaj, M. Palanikumar, Complex Tangent Trigonometric Approach Applied to (γ, τ)-Rung Fuzzy Set Using Weighted Averaging, Geometric Operators and Its Extension, Commun. Appl. Nonlinear Anal. 32 (2024), 133-144. https://doi.org/10.52783/cana.v32.2978.

[36] R. Hatamleh, A. Hazaymeh, On Some Topological Spaces Based on Symbolic n-Plithogenic Intervals, Int. J. Neutrosophic Sci. 25 (2025), 23–37. https://doi.org/10.54216/IJNS.250102.

[37] H. Qawaqneh, Fractional Analytic Solutions and Fixed Point Results with Some Applications, Adv. Fixed Point Theory, 14 (2024), 1. https://doi.org/10.28919/afpt/8279.

[38] H. Qawaqneh, M.S.M. Noorani, H. Aydi, A. Zraiqat, A.H. Ansari, On Fixed Point Results in Partial b-Metric Spaces, J. Funct. Spaces 2021 (2021), 8769190. https://doi.org/10.1155/2021/8769190.

[39] H. Qawaqneh, M.S.M. Noorani, H. Aydi, Some New Characterizations and Results for Fuzzy Contractions in Fuzzy b-Metric Spaces and Applications, AIMS Math. 8 (2023), 6682-6696. https://doi.org/10.3934/math.2023338.

[40] H. Qawaqneh, J. Manafian, M. Alharthi, Y. Alrashedi, Stability Analysis, Modulation Instability, and Beta-Time Fractional Exact Soliton Solutions to the Van Der Waals Equation, Mathematics 12 (2024), 2257. https://doi.org/10.3390/math12142257.

[41] H. Qawaqneh, New Functions for Fixed Point Results in Metric Spaces with Some Applications, Indian J. Math. 66 (2024), 55–84.

[42] H. Qawaqneh, H.A. Hammad, H. Aydi, Exploring New Geometric Contraction Mappings and Their Applications in Fractional Metric Spaces, AIMS Math. 9 (2024), 521-541. https://doi.org/10.3934/math.2024028.

[43] M. Elbes, T. Kanan, M. Alia, M. Ziad, COVD-19 Detection Platform from X-Ray Images Using Deep Learning, Int. J. Adv. Soft Comput. Appl. 14 (2022), 197-211. https://doi.org/10.15849/IJASCA.220328.13.

[44] T. Kanan, M. Elbes, K.A. Maria, M. Alia, Exploring the Potential of IoT-Based Learning Environments in Education, Int. J. Adv. Soft Comput. Appl. 15 (2023), 166-178.

[45] I.M. Batiha, S.A. Njadat, R.M. Batyha, A. Zraiqat, A. Dababneh, et al., Design Fractional-Order PID Controllers for Single-Joint Robot Arm Model, Int. J. Adv. Soft Comput. Appl. 14 (2022), 97-114. https://doi.org/10.15849/IJASCA.220720.07.

[46] A.M.A. El-latif, M.H. Alqahtani, Novel Categories of Supra Soft Continuous Maps via New Soft Operators, AIMS Math. 9 (2024), 7449-7470. https://doi.org/10.3934/math.2024361.

[47] A.M. Abd El-latif, M.H. Alqahtani, F.A. Gharib, Strictly Wider Class of Soft Sets via Supra Soft Δ-Closure Operator, Int. J. Anal. Appl. 22 (2024), 47. https://doi.org/10.28924/2291-8639-22-2024-47.

[48] A. Al-Omari, M.H. Alqahtani, Some Operators in Soft Primal Spaces, AIMS Math. 9 (2024), 10756-10774. https://doi.org/10.3934/math.2024525.

[49] A.M. Abd El-latif, A.A. Azzam, R. Abu-Gdairi, M. Aldawood, M.H. Alqahtani, New Versions of Maps and Connected Spaces via Supra Soft Sd-Operators, PLOS ONE 19 (2024), e0304042. https://doi.org/10.1371/journal.pone.0304042.

[50] A.M.A. El-latif, A.A. Azzam, R. Abu-Gdairi, M.H. Alqahtani, G.M. Abd-Elhamed, Applications on Soft Somewhere Dense Sets, J. Interdiscip. Math. 27 (2024), 1679-1699. https://doi.org/10.47974/JIM-2007.

[51] M.H. Alqahtani, Neutrosophic Primal Structure with Closure and Proximity Operators, AIMS Math. 11 (2025), 644-660. https://doi.org/10.3934/math.2026028.

[52] M.H. Alqahtani, Operators and Separation Axioms Within the Framework of Diving Topological Spaces, AIMS Math. 10 (2025), 25253-25273. https://doi.org/10.3934/math.20251118.

[53] I. Ibedou, S.E. Abbas, M.H. Alqahtani, Defining New Structures on a Universal Set: Diving Structures and Floating Structures, Mathematics 13 (2025), 1859. https://doi.org/10.3390/math13111859.

[54] M.H. Alqahtani, M. Tkachenko, Normality and N-Factorizable Topological Groups, Topol. Appl. 373 (2025), 109497. https://doi.org/10.1016/j.topol.2025.109497.

[55] S.A. El-Sheikh, A.M. Abd El-latif, Decompositions of Some Types of Supra Soft Sets and Soft Continuity, Int. J. Math. Trends Technol. 9 (2014), 37-56. https://doi.org/10.14445/22315373/IJMTT-V9P504.

[56] A.M. Abd El-latif, Specific Types of Lindelöfness and Compactness Based on Novel Supra Soft Operator, AIMS Math. 10 (2025), 8144-8164. https://doi.org/10.3934/math.2025374.

[57] A.M. Abd El-latif, M.H. Alqahtani, New Soft Operators Related to Supra Soft δ-Open Sets and Applications, AIMS Math. 9 (2024), 3076-3096. https://doi.org/10.3934/math.2024150.

[58] M.H. Alqahtani, A.M. Abd El-latif, Separation Axioms via Novel Operators in the Frame of Topological Spaces and Applications, AIMS Math. 9 (2024), 14213-14227. https://doi.org/10.3934/math.2024690.

[59] Z.A. Ameen, M.H. Alqahtani, Baire Category Soft Sets and Their Symmetric Local Properties, Symmetry 15 (2023), 1810. https://doi.org/10.3390/sym15101810.

[60] M.H. Alqahtani, O.F. Alghamdi, Z.A. Ameen, Nodecness of Soft Generalized Topological Spaces, Int. J. Anal. Appl. 22 (2024), 149. https://doi.org/10.28924/2291-8639-22-2024-149.

[61] Z.A. Ameen, M.H. Alqahtani, Some Classes of Soft Functions Defined by Soft Open Sets Modulo Soft Sets of the First Category, Mathematics 11 (2023), 4368. https://doi.org/10.3390/math11204368.

[62] Z.A. Ameen, M.H. Alqahtani, Congruence Representations via Soft Ideals in Soft Topological Spaces, Axioms 12 (2023), 1015. https://doi.org/10.3390/axioms12111015.

[63] M.H. Alqahtani, H.Y. Saleh, A Novel Class of Separation Axioms, Compactness, and Continuity via C-Open Sets, Mathematics 11 (2023), 4729. https://doi.org/10.3390/math11234729.

[64] R. Hatamleh, N. Odat, H.A. Abujabal, F. Khan, A.M. Khattak, et al., Fermatean Double-Valued Neutrosophic Soft Topological Spaces, Eur. J. Pure Appl. Math. 18 (2025), 6483. https://doi.org/10.29020/nybg.ejpam.v18i3.6483.

[65] A.M.A. El-latif, On Soft Supra Compactness in Supra Soft Topological Spaces, Tbilisi Math. J. 11 (2018), 169–178. https://doi.org/10.32513/tbilisi/1524276038.